EFFECTS OF INCREASED Q-FACTOR ON KNEE BIOMECHANICS DURING CYCLING

A Thesis Presented for the
Master of Science
Degree
The University of Tennessee, Knoxville

Tanner Austin Thorsen
August 2018

Copyright © 2018 by Tanner A. Thorsen
All rights reserved.

ACKNOWLEDGEMENTS

I would first and foremost like to thank my advisor, Dr, Songning Zhang, for his guidance and supervision throughout this thesis project. He has been a great mentor and advisor who has sincerely cared about my scholastic and professional development. His tireless support, encouragement, and feedback have made me a better researcher and scholar. Thank you!

I would also like to thank my thesis committee members, Dr. Joshua Weinhandl and Dr. Kelley Strohacker. Their advice, counsel, and mentorship throughout this thesis project have been far more valuable than I could have imagined at the onset of my graduate education. I would also like to thank several of my fellow colleagues; namely Erik Hummer, for his collaborative efforts and insights within the realm of cycling, as well as Derek Yocum, Shelby Peel, Dan Sample, and Lindsey St. Hilaire, for their help with data collection, pedal calibration, and participant recruitment.

There is a proverb of unknown origin that incorporates, in part, the love I have for my wife Christine, and the impact she has had on my life. “If you want to go fast, go alone. If you want to go far, go together”. Throughout all phases of this thesis project, Christine has been my rock and my support. She has worked tirelessly for our family so that I may have the opportunity to complete this degree. Thank you, Christine. I love you!

ABSTRACT

Q-Factor (QF), the inter-pedal width, in cycling is the analog to step-width in gait. Increased step-width has been shown to reduce peak knee abduction moment (KabM), however no studies have examined the frontal plane biomechanics with increased QF in cycling. **Purpose:** The purpose of this study was to investigate the effects of increased QF on frontal plane knee biomechanics during cycling in healthy participants. **Method:** Sixteen healthy participants (age: 22.4 ± 2.6 yr, BMI: 22.78 ± 1.43 kg/m^2) participated in this study. A motion analysis system and customized instrumented pedals were used to collect five trials of three-dimensional kinematic (240 Hz) and pedal reaction force (PRF, 1200 Hz) data in twelve testing conditions, four QF conditions of Q150 (150 mm), Q192 (192 mm), Q234 (342 mm), Q276 (276 mm), and three workrate conditions of 80 W, 120 W, and 160 W. A 3 × 4 (QF × workrate) repeated measures ANOVA was performed to analyze differences between conditions ($p < 0.05$). **Results:** Increased QF increased peak KAbM 47, 56, and 56% from Q150 to Q276 at each workrate respectively. Mediolateral PRF increased 46, 57, and 57% from Q150 to Q276 at each workrate. Frontal plane knee angle and range of motion (ROM) decreased with increased QF. No changes were observed for peak vertical PRF, knee extension moment, sagittal plane peak knee joint angles or ROM. **Conclusions:** These results indicate increasing QF will increase peak KAbM. Future studies should examine the effects of increased QF on obese and knee osteoarthritis patients.

TABLE OF CONTENTS

CHAPTER I INTRODUCTION 1
Background 1
Statement of the Problem 5
Research Hypotheses 5
Delimitations 5
Limitations 6
CHAPTER II LITERATURE REVIEW 8
Introduction 8
Knee Biomechanics of Cycling 11
Introduction 11
Sagittal Plane Knee Kinematics of Cycling 12
Frontal Plane Knee Kinematics of Cycling 13
Sagittal Plane Knee Kinetics of Cycling 14
Frontal Plane Knee Kinetics of Cycling 15
Effects of cycling Workload on knee biomechanics 18
Effects of cycling Cadence on knee biomechanics 21
Effects of Saddle Height and Fore/Aft position on knee biomechanics 22
Instrumented Pedal Design and Force Measurement 25
Q-Factor 27
Gross Mechanical Efficiency 28
Self-Selected Q-Factor 29
Bike Fit 30
Q-Factor Summary 32
CHAPTER III METHODS 33
Participants 33
Instrumentation 33
Motion Capture 33
Cycle Ergometer 34
Instrumented Bike Pedals 34
Q-Factor 35
Experimental Procedures 35
Data Treatment and Analysis 38
Statistical Analysis 41
CHAPTER IV THE EFFECTS OF INCREASED Q-FACTOR ON KNEE BIOMECHANICS DURING CYCILING 42
Abstract 43
1. Introduction 44
2. Method 46
2.1 Participants 46
2.2 Instrumentation 47
2.3 Experimental Procedures 48
3. Results 52

4. Discussion 57
5. Conclusion 62
LIST OF REFERENCES 63
APPENDICES 73
Appendix A: Individual Subject Characteristics 74
Appendix B: Informed Consent Form 76
Appendix C: Flyer 80
Appendix D: Physical Activity Readiness Questionnaire (PAR-Q) 81
Appendix E: Borg's 6-20 scale, Comfort, Pain Numeric Visual Analog scale 83
Appendix F: Individual Results for Selected Variables 84
VITA 106

LIST OF TABLES

Table 1: Group Mean RPE, comfort, and pain scores. 53
Table 2: Peak power phase pedal reaction forces (PRF). 54
Table 3: Peak power phase knee joint angles (°) and moments (Nm). 56
Table 4: Individual Subject Characteristics. 74
Table 5: Group Mean RPE, comfort, and pain scores. 75
Table 6: Individual mean peak vertical PRF (N). 85
Table 7: Individual mean peak mediolateral PRF (N). 86
Table 8: Individual mean power phase COP (cm). 87
Table 9: Individual mean knee extension ROM (°). 88
Table 10: Individual mean peak frontal plane knee angle (°). 89
Table 11: Individual mean knee abduction ROM (°) 90
Table 12: Individual mean knee external rotation ROM (°). 91
Table 13: Individual mean peak ankle eversion angle (°). 92
Table 14: Individual mean hip abduction ROM (°). 93
Table 15: Individual mean peak knee extension moment (Nm). 94
Table 16: Individual mean peak knee abduction moment (Nm). 95
Table 17: Individual mean peak knee external rotation moment (Nm). 96
Table 18: Individual mean peak ankle eversion moment (Nm). 97
Table 19: Individual mean peak ankle external rotation moment (Nm). 98
Table 20: Individual mean peak hip abduction moment (Nm). 99
Table 21: Individual RPE scores. 100
Table 22: Individual comfort scores. 101
Table 23: Individual pain scores. 102
Table 24: Group mean peak pedal reaction force (PRF) and pedal center of pressure. 103
Table 25: Group mean peak lower extremity joint angles and power phase ROM. 104
Table 26: Group mean peak lower extremity power phase joint moments. 105

LIST OF FIGURES

Figure 1. Diagram with labels of key components of the bicycle..... 11
Figure 2. The local coordinate system and arrangement of the two force sensors on the right instrumented pedal. 35
Figure 3. A) The custom jig installed on the ground used to keep the cycle ergometer aligned parallel to the antereoposterior and mediolateral axis of the lab global coordinate system, and B) Base of the cycle ergometer positioned within the custom jig..... 49
Figure 4. A) Right instrumented bicycle pedal with three QF extenders, B) Right instrumented bicycle pedal mounted on the stationary cycle ergometer at Q150 and C) Right instrumented bicycle pedal mounted on the stationary cycle ergometer at Q276. 50

CHAPTER I
INTRODUCTION

Background

Knee and hip pain are among the major causes for ambulatory pain in elderly adults all over the world (Dawson et al., 2004). A major cause of this pain stems from arthritis, specifically, Osteoarthritis (OA) (Zhang et al., 2008). In the United States alone, OA is prevalent in nearly 27 million people (Lawrence et al., 2008). OA most commonly affects the weight bearing joints of the lower extremity, namely the knee and hip (Lawrence et al., 2008), and nearly 7.7 million people in the U.S. suffer from OA that affects ambulation (Ogden et al., 2016). Although the exact cause of OA is not entirely understood, there are several known risk factors for OA. Non-modifiable risk factors include age (Felson et al., 2000) and genetics (Felson et al., 1998), and modifiable risk factors include injury (Lohmander et al., 2004), muscle weakness (Baker et al., 2004; Slemenda et al., 1997; Slemenda et al., 1998), and obesity (Felson et al., 2000; Zhang et al., 2008). Obesity is the accrual of excess body fat, which results in a body mass index (BMI) greater than 30kg/m^2 (BMI, 1998). Obesity, apart from all modifiable risk factors is the single most modifiable risk factor in the development and progression of OA. This is in part due to the increased load on lower extremity joints that result from the accumulation of excess body mass (Felson et al., 1988).

Although all joints of the lower extremity may be susceptible to the progression of OA, the knee joint is one of the most common (Mündermann et al., 2005), and knee OA is most frequently and primarily observed in the medial compartment (Thomas et al., 1975). This is in part attributable to the increased load experienced in the medial

compartment compared to the lateral compartment of the knee during level walking (Schipplein and Andriacchi, 1991).

The distribution of loads transferred through the knee joint can be estimated by the internal knee abduction moment (KAbM) (or external adduction moment) (Andriacchi et al., 2009; Paquette et al., 2015; Schipplein and Andriacchi, 1991). As a surrogate variable for medial compartment knee loading, the internal knee abduction moment, has been shown to increase with the severity of knee OA (Andriacchi et al., 2009).

In level walking, previous studies have investigated how peak KAbM may be affected by alterations made to gait. In biomechanical research, SW is a common spatiotemporal measurement used. The effects of widening step-width (SW) have been studied as it pertains to peak KAbM. During level walking wider SW has been shown to decrease peak KAbM (Bennet, 2016; Fregly et al., 2008; Zhao et al., 2007). A reduction in peak KAbM has also been shown in stair negotiation in healthy (Bennet, 2016; Paquette et al., 2014a), and OA populations (Paquette et al., 2015).

Most exercise protocols designed to reduce body fat have been focused on steady state cardiovascular exercise, such as walking and running. Another form of exercise often prescribed for weight loss is cycling (Boutcher, 2010). Cycling allows reduced knee joint loading in large part by placing the majority of the rider's weight on the saddle (seat) (Burke, 1986). During the power stroke of a cycle, great demand is placed on the knee extensor muscles, followed by the knee flexor muscles during the recovery phase.

Recently, several studies have examined changes to frontal plane knee biomechanics in response to changes in toe-in angles (Gardner et al., 2015), lateral shoe wedges (Gardner et al., 2016), cycling workload, and cycling cadence (Fang et al., 2016). Although previous literature has suggested that KAbM may potentially be reduced when some movement between the foot and pedal is allowed, no reduction was found with the manipulation of the toe-in angle at the shoe pedal interface (Gardner et al., 2015). In the study where lateral wedges were placed on the lateral aspect of the pedal, in between the pedal and the shoe, such to promote 5 or 10° ankle eversion, a significant decrease in peak KAbM was seen for the 10° wedge as compared to the neutral condition (Gardner et al., 2016). Fang et al. (2016), examined the effects of cadence and workload on frontal plane knee biomechanics and found that increased workload significantly increased peak KAbM. There was, however, no significant effect of cadence on peak KAbM (Fang et al., 2016).

The inter-pedal width, measured from the outside face of one crank arm to the outside face of the opposite crank arm, known as Q-Factor (QF), may serve as an analogous spatiotemporal variable in cycling to SW during walking. The QF is measured from the outside face of the crank arm, where the pedal attaches to the contralateral crank arm/pedal (Disley and Li, 2014a, b). Relatively unexplored in the scientific literature, the biomechanical effects of QF have yet to be fully defined.

Disley and Li (2014a) showed that in trained cyclists, a reduction in QF, to 120 mm and 90 mm from 150 mm, resulted in a significant increase in gross mechanical efficiency (GME) as well as the magnitude and muscular timing of activation was

unchanged for the vastus lateralis, vastus medialis, tibialis anterior, and gastrocnemius.. Although there was no significant difference between the GME at 120 mm versus 90 mm, bringing the pedals closer to the midline of the bicycle may increase the efficiency of force transfer at the pedal by reducing tangential force during the pedal stroke (Disley and Li, 2014a). GME was, however, decreased at 150 mm and 180 mm relative to 120 mm and 90 mm, albeit there was no significant difference in GME between these two QFs.

In a second study that permitted unrestricted mediolateral range of motion of the bicycle pedal, trained cyclists chose a narrower QF than untrained cyclists (137mm vs. 153mm). No significant differences were found between GME or knee variability. Mean self-selected QF (SSQ) was reported as 142 ± 12mm. Good correlation was found between SSQ (142mm) and knee variability (R^2 = 0.938) and at QFs ±30mm from SSQ knee variability increased with a concurrent decrease of GME. A strong correlation was found between hanging intermalleolar distance and SSQ (R^2=0.794).

Examination of the QFs of the different cycle ergometers used in the previously mentioned studies by Gardner et al. (Gardner et al., 2016; Gardner et al., 2015) and Fang et al. (Fang et al., 2016) may provide insight to the anticipated kinetic response of increasing QF for young, healthy, recreationally active adults. The QF on the cycle ergometer of Gardner's studies was measured at 150 mm (Excalibur Sport, Lode, Groningen, Netherlands). With the addition of 5° and 10° lateral shoe wedges, all participants exhibited KAbM (Gardner et al., 2016). The QF on the cycle ergometer of Fang's study was measured at 190 mm (Model 818E, Monark, Varberg, Sweden). At this

increased QF, seven of eighteen subjects exhibited an abduction moment pattern at all workloads. Eleven of eighteen participants exhibited a knee adduction moment pattern at all workloads (Fang et al., 2016).

Statement of the Problem

To our knowledge, there have been no studies that have explored the effects of increased QF on knee joint kinetics during cycling. Differences have been shown in mechanical and metabolic efficiency among trained cyclists from the manipulation of QFs. It is unknown, however, if an increase in QF will result in a change of peak KAbM, and therefore medial knee compartment loading while cycling. The purpose of this study was, therefore, to examine effects of standard and increased QFs at different workloads on knee biomechanics of healthy-weight participants during stationary cycling.

Research Hypotheses

1. As QF increases, the peak KAbM will decrease and, as QF increases further, the frontal plane knee moment will become a knee adduction moment.
2. As workrate increases, the increase in the frontal plane knee moment will be greater.
3. As QF increases, peak knee extension moment will not change significantly.

Delimitations

The exclusion criteria for this study include:

- Major injuries (e.g. fracture of bone, rupture of tendon or ligament) that require surgical repair to any of the lower extremity ever.
- Any disorder/disease/pathology affecting gait or balance.

- Any lower extremity injuries within the past year.
- Pain while performing common actives of daily living, like walking, riding a stationary bike, or walking up the stairs.
- Any cardiovascular diseases or primary risk factor that prohibited participation in aerobic exercise as indicated by the Physical Activity Readiness Questionnaire (PAR-Q). If a participant marked "yes" on any of the questions, he or she was required to provide written consent from a doctor signifying adequate health for participation in the study.

The inclusion criteria included:

- Men and women between 18 and 35 old.
- BMI between 18kg/m^2 and 24.9 kg/m^2.
- Recreationally active, defined as engaging in moderate to vigorous activity at three days a week for the past six months.

Limitations

- The tests were conducted in a laboratory setting.
- The retro-reflective tracking markers used for the feet were placed directly on the shoe, not on the foot itself, and therefore might not accurately reflected the motion of the foot within the shoe.
- The American College of Sports Medicine (ACSM) metabolic equivalent (MET) equations (Glass et al., 2007) as well as The Compendium of Physical Activities (Ainsworth et al., 2011) are limited in that energy expenditure is reported or calculated in absolute MET values for able-bodied adults who are 18-65 years of

age. As such, energy expenditure comparisons between alternative populations (e.g. youth, older adults, and those with disabilities) may consider including additional adjustments for population specific energy expenditure reporting (Ainsworth et al., 2011).

CHAPTER II
LITERATURE REVIEW

Introduction

The purpose of this study was to examine effects of standard and increased QFs on knee biomechanics of healthy-weight participants during stationary cycling. This literature review includes background information about bicycle construction, bicycle fit, cycling biomechanics, and the influence of cycling QF on cycling efficiency and knee kinetics.

Knee and hip pain are among the major causes for ambulatory dysfunction in elderly adults all over the world (Dawson et al., 2004). A major cause of this pain is from arthritis, specifically, osteoarthritis (OA) (Zhang et al., 2008). In the United States alone, OA is prevalent in nearly 27 million people (Lawrence et al., 2008). OA most commonly affects the weight bearing joints of the lower extremity, namely the knee and hip (Lawrence et al., 2008), and nearly 7.7 million people in the U.S. suffer from OA that affects ambulation (Ogden et al., 2016). Although the exact cause of OA is not entirely understood, there are several known risk factors for OA. Non-modifiable risk factors include age (Felson et al., 2000) and genetics (Felson et al., 1998), and modifiable risk factors include injury (Lohmander et al., 2004), muscle weakness (Baker et al., 2004; Slemenda et al., 1997; Slemenda et al., 1998), and obesity (Felson et al., 2000; Zhang et al., 2008). Obesity, apart from all modifiable risk factors, is the single most modifiable risk factor in the development and progression of OA. This is in part due to the increased load on lower extremity joints that result from the accumulation of excess body mass (Felson et al., 1988).

Obesity is the accrual of excess body fat, which results in a body mass index (BMI) greater than 30kg/m^2 (BMI, 1998). In the last 75 years the trend of adult obesity has been increasing. Contrast, for example, obesity statistics from 2012 in which 34.9% of Americans were classified as obese (Ogden et al., 2016) with that of 13.3% in the early 1960's (Flegal et al., 2016). The growing epidemic of obesity is not confined to the United States alone. In 2016, the World Health Organization reported that worldwide, 39% of adults over the age of 18 were overweight and 13% were obese (WHO, 2016).

Weight loss has, however, been shown to reduce risk of symptomatic OA as well as reduce the problematic symptoms experienced by those diagnosed with OA (Focht et al., 2005; Messier et al., 2005). Messier (2005) observed that a 1 kg decrease in body mass was associated with a decrease of 40.6 N and 38.7 N in tibiofemoral compressive and resultant ground reaction forces respectively . Additionally, it was found that this 1 kg decrease in body mass resulted in a 1.4% reduction in the knee abduction moment (Messier et al., 2005). Other researchers have furthermore noted that healthy weight loss resulted improved functional ability and decreased knee pain (Focht et al., 2005; Messier et al., 2004).

Further support for weight loss as a non-surgical treatment for knee OA has been recommended by many global health organizations including The Osteoarthritis Research Society International (OARSI) (Zhang et al., 2008), the American College of Rheumatism (Rheumatology, 2000), and the European League Against Rheumatism (Pendleton et al., 2000). In 2007, OARSI released 25 recommendations for the management of hip and knee OA aimed at assisting physicians and allied health care

professionals who work with OA patients in primary and secondary care settings (Zhang et al., 2008). These guidelines are current, evidence based, globally relevant recommendations for the treatment of OA. Healthy weight loss via diet and exercise are among the first non-pharmacologic recommendations (Zhang et al., 2008).

It important that if overweight or obese, people lose weight. The position stance of the American College of Sports Medicine (ACSM) recommends that most adults engage in moderate to vigorous cardiorespiratory exercise (Garber et al., 2011). Current recommendations of physical activity for adults are for at least 30 minutes a day, 5 days per week, of moderate-intensity physical activity (3-5.9 METs) or at least 3 days per week of vigorous physical activity (> 6 METs) (Garber et al., 2011). Furthermore, ACSM guidelines suggest that resistance training may decrease the risk of musculoskeletal diseases (e.g. OA) and that resistance training may reduce the pain and disability in patients suffering from OA (Garber et al., 2011).

Although diet and exercise continue to be the best forms of weight loss, it is still challenging. Specifically, for the obese and osteoarthritic populations, excess body mass increases the loads experienced by the lower extremity joints during exercise (Messier et al., 2005). This often makes aerobic weight bearing exercises difficult and painful (Focht et al., 2005; Skender et al., 1996).

Most exercise protocols designed to reduce body fat have been focused on steady state cardiovascular exercise, such as walking and running. Another form of exercise often prescribed for weight loss is cycling (Boutcher, 2010). Cycling allows reduced knee joint loading in large part by placing the majority of the rider's weight on the saddle

(seat) (Burke, 1986). During the power stroke of a cycle, great demand is placed on the knee extensor muscles, followed by the knee flexor muscles during the recovery phase.

Knee Biomechanics of Cycling

Introduction

The basic components of a bicycle include the frame, saddle, handlebar, crank, crank arms, and pedals (Figure 1). The bicycle frame is further defined by the top tube, down tube, seat tube, head tube, and both chain and seat stays (Figure 1). One complete cycle of pedal circular movement defined by the crank arm can be divided in to a two-phase cycle: power phase (from 0º to 180º) and recovery phase (from 180º to 360º) (Asplund and St Pierre, 2004). During the pedal cycle, the top most position of the crank arm and pedal is referred to as top dead center (0º), while the bottom mot position is referred to as bottom dead center (180º). One complete pedal cycle (revolution) is typically defined as from the top dead center.



Figure 1. Diagram with labels of key components of the bicycle.

During the pedal cycle, the knee travels through approximately 60-80º of sagittal plane (flexion/extension) motion (Ercison et al., 1988). The knee begins the power phase at top dead center, flexed to about 110º, and ends the power phase at bottom dead center having extended to about 35º of flexion. Much of the literature surrounding lower extremity kinematics during cycling have reported the two-dimensional sagittal plane motions (flexion/extension) of the knee. It has been suggested (Asplund and St Pierre, 2004; Burke, 1986) however, that movements critical to joint safety occur in all 3 cardinal planes of motion, and therefore examination of joint kinematics in the frontal and transverse planes merit inclusion in this review. For sake of clarity and relationship to the current research, only sagittal and frontal plane knee kinematics and kinetics will be discussed in this review.

Sagittal Plane Knee Kinematics of Cycling

Previous research of knee joint range of motion (ROM) in the sagittal plane shows general patterns, albeit the specific ranges of motion differ. To illustrate knee joint ROM in the sagittal plane during cycling, Ericson et al. (Ercison et al., 1988; Ericson, 1986) showed that during normal cycling, defined as cycling at 120 Watt (W) workrate and pedal cadence of 60 revolutions per minute (RPM) with a seat height of 113% the distance from the ischial tuberosity to the medial malleolus, mean knee flexion ROM was 66º (46º-112º knee flexion). Two decades later, Bini et al. (2010) found comparable knee ROM, 65º, while investigating knee kinematics during cycling at 80% of the subjects maximum power output with a self-selected pedal cadence and a saddle height of 100% the distance from the greater trochanter to the floor.

Other studies, however, have found differing mean knee ROM while cycling when manipulating factors such as cadence, workload, or bike fit. While performing 30-second Wingate test, Too and Landwer (2000) reported a mean knee ROM of 74º ± 6º with a saddle height of 109% the distance of the pubic symphysis to the floor. The authors further reported changes in knee joint ROM as crank arm length was manipulated. As the crank arm length was increased between 110 mm and 265 mm, knee joint range of motion was shown to increase from 67 ± 13.9º to 102 ± 4.0º (Too and Landwer, 2000). Fang et al. (2016) reported a mean knee ROM of 77.4º when increasing the workload from 0.5 kg to 1.0 kg at a constant 60 RPM pedal cadence (Fang et al., 2016). It was also reported that there was no significant effect on sagittal plane knee ROM when cycling at a workload of 1 kg and increasing cadences (60, 70, 80, and 90 RPM) (Fang et al., 2016).

Frontal Plane Knee Kinematics of Cycling

Previous research has reported frontal plane knee ROM of 3-10°; from about 2º-4º of abduction to about 1º-6º of adduction during the crank cycle (Bailey et al., 2003; Fang et al., 2016; Umberger and Martin, 2001). Bailey et al. (2003) investigated frontal plane knee kinematics during cycling, in addition to sagittal plane kinematics at a power output of 200 W with a cadence of 90 RPM. In this study, each participant rode their own cycle which was mounted to a stationary cycle trainer. Under these conditions a narrower frontal plane ROM of 3º (º adduction – 2º abduction) was observed. They further reported that the maximum knee abduction angle occurred between 90 and 200º of the crank cycle, and the maximum adduction angle occurred between 300 and 360º of the crank cycle

(Bailey et al., 2003). Gardner et al. (2016) found a peak knee adduction angle of 2.2º at a power output of 80 W and 60 RPM while participants cycled on an cycle ergometer. Fang et al. (2016) reported frontal plane knee ROM of nearly 10º (6.0º adduction – 3.9º abduction) with a workload of 1 kg a and cadence of 90 RPM while participants cycled on a cycle ergometer.

Sagittal Plane Knee Kinetics of Cycling

Much like kinematics, the lower extremity kinetics of cycling has been studied by many researchers (Ericson et al., 1986; Fang et al., 2016; Gardner et al., 2016; Gregor et al., 1985; Neptune and Hull, 1998; Too and Landwer, 2000). Knee joint kinetics have been shown to be far more sensitive to changes to, workload, seat height, and cadence (Bini and Diefenthaeler, 2010), and these differences have led to discrepant results among studies.

Broker (2003) demonstrated that during the power stoke of the pedal cycle (0 to 180º) the hip, knee, and ankle predominantly generate extensor moments. That is, the extensor muscles associated with these joints act to forcefully extend these joints as the pedal descends. About the knee joint specifically, Broker (1990) showed that the magnitude of the peak knee extensor moment is greater than the peak moments at the hip or ankle, reaching a peak extensor torque of about 40 Nm (at 250 W and 90 RPM). This peak knee extensor moment was seen at approximately 90º of the crank cycle and soon switched to a flexor moment around 125º of the pedal cycle, well before the knee is fully extended. This mechanism of transition from extensor to flexor moment prior to bottom

dead center of the pedal stroke serves to redirect pedal loading from inferior to posterior promoting a more effective pedal loading orientation.

Neptune and Hull (1998) compared sagittal plane kinetics and kinematics among 6 male competitive cyclists. Each participant cycled for 2 minutes at a constant workload of 225 W at 90 RPM. The results of this study indicated both peak knee extensor (power phase) and flexor moments (recovery phase) to be around 30 Nm (Neptune and Hull, 1998). Ericson et al. (1986) studied sagittal plane knee joint loading during ergometer cycling at 60 RPM, at a workload of 120 W, and a saddle height of 113% the distance between the ischial tuberosity and medial malleolus. In this study, the peak knee extensor moment was reported as 28.8 Nm with the peak knee flexor moment reported at 11.9 Nm. Gregor et al. (1985) investigated sagittal plane knee kinematics using only 5 recreational cyclists where power output was held constant at 160 W at a cadence of 60 RPM. The peak knee extension moment of this study was reported at 53 Nm with a peak knee flexion moment of 34 Nm. Given that these reported moments are not normalized to body mass (Nm/kg), the discrepancy of the above reported extensor and flexor moments may be a result of the sensitivity of sagittal plane knee joint kinetics to the adjustment of seat height, workload, and cadence.

Frontal Plane Knee Kinetics of Cycling

There are a limited number of studies that examine frontal plane knee kinetics in cycling. Up to this point, these studies have used an instrumented bicycle pedal and an inverse dynamics approach to estimate lower extremity joint moments. Early studies used bicycle pedals which were instrumented with only one force sensor (Ericson et al., 1984;

Gregersen and Hull, 2003a; Ruby et al., 1992). These types of pedals cannot measure the frontal plane and sagittal plane center of pressure (COP) displacement in that two sensors are needed, and therefore the calculated kinetic variables, such as knee frontal-plane moment, are less accurate than a pedal instrumented with two sensors. More recent studies (Fang et al., 2016; Gardner et al., 2016; Shen et al., 2018) have utilized bicycle pedals instrumented with two sensors.

In a study by Ruby et al. (1992), participants cycled at 90 RPM and 225 W with the right pedal instrumented with one force sensor. The authors modeled the lower extremity with a bar linkage model and calculated the three-dimensional (3D) knee joint loads using inverse dynamics. They reported KAbM of 15.3 Nm and peak knee adduction moment of 11.2 Nm. Gregersen and Hull (2003a) also used 3D inverse dynamics to calculate the frontal plane knee load of the right leg using a bicycle pedal instrumented with one force sensor. Participants pedaled at a workrate of 225 W at 90 RPM, and the peak external knee adduction moment (KAbM) was 7.8 Nm during the power stroke (defined as the crank angle between 306-119º) and peak knee abduction moment was 8.1 Nm during the recovery stroke. It is important to point out, though, that these reported joint moments were highly variable from subject to subject. Ericson et al. (1984) studied frontal plane knee kinetics while subjects cycled at 120 W and 60 RPM. They reported the external peak knee adduction moment to be 25.4 Nm and the external knee abduction moment to be 2.9 Nm.

More recently, Gardner et al. (2016) examined frontal plane knee loading in eleven healthy participants while cycling at a power output of 80 W and 60 RPM. They

reported a mean peak internal knee abduction moment of 9.0 Nm. Similarly, Fang et al. (2016) reported the mean peak internal knee adduction moment of 7.0 Nm and the mean internal knee abduction moment was 7.8 Nm while cycling at a workload of 1kg at an RPM between 60 and 90. Finally, while examining the effects of varus knee alignment on frontal plane kinetics during cycling, Shen et al. (Shen et al., 2018) reported a mean peak internal knee adduction moment of 7.2 Nm which is consistent with the more recent studies that utilized a two-sensor instrumented bicycle pedal.

As demonstrated above, the kinetic results that have been reported in the literature are highly variable. There may be several factors that contribute to the variation of reported frontal plane knee kinetics. First, both cadence and particularly workload differed among studies. Fang et al. (2016) demonstrated the effect that increasing workload at a constant cadence can have to frontal plane knee loading, which may have shed some light as to the variance of reported kinetic variables from previous studies. Second, even when cadence and workload were held constant, differences in frontal-plane knee joint kinetics existed (Gregersen and Hull, 2003a; Ruby et al., 1992) and may likely be attributed to differences in saddle height or depth which was unstandardized in the above-mentioned studies. Finally, as previously discussed, the use of a bicycle pedal instrumented with one sensor compared to a pedal that was instrumented with two sensors may be a source of discrepancy in the results between studies.

In summary, it appears that the knee kinetic variables of the lower extremity during cycling are far more sensitive to cadence, workload, and posture than the knee kinematic variables. Furthermore, studies used different instrumented bicycle pedals to

measure and calculate these kinetic variables. As a result, there has been discrepancies reported. It is therefore important to relate cycling posture, cadence, and workload to frontal plane kinetic variables when interpreting the results from cycling studies. Of the studies that utilized a two-sensor instrumented bicycle pedal, the mean peak internal knee abduction moment ranged from 7.2 Nm to 9.0 Nm with the mean peak internal knee adduction moment of 7.0 Nm.

Effects of cycling Workload on knee biomechanics

Kinematics

Research has shown that the manipulation of cycling workload does not have a significant effect on lower extremity kinematics. Bini et al. (2010), investigated the influence that changing workload would have on sagittal plane knee ROM and peak knee angles. The participants rode at two cadences (40 and 70 RPM), three saddle heights (reference height at 100% of trochanteric height; high, +3 cm; low, -3 cm), and three workloads (0, 5, and 10 N of braking force) under all conditions. Both the peak knee extension angle or ROM were unaffected as workload increased. Ediline et al. (2004), reported sagittal plane knee kinematics while cycling at 90 RPM and with a starting workrate of 100 W, with an increase of workrate of 50 W every three minutes. They reported no difference in knee ROM when cycling at different work rates. They reported peak knee flexion angle to be 71º, peak knee extension angle of 138º and knee flexion ROM to be 67º under all conditions.

One study, however, did report a significant change of peak knee angle under different work rates. Ericson et al. (1988) used work rates of 0, 120, and 240 W at

cadences of 40, 60, 80, and 100 RPM. The results showed that the maximum knee extension angle was significantly decreased from 49º to 42º with increased work rate. The maximum knee flexion angle and mean knee flexion ROM were, however, not affected, which supported findings of the other studies (Bini and Diefenthaeler, 2010; Edeline et al., 2004). In support of Ericson's findings, Fang et al. (2016) showed that the cycling workload significantly increased the knee extension and knee abduction ROM by 3.1° and 1.3° respectively. In this study participants pedaled at five workload conditions (0.5, 1.0, 1.5, 2.0, 2.5 kg) at a constant 60 RPM.

Kinetics

Previous studies have shown a direct relationship between knee moments and cycling work rate. Ericson et al. (1986) asked participants to cycle at work rates of 0, 120, and 240 W with incremental increases in cadence. They reported the external knee flexion moment to be influenced the most, increasing from 9 to 50 Nm, with increased work rate.

Mornieux and Guenette (2007) studied the effect of work rate on of the kinetics of each lower extremity joint. The participants of this study pedaled at 80 RPM with power outputs of 150, 250, and 350 W. As the workrate increased, the total net moment generated at the lower extremity joints increased from 86.0 Nm to 152.0 Nm. With this increase in work rate, the knee joint's contribution to the net moment decreased significantly from 30% to 25%.

Changes to knee the knee joint compressive contact force with respect to workload tend to follow similar patterns where an increase in cycling workload may

produce significant changes in knee joint compressive contact forces. In a study by Ericson et al. (1986), participants pedaled at 60 RPM with workloads of 0, 2 and 4 kg. Calculation of the tibiofemoral joint forces were performed using an inverse dynamics model of the knee. Significant increases were observed for the peak tibiofemoral compressive force and the peak anterior tibiofemoral shear force. Similarly, Kutzner (2012) used an instrumented knee implant to measure tibiofemoral contact forces. Subjects pedaled at 60 RPM and power output levels were set at 50, 75, 95, and 120 W. The cycle ergometer saddle was positioned at the standard seat height, adjusted to each subject such that the shoe sole of the outstretched leg was approximately 2 cm below the pedal. Peak knee resultant contact forces were measured to be 0.65, 0.96, 1.18, and 1.31 body weight (BW), respectively. When cycling at 40 RPM, the peak knee resultant force significantly increased from 0.5 to 1.63 BW as the power increased from 25 to 95 W. The authors reported a significant correlation between peak knee force magnitude and pedal power. The authors furthermore reported a mean compressive knee force, while pedaling at 60 RPM and 120W of 1.31 BW. On average, they reported the measured knee contact forces between 13 and 20% higher than those reported previously by Ericson and Nisell (1986). The differences among studies may be attributed to the models used to measure/calculate knee forces. Ericson and Nisell did not account for muscle cocontraction in their inversed dynamics-based knee model, and subsequently, their calculated compressive forces should be regarded minimum values.

Fang et al. (2016) reported that workload had a significant effect on frontal plane knee joint kinetics. The knee extension moment increased from 11.6 to 37.2 Nm and

KAbM increased from 5.8 to 14.4 Nm as the workload increased from 0.5 to 2.5 kg at a cycling cadence of 60 RPM.

Effects of cycling Cadence on knee biomechanics

Kinematics

In the late 1980's, Ericson and his colleagues studied the effects of manipulating many variables of cycling, as shown earlier (Ercison et al., 1988; Ericson, 1986; Ericson et al., 1984; Ericson et al., 1986; Ericson and Nisell, 1986). While studying the effects of changing cadence on kinematic variables (1988), participants were asked to pedal at a constant workload of 2 kg with increasing cadences of 40, 60, 80, and 100 RPM. Furthermore, as was discussed earlier, participants were asked to pedal at a constant 60 RPM with increasing workloads of 0, 2, and 4 kg. Although knee ROM was shown to decrease with increasing workload, knee ROM was shown to not be influenced by the change of cadence.

In 2010, Bini et al. (2010) performed a study that examined changes of knee kinematics as a result of changes to cycling cadence. Participants cycled at cadences of 40 and 70 RPM at three workloads of 0, 5, and 10 N. They found that mean knee angles and knee ROM were not affected by cadence in any condition. Additionally, Fang et al. (2016) reported that cycling cadence had a significant but small effect on the frontal plane knee abduction ROM as cadence increased from 60 to 90 RPM.

Kinetics

Previous literature has shown that changes in pedaling cadence do not affect knee joint kinematics while cycling (Bini, 2010; D'Lima et al., 2008; Ericson and Nisell,

1986). Ericson and Nisell (1986) had participants pedal at cadences of 60, 80, 100 and 120 RPM with 2 kg workload. Neither the peak tibiofemoral compressive force nor the peak anterior tibiofemoral shear force was affected by changing cadence. Using a total knee replacement instrumented with strain gauges, D'Lima et al. (2008) asked subjects to pedal at 60, 70, 80, and 90 RPM. They reported the peak knee compressive force to be about 1.03 BW and the anterior tibiofemoral shear force was about 0.21 BW for all conditions. In the study by Bini et al. (2010) subjects cycled with a free chosen cadence (FCC), a cadence 20% higher than FCC (FCC + 20%), and a cadence 20% lower than FCC (FCC – 20%). Workload was held constant during the different cadence trials at either 60% (3.05 ±0.27 $W*kg^{-1}$) or 80% (4.06 ± 0.36 $W*kg^{-1}$) of the peak power output of each participant. The knee joint reaction forces at the knee, derived by an inverse dynamics approach, was not different between conditions. The knee joint resultant forces at FCC - 20%, FCC, and FCC + 20% were 106.6 N (0.15 BW), 107.8 N (0.15 BW), and 90.3 N (0.13 BW), respectively.

In summary, most studies have found that knee joint kinematics are hardly influenced by changes in cycling cadence and workload, yet, noteworthy differences have been seen for knee joint kinetics.

Effects of Saddle Height and Fore/Aft position on knee biomechanics

Saddle height and depth are modifiable variables directly related to cycling posture. Probably the most influential factor in cycling performance is the saddle height, and over the years there have been many methods developed to find the optimal saddle height (Wozniak Timmer, 1991). Adjusting the saddle height and/or saddle fore/aft

position changes the joint angles and ranges of motion of the lower extremity, which may be related to potential risk for injury. This, in turn, can change the load that the knee joint experiences during the pedal cycle.

Previous studies have identified several ways to determine saddle height. An early study by Hamley and Thomas (1967) suggested that the optimal seat position was located at 109% of the distance from pubic symphysis height to the floor with cycling shoes on. Similarly, Greg Lemond, a three time Tour de France winner, recommended multiplying the pubic symphysis height by 88.3% to determine the seat height from the center of the bottom bracket to the top of the saddle (Broker, 2003). In 1977, Nordeen-Snyder (1976) found that oxygen consumption was the most efficient at a saddle height of 100% of trochanteric height.

From a biomechanical perspective, only a few studies have focused on the effects that saddle height has on the knee joint biomechanics while pedaling (Bini, 2011; Bini, 2010; Ercison et al., 1988; Holmes et al., 1994; Tamborindeguy and Bini, 2011). In a review of literature, Bini et al. (2011) stated that the limited number of articles surrounding the effects of saddle height on lower extremity, especially knee joint, biomechanics and injury prevention during cycling leads to inconclusive results. They recommend that, in consideration of cycling economy (Peveler, 2008), injury prevention, and knee joint loading (de Vey Mestdagh, 1998), the Holmes method (Holmes et al., 1994) should be used for determining saddle height; a saddle height that produces 25-30º of knee flexion at bottom dead center.

In a study by Bini et al. (2010), the effects of saddle height were demonstrated by the change in contribution to total mechanical work by the ankle, knee and hip joints at a saddle height of 100% trochanteric height as well as ± 3cm from 100% trochanteric height. They reported an inverse relationship between saddle height and the total mechanical work contribution of the knee joint. In fact, when the saddle height was lowered 3 cm from the reference height, increased mechanical work (which may be related to higher quadriceps force (Ericson, 1988)) was seen. This study was in agreement with work done by Ericson et al. (1987) who examined the effect that three different saddle heights (102, 113, and 120% of the distance between the ischial tuberosity and the medial malleolus) had on sagittal plane knee joint kinetics. They observed increased peak patellofemoral compressive forces as saddle height was decreased.

The seat tube angle is defined as the angle that is formed between the seat tube and the level horizon. Conventional manufacturer standard seat tube angles for standard road bicycles are approximately 74º (Price and Donne, 1997). A larger seat tube angle (> 74º) allows the ride to sit more forward on the saddle (without further adjustment to the fore/aft position of the seat). A shallower seat tube angle (< 74º) provides the opposite effect. It has been shown by Price and Donne (1997) as well as Umberger et al. (1998) that a greater seat tube angle and/or saddle fore position can increase the hip extension angle as well as the ankle ROM. These two studies reported no kinematic changes at the knee joint with respect to seat tube angle or saddle fore/aft position. Saddle fore/aft position, sometimes referred to as saddle depth, can serve similar function to the seat tube

angle in determining the fore/aft position of the cyclist on the bicycle. The recommendation of Burke and Pruitt (Broker, 2003; Burke and Pruitt, 2003) is that, through combination of the seat tube angle and the saddle fore/aft position, the anterior aspect of the patella be positioned directly in line with the axis of rotation of the pedal spindle with the crank is in the forward horizontal (90º) position.

Instrumented Pedal Design and Force Measurement

Bicycle pedals represent two of the five contact points between the body and the bicycle (two pedals, one saddle, two handlebars). The pedals are the primary location of the energy transfer between the rider and the bicycle, and as has been discussed previously, pedal loading directly impacts how the lower extremity moves and is stressed during cycling (Broker, 2003).

Instrumented bicycle pedals offer the ability to study the kinetic exchange between the rider and the bicycle. Since first introduced into the scientific literature in 1896 by Archibald Sharp (Sharp, 1896), many modern-day designs of instrumented pedals have since evolved, each with distinct advantages, and all with common limitations. Generally, there are three designs of instrumented bicycle pedals: pedal-body strain gauge (Álvarez and Vinyolas, 1996; Reiser, 2001; Rowe et al., 1998), piezoelectric (Ericson et al., 1984; Fang et al., 2016; Gardner et al., 2016; Gregersen and Hull, 2003a; Ruby et al., 1992; Shen et al., 2018), and fixed-shaft strain gauges.

Pedal-body instrumented pedal designs measure pedal loading via strain gauges within the pedal body. These strain gauges can measure normal and tangential forces applied to the pedal body. Piezoelectric designs contain one (Ericson et al., 1984;

Gregersen and Hull, 2003a; Ruby et al., 1992) or two (Fang et al., 2016; Gardner et al., 2016; Shen et al., 2018) piezoelectric transducers between two rigid plates. In addition to the normal and tangential forces, these instrumented pedals allow for the determination of the location of the applied load in the mediolateral plane as well as the torque applied about all three cardinal planes. Fixed-shaft designs measure pedal loading at the pedal spindle shaft. Due the intricate installment of the strain gauge at the pedal-crank arm interface, these designs are unsuitable for high loads and currently do not identify medial-lateral loading pattern (Álvarez and Vinyolas, 1996; Reiser, 2001; Rowe et al., 1998). According to Broker (Broker, 2003), piezoelectric sensors have the advantage over strain gauge sensors in part because they allow for a greater measurement range over which the loads placed on the pedal, simpler calibration capabilities, and minimal cross-sensitivity, meaning that the loads applied in one axis do not affect the measurement of loads applied in other axes.

Although current instrumented bicycle pedals provide meaningful information about pedal reaction forces allow computation of lower extremity kinetics, it is worth noting a few limitations of these common designs. First, no instrumented pedal designs have wireless data transmission capabilities. This means that there are necessary wires that transmit force data from the pedal to a nearby computer. These wires are often free hanging or attached to the rider. Understandably, this creates an unrealistic cycling environment for a rider and may confound obtained results. Second, these instrumented pedals are considerably bulkier than traditional bicycle pedals. With the piezoelectric design, for example, two sensors are fixed between two rigid plates. This increased size,

as compared to traditional bicycle pedals, renders the pedals poorly suited for non-laboratory work.

Q-Factor

Relatively unexplored in the scientific literature, the QF refers to the horizontal width between pedals (Disley and Li, 2014a). This mediolateral distance is sometimes referred to as 'tread' and is measured from the outside face of the crank arm/pedal attachment to the outside face of the contralateral crank arm/pedal attachment (Disley and Li, 2014a). The term 'Q-Factor' was coined in the 1990's by Grant Pedersen, short for 'Quack Factor', in that alteration to the mediolateral distance between pedals can make a cyclist appear to waddle like a duck as the pedal their bicycle (Disley and Li, 2014a). This rather comical nomenclature has nevertheless been adopted in mainstream cycling vocabulary describing the mediolateral distance between pedals.

Generally, QFs range from ~150 mm on a road bike to ~180 mm on a mountain bike, with no mass-produced bicycle having a QF lower than 135 mm (Disley and Li, 2014a). QF size is largely determined by frame clearance. Mountain bikes, for instance, often employ a triple chainring system at the bottom bracket, thus reducing frame clearance. Newer bottom bracket designs on road bikes allow for narrower QFs by reducing frame clearance. This is accomplished by housing proprietary bearing sets within the frame coupled with a compatible crankset. Even with current manufacturer designs, many bicycles would be able to support QFs lower that 150 mm. For cycle ergometers often employed in exercise testing (Beekley et al., 2004), exercise (Poole et al., 1990), or rehabilitation (Lacasse et al., 1996; Liebs et al., 2010), QFs can range from

~150 mm (Lode Excalibur Sport) to approaching ~200 mm (170 mm for the Peloton Bike, 194 mm for the Monark 818e).

Despite the depth of scientific literature surrounding manipulation of the modern components the bicycle, only a handful of studies have examined the impact of QF manipulation on biomechanical and physiological variables.

Gross Mechanical Efficiency

Disley and Li (2014a) hypothesized that narrowing a QF would result in lower oxygen consumption – for a given power output – and thus an increase in gross mechanical efficiency (GME) defined by using the ratio of mechanical work accomplished in kcal/min to energy expended in kcal/min during the final 120 seconds of each cycling stage (Disley and Li, 2014a). Furthermore, they hypothesized that the level of muscular activation of major muscles involved in the pedal stroke would decrease with narrower QFs. Rationale for this study stems from bipedal walking where it has been shown that the metabolic cost of walking decreases at lower SW (Donelan and Kram, 2001). In the twenty-four trained cyclists studied, a reduction in QF resulted in an increase of GME, while the level and timing of muscular activation was unchanged in the lower extremity muscles studied. It was observed that the GME for Q90 (QF of 90mm) and Q120, when compared to the standard Q150 and large Q180, were significantly higher ($P < 0.006$). There was no significant difference between Q90 and Q120 nor was there a difference between Q150 and Q180. Moving the pedals closer to the midline of the bicycle may increase the efficiency of force transfer at the pedal by reducing tangential force during the pedal stroke (Disley and Li, 2014a).

Self-Selected Q-Factor

Having shown that a narrower QF is more efficient at submaximal workloads, Disley et al. (2014b) devised a study to explore how cyclists would self-select foot position; both in terms of pedal angle and QF. Although aspects of this study examined the self-selection of pedal angle with and without commercial cleat systems, the focus of the inclusion in this review will be the effects of a self-selected QF.

Experimental testing was performed on a custom-made bicycle with custom floating pedals (Disley and Li, 2014b). The floating pedals permitted lateral adjustments of the pedal along the pedal axle as well as rotational freedom of the pedal footplate. Participants were asked to pedal in four different conditions: the fixed condition - permitting no movement of the pedal, the lateral condition - permitting lateral movement of the pedal along the pedal axle while restricting rotational movement of the pedal footplate, the rotation condition - permitting rotational movement of the pedal footplate but restricted lateral movement, and the free condition - permitted both lateral and rotational movement. Participants of this study, all of whom were accustomed to cycling, were divided in to two groups. The 12 cyclists that had the highest knee variability in the free condition were grouped in to the unstable (UST) group, and the 12 cyclists that had the lowest knee variability were grouped in the stable (ST) group. Among the two groups of cyclists included in this study, there was no main effect of group on self-selected QF during the lateral condition but there was small yet significant difference during the free condition between groups (ST=137±16.8mm, UST=152.6±18.9mm, $F(1,1)=4.343$, $p=0.49$, $eta2 =0.165$).

Given an unrestricted pedal range of motion, ST cyclists chose a narrower QF than UST cyclists (137mm vs. 153mm). Previous research may validate this finding, showing that more coordinated cyclists choose a lower QF, 137 mm, that falls within the range of the more mechanically efficient QFs of <150mm (Disley and Li, 2014a). What is yet unclear from this study is how efficient untrained cyclists are at QFs closer to 150mm.

Bike Fit

Disley (Disley and Li, 2014b) postulated that any self-selection of the suspended position on the bicycle for comfort or injury prevention should be based upon the action of bipedal walking (Disley and Li, 2014b). Rationale for this claim stems from the understanding that the bicycle was designed to use the natural locomotive ability of the human body to provide assisted forward motion. In this study, the aims included determining if a self-selected QF would decrease knee variability and improve efficiency as well as whether self-selected QF can be predicted off the bike (Disley and Li, 2014b). The authors hypothesized that the use of self-selected QF would decrease knee variability and increase GME and that self-selected QF can be predicted using suspension and locomotion tasks.

To determine self-selected QF, participants cycled on an adjustable cycle ergometer equipped with the previously mentioned floating pedals (Disley and Li, 2014a). To estimate the self-selected QF of the participants while off the bike, participants were required to complete two tasks. To predict self-selected QF from a locomotion task, participants walked 6 m barefoot before stepping onto a box 15 cm high.

The second task required participants to suspend themselves for a period of time greater than 5 seconds off of the ground in gymnastics support position (using parallel bars, feet off of the floor, using only straight extended arms to support body weight). Hanging intermalleolar distance was measured as the distance between left and right medial malleoli. Participants then pedaled at different QFs: self-selected QF (SSQ), determined by using custom built floating pedals (Disley and Li, 2014b), SSQ-30 mm, SSQ+30 mm and 150 mm.

No significant differences were found between GME or knee variability (calculated as the standard deviation of the lateral movement of the femoral epicondyle marker along the frontal plane). Mean SSQ was reported as 142 ± 12 mm. Good correlation was found between SSQ (142mm) and knee variability ($R^2 = 0.938$) and at QFs ±30 mm from SSQ knee variability increased with a concurrent decrease of GME. A strong correlation was found between hanging intermalleolar distance and SSQ (R^2=0.794). The walking step test resulted in a SW that had poor correlation with SSQ ($R^2 = 0.091$).

Examination of the QFs of the different cycle ergometers used in the previously mentioned studies by Gardner et al. (Gardner et al., 2016; Gardner et al., 2015) and Fang et al. (2016) may provide insight to the anticipated kinetic response of increasing QF for young, healthy, recreationally active adults. The QF on the cycle ergometer of Gardner's studies was measured at 150 mm (Excalibur Sport, Lode, Groningen, Netherlands). With the addition of 5° and 10° lateral shoe wedges, all participants exhibited KAbM (Gardner et al., 2016). With the introduction of 5° and 10° toe in angles at the pedal, all

participants exhibited KAbM (Gardner et al., 2015). The QF on the cycle ergometer of Fang's study was measured at 194 mm (Model 818E, Monark, Varberg, Sweden). At this increased QF, seven of eighteen subjects exhibited KAbM at all workloads. Eleven of eighteen participants exhibited a knee adduction moment (KAdM) at all workloads (Fang et al., 2016). Comparison of these two cycling studies suggests that increasing QF – analogous to increasing SW in gait – may reduce KAbM, and even change the moment pattern to a knee adduction moment pattern.

Q-Factor Summary

In summary, most commercially available bicycles are manufactured with a QF of ~150 mm on a road bike to ~180 mm on a mountain bike. As the QF is brought closer to the midline of the bicycle, an increase of gross mechanical efficiency was shown in trained cyclists. Furthermore, it has been shown that trained cyclists, when given unrestricted free range of motion at the pedal, choose a narrower QF when compared to untrained cyclists. Finally, intermalleolar distance, measured during the gymnastics support position, showed a strong correlation to SSQ and can therefore be used to predict SSQ during or prior to a bicycle fit. Although these select studies examine the relationship between QF and cycling physiological response and kinematics, there have been no reported studies examining lower extremity kinetic response to changes in QF. The reported frontal plane knee moment patterns between related cycling studies, with cycle ergometers of differing QFs, may suggest that peak KAbM may decrease as QF increases.

CHAPTER III
METHODS

Participants

For this study, healthy weight ($19.0 \leq BMI \leq 24.9$ kg/m^2), recreationally active adults (18-40 years) were recruited through email, posted flyers, and word of mouth. Recreationally active was defined as engaging in moderate to vigorous activity 3 days or more per week for a total of ≥ 150 min·wk (Garber et al., 2011) with less than three hours per week cycling in any form. All participants were free from lower extremity injury within the past six months and were able to ride a stationary bike without assistance. All participants completed a physical activity readiness questionnaire (PAR-Q) (American College of Sports Medicine, 1995) and signed an informed consent document approved by the Institutional Review Board of the University of Tennessee, Knoxville.

An *a priori* power analysis, using results from previous research (Fang et al., 2016; Gardner et al., 2016; Shen et al., 2018) indicated that a total of 6-16 participants were needed for an *alpha* of 0.05 and a *beta* of 0.80. Variables used in the power analysis included peak KAbM, knee extension moment and knee adduction/flexion/extension angles during the power phase of the pedal cycle.

Instrumentation

Motion Capture

A twelve-camera motion analysis system (240Hz, Vicon Motion Analysis Inc., Oxford, UK) was used for three-dimensional (3D) kinematic data collection. Participants wore tight-fitting spandex shorts, a t-shirt, and neutral running shoes (AIRMAX, Nike,

USA). Retroreflective anatomical markers were placed bilaterally on the acromion process, iliac crest, greater trochanter of the femur, medal and lateral epicondyles of the femur, medial malleolus of the tibia, lateral malleolus of the fibula, lateral aspect of the head of the 5th metatarsal, medial aspect of the head of the 1st metatarsal, and the distal end of the 2nd toe. A semi-rigid thermoplastic shell with four retroreflective tracking markers was placed on the posterolateral aspect of both shanks and thighs, as well as on the posterior trunk. Two additional shells, each with two tracking markers, were placed on the posterior-lateral aspect of the pelvis and four individual retroreflective tracking markers were affixed to the mid to lateral aspect of the heel counter of each shoe.

Cycle Ergometer

A Lode cycle ergometer (Excalibur Sport, Lode, Groningen, Netherlands), was used for cycling data collection. The ergometer is electro-mechanically braked, which allows for precise control of work rate, independent of pedal cadence. The ergometer had an adjustable saddle and handlebars to allow a specific bike fit for each participant.

Instrumented Bike Pedals

Two customized instrumented bike pedals were used to collect pedal reaction forces (PRF) on the Lode cycle ergometer. Each pedal assembly contained two 3D force sensors (Type 9027C, Winterthur, Kistler, Switzerland) coupled with two industrial charge amplifiers (Type 5073A, Kistler, Winterthur, Switzerland). The coordinate system for the pedal is shown in Figure 2 (Gardner, 2013). The charge amplifiers were necessary to convert the analog charge measured by the force sensors to a voltage value used by the Vicon Nexus software. A custom jig was built and secured to two holes in a floor-

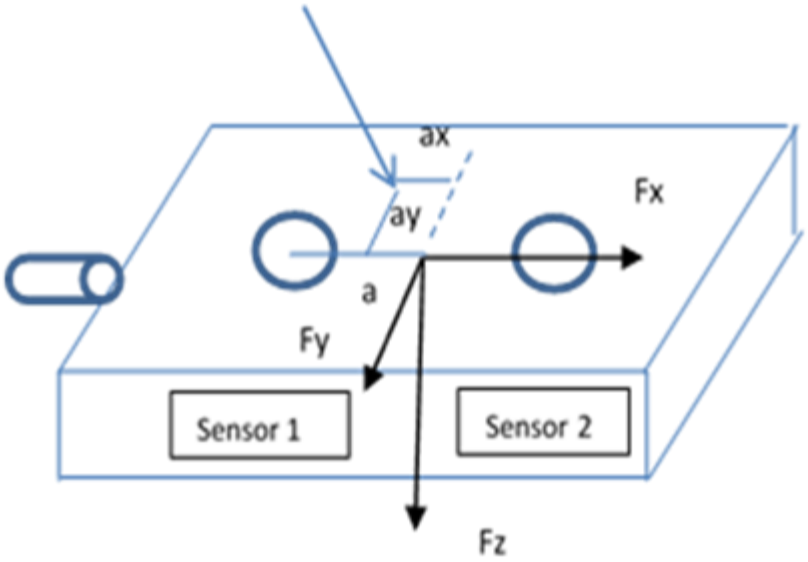


Figure 2. The local coordinate system and arrangement of the two force sensors on the right instrumented pedal.

mounted force plate to ensure that the cycle ergometer was aligned with the antereoposterior and mediolateral axes of the lab global coordinate system. Prior to using the pedal assemblies, extensive calibration testing was done to ensure that the pedal measurements were accurate. The 3D pedal reaction forces from the instrumented pedals and 3D kinematics were recorded through the Vicon Nexus system simultaneously.

Q-Factor

QF was increased using three pairs of Sunlite Pedal Extenders (Sunlite, Booklyn, NY). Each single pedal extender increased the unilateral QF by 21 mm, such that a pair (1 on the left pedal and 1 on the right pedal) increased the total QF by 42 mm.

Experimental Procedures

Upon arrival to the biomechanics laboratory, participant height was measured with a physician's scale. Once the anatomic and tracking markers were placed, a static

trial was collected and participant weight was recorded. A body mass index (BMI) score (kg/m^2) was calculated for each participant.

The cycle ergometer was then fit to the specification of each participant. The saddle height on the cycle ergometer was set in accordance with the Holmes method (Holmes et al., 1994), such that the angle of the participant's knee was between 25-30° knee flexion, verified with a handheld goniometer, when the crank was set at bottom dead center. The saddle fore/aft position was set such that the participant's knee was in line with the pedal spindle when the crank was in the forward horizontal (90°) position (Burke and Pruitt, 2003). Each participant's trunk angle was determined by adjusting the handlebars such that a 90° angle was created, again verified with a handheld goniometer, between the midline of the femur and a line connecting the greater trochanter of the femur to the acromion process of the scapula with the pedal at bottom dead center (Fang et al., 2016; Gardner et al., 2016; Shen et al., 2018). Handlebar height was set at a comfortable position for the participant such that the top of the handlebars were positioned approximately 5-8 cm below the top of the saddle, depending on the flexibility and comfort of the participant (Silberman et al., 2005). Handlebar fore/aft position was determined such that while the participant was in a comfortable position with the hands on the handlebars, looking straight ahead, a plumb bob dropped from the tip of the nose of the participant intersected the handlebar stem of the cycle ergometer (Asplund et al., 2005; Burke, 1994).

Participants performed a two-minute warm-up on the cycle ergometer at a QF of 150 mm, a workrate of 80 W, and at a self-selected cadence. A minimum of a two-minute

rest period was given between the warm-up and commencement of testing. The participants performed in a total of 12 testing conditions, pedaling for two minutes at workloads of 80, 120, and 160 W while maintaining a constant cadence of 80 RPM (Martin and Spirduso, 2001) in each of four QFs: QF of 150 mm, the manufactured QF of the stationary cycle ergometer (Q150), QF of 192 mm (Q192), QF of 234 mm (Q234), and QF of 276 mm (Q276). The range of workloads in this study was set to meet exercise recommendations of moderate to vigorous activity for young (20-39 yrs) adults by the American College of Sports Medicine (ACSM) for healthy young adults (Garber et al., 2011; Glass et al., 2007). For example, a 75-kg young adult cycling at 80 W and 80 RPM would be doing moderate activity (5.3 METs) whereas the same young adult cycling at 160 W would be doing vigorous activity (8.6 METs). The following equation was used to calculate METs with respect to workload (Glass et al., 2007; Thompson et al., 2013):

$$METs = (10.8 \times Workload\ (Watts) \div Body\ Mass\ (Kg) + 7) \div 3.5$$

All conditions were randomized first by QF, and then by workload. Data were collected on 5 consecutive pedal cycles beginning in the last 30 seconds of each test condition (Fang et al., 2016; Gardner et al., 2016; Shen et al., 2018). Following the conclusion of each QF condition, a two-minute rest period was given to each participant where they indicated their Rating of Perceived Exertion (RPE) with the Borg 6-20 scale (Borg, 1998), comfort, and knee pain via numeric visual analog scales while the next condition (QF or workload) was set. Participants were instructed to remain on the cycle ergometer during the rest period.

Data Treatment and Analysis

Before cycling data were collected the participant performed one static standing trial. The static trial consisted of the participants standing erect behind the cycle ergometer within the motion capture volume, with feet planted parallel at shoulder width on the ground, and arms crossed in front of their chest. Approximately one second of data were recorded while the participant stood motionless. The markers were then labeled. Once the model was built in the Nexus software, the anatomical markers were removed and tracking markers were left for data collection. During movement trials, the labeling template was then changed to a template that included only tracking markers. Following data collection, all dynamic trails were processed according to the appropriate (QF) static calibration trial in the Nexus software.

The marker coordinate data were processed in Vicon Nexus 2.6 (Vicon Motion Analysis Inc., Oxford, UK). Correct labeling of these data were checked for each trial. If any gaps in the marker coordinate data were found, those gaps were filled with either a rigid body fill or a pattern fill. If a minimum of the three other makers on the same shell were present throughout the gap the rigid body fill filled the gaps in the maker coordinate data by assuming a consistent trajectory of all four makers on the same shell. If, however, less than three makers on the same shell were missing during the selected gap, the pattern fill filled the gap relative to the trajectory of any of the selected visible markers during that gap.

Using the signals from the two force sensors, the PRF, moments, and center of pressure (COP) of the right pedal were calculated using the following equations:

$$F_x = F_{x1} + F_{x2} \quad (2)$$

$$F_y = F_{y1} + F_{y2} \quad (3)$$

$$F_z = F_{z1} + F_{z2} \quad (4)$$

$$M_x' = a_{z0} \times F_y \quad (5)$$

$$M_y' = (a \times F_{z1} - a \times F_{z2}) - a_{z0} \times F_x \quad (6)$$

$$M_z' = -a \times F_{y1} + a \times F_{y2} \quad (7)$$

$$a_x = \frac{-M_{y\prime}}{F_z} \quad (8)$$

$$a_y = \frac{M_{x\prime}}{F_z} \quad (9)$$

Where F_{x1}, F_{y1} and F_{z1} are the forces measured by Sensor 1 in the x, y, and z direction, respectively; F_{x2}, F_{y2} and F_{z2} are the forces measured by Sensor 2 in the x, y, and z direction, respectively; a is half the distance between two sensors, and a_{z0} is the distance from the sensors to the top of the pedal; F_x is the mediolateral pedal reaction force, F_y is the anteroposterior pedal reaction force, and F_z vertical pedal reaction force; M_x', M_y', M_z' are the moment at the top of the pedal about x-axis, y-axis, and z-axis, respectively; a_x and a_y are COP in the x and y direction, respectively (Figure 2).

The five consecutive pedal cycles at each condition were truncated in Vicon Nexus to obtain five individual trials for each condition. The data exported into Visual3D biomechanical analysis suite (Version 6, C-Motion, Inc., Germantown, MD, USA) to compute pedal reaction forces as well as lower extremity joint kinematics and kinetics. Angular computations were completed using a Cardan rotational sequence (X-Y-Z) and a right-hand rule to define angular kinematic and kinetic variable conventions. Positive

values indicated ankle dorsiflexion, inversion, and internal rotation, knee extension, adduction, and internal rotation, as well as hip flexion, adduction, and internal rotation angles and moments. Anthropometric data were estimated using Dempster model and Hanavan model (Dempster et al., 1959; Hanavan Jr, 1964). More specifically, segment circumferences and moment of inertia estimations used the Hanavan model, while segment weights as a percent of body weight used the Dempster model. Kinematic and pedal reaction force data were filtered using a zero lag, fourth-order Butterworth low-pass filter at 6 Hz (Gregersen and Hull, 2003b), with joint moment calculations expressed in the proximal segment's reference frame. Two customized computer programs (VB_V3D and VB_Table, version 6.0, MS Visual Basic) were used to determine discrete events of variables of interest and organized data from Visual3D outputs for subsequent statistical analysis. For kinetic and kinematic data, peak values were chosen during the power phase of the crank cycle. It should be noted that the moment variables were not normalized to any anthropometric features (i.e. body height or mass) as in cycling the majority of the body weight is supported by the cycle ergometer saddle and handlebars.

VB_V3D was used to identify points of interest during the pedal cycle. The variables of interests included peak knee angles and ranges of motion (ROM), as well as peak moments in the sagittal, frontal and transverse planes. To ensure accuracy and consistency, the researcher picked these discrete events for all trials. The selected variables were then organized and saved in a separate Excel file for each participant. The VB_Table program organized and computed mean values for each participant, with

variables organized into separate sheets of an Excel file. This program generated the global mean for each variable.

Statistical Analysis

The data were checked for normality using a Shapiro-Wilks test. A 3×4 (Workload × QF) repeated measures analysis of variance (ANOVA) was used to detect differences between workload and QF conditions (25.0 IBM SPSS, Chicago, IL). When an interaction was present, a pairwise t-test was performed in the post hoc analysis with Bonferroni adjustments to determine the location of the statistical differences between QF and workload. An alpha level of 0.05 was set a priori and adjusted for post hoc comparison such that such that workrate $\alpha < 0.017$, QF $\alpha < 0.008$, interaction $\alpha < 0.008$.

CHAPTER IV
THE EFFECTS OF INCREASED Q-FACTOR ON KNEE BIOMECHANICS DURING CYCILING

Abstract

Q-Factor (QF) in cycling, or the inter-pedal width, is the analog to step-width in gait. Increased step-width has been shown to reduce peak knee abduction moment (KabM), however no studies have examined the frontal plane biomechanics of increased QF in cycling. **Purpose:** The purpose of this study was to investigate the effects of increased QF on frontal plane knee biomechanics during cycling in healthy participants. **Method:** Sixteen healthy participants (age: 22.4 ± 2.6 yr, BMI: 22.78 ± 1.43 kg/m2) participated in this study. A motion analysis system and customized instrumented pedals were used to collect five trials of three-dimensional kinematic (240 Hz) and pedal reaction force (PRF, 1200 Hz) data in twelve testing conditions, four QF conditions of Q150 (150 mm), Q192 (192 mm), Q234 (342 mm), Q276 (276 mm), and three workrate conditions of 80 W, 120 W, and 160 W. A 3 × 4 (QF × workrate) repeated measures ANOVA was performed to analyze differences between conditions ($p < 0.05$). **Results:** Increased QF increased peak KAbM 47, 56, and 56% from Q150 to Q276 at each workrate respectively. Mediolateral PRF increased 46, 57, and 57% from Q150 to Q276 at each workrate. Frontal plane knee angle and range of motion (ROM) decreased with increased QF. No changes were observed for peak vertical PRF, knee extension moment, sagittal plane peak knee joint angles or ROM. **Conclusions:** These results indicate increasing QF will increase peak KAbM. Future studies should examine the effects of increased QF on obese and knee osteoarthritis patients.

Keywords: Cycling, Q-Factor, Knee Abduction Moment, Knee Osteoarthritis

1. Introduction

Cycling is a common form of recreation and is often prescribed as an exercise intervention for patients with knee osteoarthritis (OA) (Kutzner et al., 2012; Mangione et al., 1999), in part because great demand is placed on the knee joint muscles without any high impact loading to the lower extremity joints as in walking or running (Johnston, 2007; Kutzner et al., 2012). The peak internal knee abduction moment (KAbM) is a common surrogate variable for medial compartment knee loading during walking (Paquette et al., 2015; Paquette et al., 2014b; Schipplein and Andriacchi, 1991; Sharma et al., 1998; Yocum et al., 2018) and cycling (Fang et al., 2016; Gardner, 2013; Gardner et al., 2016; Shen et al., 2018). Increased step-width has been shown to reduce KAbM in level walking (Zhao et al., 2007)(Zhao 17, 18) as well as stair ascent (Bennett et al., 2017b; Paquette et al., 2015; Yocum et al., 2018), and stair descent (Paquette et al., 2014b; Yocum et al., 2018).

Relatively unexplored in the scientific literature, Q-Factor (QF) refers to the horizontal width between pedals (Disley and Li, 2014a). This mediolateral distance is sometimes referred to as 'tread' and is measured from the outside face of the crank arm where the pedal is inserted to the outside face of the opposite crank when it is positioned in the same plane (Disley and Li, 2014a). QF in cycling is analogous to step-width in gait. In normal walking, preferred step-width has been reported to be between 7-12 cm (Helbostad and Moe-Nilssen, 2003; Hollman et al., 2011; Wert et al., 2010), and between 13-17 cm in stair ascent (Paquette et al., 2015; Paquette et al., 2014b; Yocum et al., 2018), and 15-17 cm in stair descent (Paquette et al., 2014b; Yocum et al., 2018).

Generally, QFs range from ~150 mm on a road bike to ~180 mm on a mountain bike, with no mass-produced bicycle having a QF lower than 135 mm (Disley and Li, 2014a).

Recent research investigating frontal plane knee biomechanics during cycling suggested that increasing QF may change the frontal plane knee alignment, potentially decreasing KAbM during cycling. Gardner et al. (2016), using Lode cycle ergometer with a QF of 150 mm, reported mean KAbM of -9.00 Nm in healthy adults while cycling at 60 RPM and a workrate of 80 W. Fang et al. (2016), using a Monark cycle ergometer with a QF of 194 mm, reported seven of eighteen participants exhibiting KAbM of -5.82 Nm, while the remaining eleven exhibited peak knee adduction moment of 9.52 Nm during the power phase of the cycle, while cycling 60 RPM and workloads of 0.5, 1, 1.5, 2, and 2.5 kg. These differences suggest that increased QF between the two studies may have played a role in the different frontal plane knee moments. In a follow up study from our group examining the effects of knee alignment on frontal plane knee biomechanics, Shen et al. (2018), using a similar Monark cycle ergometer with the same QF of 192 mm, reported that eight of ten varus aligned participants exhibited KAbM during the power phase of the cycle as compared to eight of eleven neutral aligned and five of ten valgus aligned participants.

No studies have examined the effects of increased QF on knee joint kinetics during cycling. To our knowledge, only one prior dissertation has examined mechanical and metabolic efficiency among trained and recreational cyclists from the manipulation of QF (Disley and Li, 2014a, b). It is unknown that if an increase in QF will result in a change of peak KAbM. Therefore, the purpose of this study was to examine effects of

standard and increased QFs at different workrates on knee biomechanics of healthy-weight participants during stationary cycling. It was hypothesized that as QF increases, peak KAbM will be decrease, and as QF increases further, the frontal plane knee moment will become a knee adduction moment. Furthermore, it was hypothesized that as workrate increases, the increase in the frontal plane knee moment will be greater, and that as QF increases, peak knee extension moment will not change significantly.

2. Method

2.1 Participants

Sixteen recreationally active adults 18-35 years of age (8 male, 8 female age: 22.4 ± 2.6 yr, height: 1.74 ± 0.11 m, BMI: 22.78 ± 1.43 kg/m^2) participated in this study. Recreationally active was defined as engaging in moderate to vigorous activity 3 days or more per week for a total of ≥ 150 min·wk (Garber et al., 2011), with less than three hours per week cycling in any form. All participants were free from lower extremity injury within the past six months and were able to ride a stationary bike without assistance. An *a priori* power analysis for a repeated measures analysis of variance, using results from previous research (Fang et al., 2016; Gardner et al., 2016) indicated that a sample size of 16 participants were needed for an *alpha* of 0.05 and a *beta* of 0.80 with a conservative effect size of 0.25 (G*Power 3.1). All participants were asked to read and sign a Physical Activity Readiness Questionnaire (PAR-Q) (American College of Sports Medicine, 1995) and an informed consent document approved by the institutional review board.

2.2 Instrumentation

A twelve-camera motion analysis system (240Hz, Vicon Motion Analysis Inc., Oxford, UK) was used for three-dimensional (3D) kinematic data collection. Participants wore tight-fitting spandex shorts, a t-shirt, and neutral running shoes (AIRMAX, Nike, USA). Retroreflective anatomical markers were placed bilaterally on the acromion process, iliac crest, greater trochanter, medial and lateral epicondyles, medial malleolus, lateral malleolus, lateral aspect of the head of the 5th metatarsal, medial aspect of the head of the 1st metatarsal, and the distal end of the 2nd toe. A semi-rigid thermoplastic shell with four retroreflective tracking markers was placed on the posterolateral aspect of both shanks and thighs, as well as on the posterior trunk. Two additional shells, each with two tracking markers, were placed on the posterior-lateral aspect of the pelvis and four individual retroreflective tracking markers were affixed to the posterior and lateral aspect of the heel counter of each shoe.

Participants cycled on a Lode cycle ergometer (Excalibur Sport, Lode, Groningen, Netherlands). Saddle height was set at 25-30° knee flexion, verified with a handheld goniometer, when the crank was placed at bottom dead center (Holmes et al., 1994). The saddle fore/aft position was set such that the participant's knee was in line with the pedal spindle when the crank was in the forward horizontal (90°) position (Burke and Pruitt, 2003; Fang et al., 2016; Shen et al., 2018). The handle bar position was set such that the angle between the participant's trunk and thigh was 90°, verified with a handheld goniometer when the crank was at 90° (Fang et al., 2016; Gardner et al., 2016; Shen et al., 2018).

Two customized instrumented bike pedals were used to collect pedal reaction forces (PRF) on the Lode cycle ergometer. Each pedal assembly contained two 3D force sensors (Type 9027C, Winterthur, Kistler, Switzerland) and each force sensor was coupled with an industrial charge amplifier (Type 5073A, Kistler, Winterthur, Switzerland) (Fang et al., 2016; Gardner, 2013; Gardner et al., 2016; Gardner et al., 2015; Shen et al., 2018). The charge amplifiers converted the analog charge measured by the force sensors to a voltage value. A custom jig was built and secured to two holes in a floor-mounted force plate to ensure that the cycle ergometer was aligned with the antereoposterior and mediolateral axes of the lab global coordinate system (Figure 3). Prior to using the pedal assemblies, extensive calibration testing was done to ensure that the pedal measurements were accurate.

QF was increased using three pairs of pedal extenders (Sunlite, Booklyn, NY) (Figure 4). Each single pedal extender increased the unilateral QF by 21 mm, such that a pair (1 on the left pedal and 1 on the right pedal) increased the total QF by 42 mm.

2.3 Experimental Procedures

Participants performed a two-minute warm-up on the cycle ergometer. A minimum rest period of 2 minutes was given between the warm-up and the commencement of testing. The participants then completed a total of 12 testing conditions, pedaling for two minutes at workrates of 80 W, 120 W, and 160 W, while maintaining a constant cadence of 80 RPM (Martin and Spirduso, 2001) in each of four QFs: QF of 150 mm, the manufactured QF of the stationary cycle ergometer (Q150), QF of 192 mm (Q192), QF of 234 mm (Q234), and QF of 276 mm (Q276).

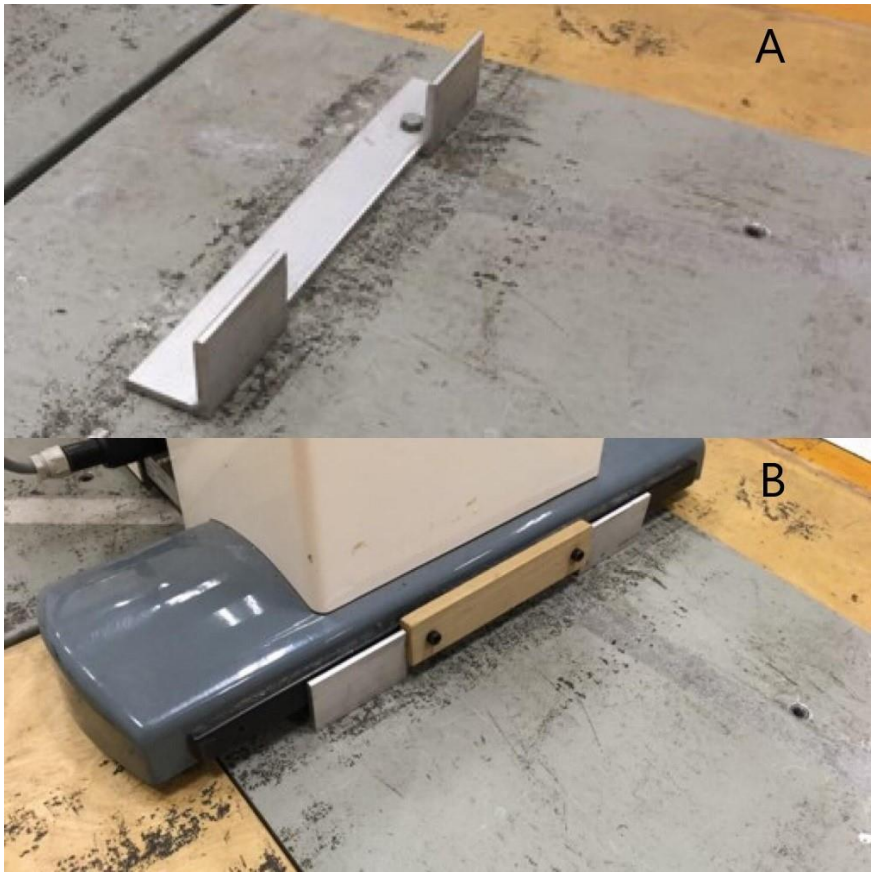


Figure 3. A) The custom jig installed on the ground used to keep the cycle ergometer aligned parallel to the antereoposterior and mediolateral axis of the lab global coordinate system, and B) Base of the cycle ergometer positioned within the custom jig.

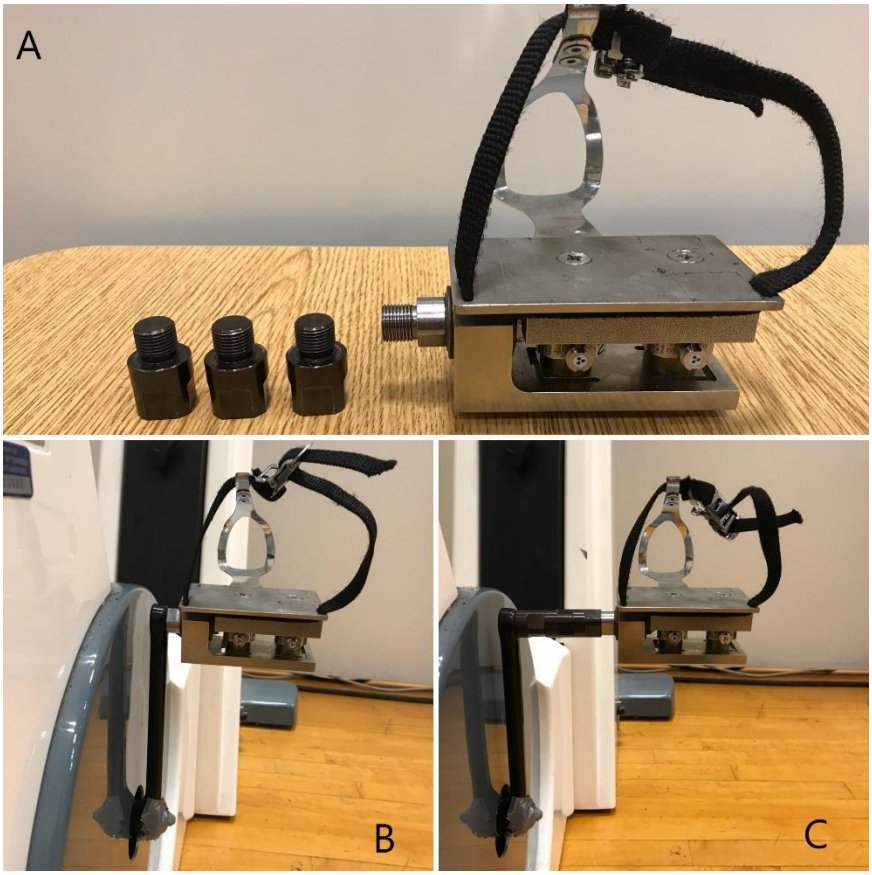


Figure 4. A) Right instrumented bicycle pedal with three QF extenders, B) Right instrumented bicycle pedal mounted on the stationary cycle ergometer at Q150 and C) Right instrumented bicycle pedal mounted on the stationary cycle ergometer at Q276.

All conditions were randomized first by QF, followed by workrate within each QF. Simultaneous recordings of kinematic (240 Hz) and kinetic (1200 Hz) data were collected on a minimum of five consecutive pedal cycles beginning in the last 30 seconds of each test condition (Fang et al., 2016; Gardner et al., 2016; Shen et al., 2018). Following the conclusion of each QF condition, a two-minute rest period was given to each participant where they indicated their Rating of Perceived Exertion (RPE) with the Borg 6-20 scale (Borg, 1998), as well as comfort, and knee pain via numeric visual analog scales (Table 1) while the next condition (QF or workrate) was set. Participants were instructed to remain on the cycle ergometer during the rest period.

The data were exported into Visual3D biomechanical analysis suite (Version 6, C-Motion, Inc., Germantown, MD, USA) to compute pedal reaction forces as well as lower extremity joint kinematics and kinetics. Angular computations were completed using a Cardan rotational sequence (X-Y-Z) and a right-hand rule to define angular kinematic and kinetic variable conventions. Kinematic and pedal reaction force data were filtered using a zero lag, fourth-order Butterworth low-pass filter at 6 Hz (Gardner et al., 2016; Gregersen and Hull, 2003b), with joint moment calculations expressed in the proximal segment's reference frame. Two customized computer programs (VB_V3D and VB_Table, version 6.0, MS Visual Basic) were used to determine discrete events of variables of interest and organized data from Visual3D outputs for subsequent statistical analysis. For kinetic and kinematic data, peak values were chosen during the power phase of the crank cycle. The force and moment variables were not normalized to body weight

and mass, respectively as in cycling the majority of the body weight is supported by saddle and handlebars (Fang et al., 2016; Gardner et al., 2015; Shen et al., 2018).

A 3×4 (workrate × QF) repeated measures analysis of variance (ANOVA) was used to detect differences between workrate and QF conditions (25.0 IBM SPSS, Chicago, IL). The data were then checked for normality using a Shapiro-Wilks test. When an interaction was present, a pairwise t-test was performed in the post hoc analysis with Bonferroni adjustments to determine the location of the statistical differences between QF and workrate. An alpha level of 0.05 was set a priori, and adjusted for post hoc comparisons such that workrate $\alpha < 0.017$, QF $\alpha < 0.008$, interaction $\alpha < 0.008$.

3. Results

There was a significant effect of workrate for RPE ($p < 0.001$, Table 1), and post hoc comparisons showed significant differences between 80 W and 120 W, 80 W and 160 W, and 120 W and 160 W ($p < 0.001$ for all comparisons).

There was a significant main effect of workrate for peak vertical PRF ($p < 0.001$, Table 2), and post hoc comparisons showed significant differences between 80 W and 120 W, 80 W and 160 W, as well as 120 W and 160 W ($p < 0.001$ for all comparisons). There was a significant interaction between workrate and QF for peak mediolateral PRF ($p = 0.016$, Table 2). Post hoc comparisons showed significant differences between Q150 and Q234, Q150 and Q276, and Q192 and Q276 ($p < 0.001$ all comparisons) at 80 W. At 120 W, significant differences were shown between Q150 and Q192, Q150 and Q234, Q150 and Q276 ($p < 0.009$ for all comparisons), and Q192 and Q276 ($p < 0.009$ for all comparisons). Finally, differences were shown at 160 W between Q150 and Q192,

Table 1: Group Mean RPE, comfort, and pain scores.

Variables	Workload (W)	Q150	Q192	Q234	Q276	Workrate	Q-Factor	Int
RPE	80	7.44±1.03	7.88±1.54	8.13±1.93	8.31±1.70	**p < 0.001**	0.101	0.110
	120[a]	9.38±1.71	10.06±1.84	9.63±2.13	9.56±2.10			
	160[a,b]	11.31±2.33	11.63±2.22	12.25±2.38	12.88±2.94			
	Q-Factor Test							
Comfort	80	0.80±0.63	1.10±1.20	1.50±1.18	2.40±1.84	0.061	0.179	0.881
	120	1.00±0.82	1.40±1.17	1.90±0.99	2.80±1.87			
	160	1.50±1.08	1.70±1.42	2.40±1.26	3.50±1.72			
	Q-Factor Test							
Pain	80	0.00±0.00	0.00±0.00	0.00±0.00	0.00±0.00	0.251	0.447	0.447
	120	0.00±0.00	0.10±0.3	0.00±0.00	0.00±0.00			
	160	0.10±0.3	0.10±0.3	0.10±0.3	0.20±0.4			
	Q-Factor Test							

Note:
[a]: significantly different from 80W, [b]: significantly different from 120W
[α]: significantly different from Q150, β: significantly different from Q192, γ: significantly different from Q234
[1]: significantly different from Q150 at same work load, [2]: significantly different from Q192 at same work load, [3]: significantly different from Q234 at same work load
Q-Factor Test: post hoc comparisons for Q-factor main effect.

Table 2: Peak power phase pedal reaction forces (PRF).

Variables	Workrate (W)	Q150	Q192	Q234	Q276	Workrate	Q-Factor	Int
Vertical PRF (N)	80	214.8±27.9	197.3±24.6	205.6±25.9	205.7±27.0	**p < 0.001**	0.183	0.339
	120$^{\alpha}$	256.1±29.5	243.0±27.5	251.1±39.7	255.5±29.1			
	160$^{\alpha,\beta}$	291.4±33.0	290.8±33.5	286.0±41.6	289.0±34.5			
	Q-Factor Test							
Mediolateral PRF (N)	80	-33.2±10.8	-38.7±9.2	-42.9±9.1^{1}	-48.5±12.5^{1,2}	**p < 0.001**	**p < 0.001**	**0.016**
	120$^{\alpha}$	-42.8±12.0	-52.8±12.6^{1}	-60.2±14.9^{1}	-67.6±14.6^{1,2}			
	160$^{\alpha,\beta}$	-50.6±12.5	-66.0±14.9^{1}	-72.5±17.7^{1}	-79.9±18.5^{1,2}			
	Q-Factor Test		α	α,β	α,β,γ			

Note:
^{a}: significantly different from 80W, ^{b}: significantly different from 120W
$^{\alpha}$: significantly different from Q150
^{1}: significantly different from Q150 at same work load, ^{2}: significantly different from Q192 at same work load, ^{3}: significantly different from Q234 at same work load
Q-Factor Test: post hoc comparisons for Q-factor main effect.

Q150 and Q234, and Q150 and Q276, and Q192 and Q276 ($p < 0.001$ for all comparisons).

There was a significant main effect of QF on knee extension ROM ($p < 0.001$, Table 2). Post hoc comparison showed significant differences existed between all QFs ($p < 0.043$ for all comparisons). There was a significant main effect of QF on knee abduction angle ($p = 0.006$, Table 3). Post hoc comparison showed that a significant difference existed only between Q150 and Q276 ($p < 0.002$). Finally, a significant main effect of QF was found for peak knee abduction ROM ($p = 0.022$, Table 3). Significant differences existed between Q150 and Q276, and Q192 and Q276 ($p < 0.005$ for all comparisons).

There was a significant main effect of workrate on peak knee extension moment ($p < 0.001$, Table 3). Significant differences existed between 80 W and 120 W, 80 W and 160 W, and 120W and 160 W ($p < 0.003$ for all comparisons). There was a significant interaction between workrate and QF for peak knee abduction moment ($p = 0.020$, Table 3). Post hoc comparisons showed significant differences between Q150 and Q234, and Q150 and Q276 at 80W ($p < 0.001$ for all comparisons). At 120 W, significant differences were shown between Q150 and Q192, Q150 and Q234, and Q150 and Q276, and Q192 and Q234, as well between Q192 and Q276 ($p < 0.007$ for all conditions). Finally, at 160 W, significant differences were shown between Q150 and Q192, Q150 and Q234, and Q150 and Q276, as well at Q192 and Q276 ($p < 0.003$ for all comparisons).

Table 3: Peak power phase knee joint angles (°) and moments (Nm).

Variables	Workrate (W)	Q150	Q192	Q234	Q276	Workrate	Q-Factor	Int
Knee Extension ROM	80	71.12±5.8	71.6±5.7	72.1±5.6	73.1±5.6	0.603	**p < 0.001**	0.663
	120	70.9±6.5	72.3±6.3	72.7±5.9	73.4±5.9			
	160	71.0±6.9	72.0±6.6	73.2±7.0	73.9±6.8			
	Q-Factor Test		α	α,β	α,β,γ			
Frontal Plane Knee Angle	80	2.6±5.3	1.4±4.9	0.9±4.9	0.2±5.2	0.770	**0.006**	0.155
	120	2.3±4.8	1.5±5.0	0.8±4.5	0.8±4.9			
	160	1.9±4.8	1.3±4.920	0.8±4.8	0.0±5.0			
	Q-Factor Test				α			
Knee Abduction ROM	80	-7.8±4.957	-7.2±5.1	-7.0±4.8	-6.2±4.3	0.083	**0.022**	0.562
	120	-8.0±5.5	-7.8±4.9	-7.0±4.6	-6.3±4.5			
	160	-8.8±5.8	-7.8±4.9	-8.5±4.3	-6.7±4.2			
	Q-Factor Test				α,β			
Knee Extension Moment	80	21.3±9.1	22.2±8.1	21.8±9.5	23.9±10.3	**p < 0.001**	0.146	0.332
	120[a]	29.2±10.0	29.0±9.1	30.7±13.0	33.1±12.2			
	160[a,b]	32.5±12.3	35.6±12.2	35.2±13.4	35.9±12.8			
	Q-Factor Test							
Knee Abduction Moment	80	-9.3±3.0	-11.0±4.0	-12.7±3.9[1]	-13.7±4.8[1,2]	**p < 0.001**	**p < 0.001**	**0.020**
	120[a]	-12.0±4.31	-14.6±5.6[1]	-16.7±5.5[1,2]	-18.7±5.3[1,2]			
	160[a,b]	-13.9±3.9	-18.1±5.5[1]	-19.8±6.3[1]	-21.7±6.5[1,2]			
	Q-Factor Test		α	α,β	α,β,γ			

Note:
[a]: significantly different from 80W, [b]: significantly different from 120W
[α]: significantly different from Q150, β: significantly different from Q192, γ: significantly different from Q234
[1]: significantly different from Q150 at same work load, [2]: significantly different from Q192 at same work load, [3]: significantly different from Q234 at same work load
Q-Factor Test: post hoc comparisons for Q-factor main effect.

4. Discussion

The purpose of this study was to examine effects of standard and increased QFs at different workrates on knee biomechanics of healthy-weight participants during stationary cycling. It was first hypothesized that as QF increases peak KAbM would decrease and, as QF increased further the frontal plane knee moment would become a knee adduction moment. This hypothesis was not supported by our results. Changes in the KAbM were in the opposite direction as we hypothesized and, as workload increased, KAbMs increased in general.

QF effects on knee frontal-plane kinematics and alignment were, in part, thought to explain the differences in knee joint moments between previous cycling studies (Fang et al., 2016; Gardner et al., 2016; Shen et al., 2018). Although a statistically significant QF effect was observed for frontal plane kinematic variables, the changes in the peak knee adduction angle (2.4, 1.5, 2.0° at each increasing workload) and knee abduction ROM (1.6, 1.7, 2.1° at each increasing workload) may not be meaningful in fully explaining the peak KAbM differences seen amongst these cycling studies. In this study peak KAbM increased by 47%, 56%, and 56% from Q150 to Q276 at three respective workloads as QF was increased. This suggests that although frontal plane knee alignment may play a role in the loading patterns of the knee during cycling, QF does not appear to significantly change this alignment.

These results from cycling also differ from observations of KAbMs in gait modification using wider step width in level walking and stair ascent. Step-width is the spatiotemporal analog in gait to QF in cycling. In normal walking, preferred step-width

has been reported between 7-12 cm (Helbostad and Moe-Nilssen, 2003; Hollman et al., 2011; Wert et al., 2010), and between 13-17 cm in stair ascent (Paquette et al., 2015; Paquette et al., 2014b; Yocum et al., 2018). Gait modification studies have demonstrated that with increased step-width, KAbM decreases in level walking (Fregly et al., 2008; Zhao et al., 2007), stair ascension (Paquette et al., 2015; Paquette et al., 2014b; Yocum et al., 2018). In recent wide step-width stair ascent studies, mean wide step-widths were reported as 0.32 m (Paquette et al., 2015) and 0.30 m (Yocum et al., 2018) which is similar in absolute distance to Q192 of the current study. QF is measured from crank arm to crank arm (Disley and Li, 2014a, b), while step width was measured as the distance from left to right foot COM (Bennett et al., 2017a; Bennett et al., 2017b; Paquette et al., 2015; Paquette et al., 2014b; Yocum et al., 2018). The actual horizontal distance between the centers of the two pedals (a closer approximation of foot COM) in the current study was 0.32 cm at Q192 (19.2 cm + additional 13 cm, the combined distance from center of pedal to crank arm). KAbM was shown to reduce by 19.4% (Paquette et al., 2015) and by 5.1% (Yocum et al., 2018) at wider step widths in healthy adults. However, as QF increased from Q150 (similar to the preferred walking step-width) to Q192 (similar to the wider step-width), KAbM increased by 18%, 22%, and 30% and each workload. KAbM continues to increase as QF widens to Q234 and Q276 with increases of peak KAbM of 13% and 10% respectively at each workload. At Q276 peak KAbM is on average 24% greater than at Q150 at across all workloads.

During cycling, the body weight of the rider is supported primarily by the saddle, and secondarily by the handle bars. In level walking, stair ascent, and stair descent, the

lower extremities support the entirety of the body weight. One explanation for the reduction of peak KAbM in walking is a reduction in the frontal plane moment arm from the frontal-plane GRF to the knee joint (Guo et al., 2007; Paquette et al., 2014b). Previous gait modification research suggests that during the weight acceptance phase of stance, the whole-body COM shifts laterally closer to the support leg to establish balance and, as a result, the GRF vector shifts from the medial side of the knee laterally, closer to the knee joint, thereby decreasing the frontal plane moment arm and KAbM (Guo et al., 2007; Paquette et al., 2014b). In cycling, the whole-body COM does not shift significantly relative to the knee joint due to constraint from the seat and cycling movement. As QF was increased, the frontal plane moment arm was likely increased from knee joint center without the compensation of whole-body COM, and an increase of KAbM was observed. The differences between decreased KAbM with wider step-width and increased KAbM with wider QF seem to be in part attributable to the lack of manipulation of body COM by the lower extremity in cycling to effectively reduce the frontal-plane GRF moment arm.

The other contributing factor for differing KAbM is mediolateral PRF. A QF main effect of mediolateral PRF was present for all conditions. An interaction for peak mediolateral PRF showed greater increases at higher workloads (Table 2). KAbM is observed when the knee joint is in the adducted position (Paquette et al., 2014b). Increased KAbM in this study, when considered with the small changes to knee adduction angle (Table 3) provide support that the increased mediolateral GRF may be also a key player in the increase of KAbM. It is worth noting that mediolateral PRF

increased significantly with increased QF, and the mediolateral PRF changes seem to closely parallel those of KAbM. Although this magnitude was, in absolute terms, relatively small compared to peak vertical PRF, these results suggest that increased mediolateral PRFs are partially responsible for the increase in peak KAbM.

The hypothesis that as workload increases, the increase in the frontal plane knee moment will become greater was supported by our data as a QF x workload interaction was observed for KAbM. In general, the magnitude of change of KAbM increased with wider QFs at higher workloads. At 160 W, KAbM increased by 7.8 Nm from Q150 to Q276 as compared to 4.4 Nm for the same QFs at 80 W. These results provide evidence that QF manipulation, in conjunction with workload manipulation, may be used in designing protocols used in prevention and rehabilitation for patients with knee OA or total knee replacement, which modulate knee joint loading.

To our knowledge, our study is the first study to comprehensively examine the knee biomechanics with focus on frontal-plane kinematics and kinetics during cycling with increased QF. Disley and Li (2014b) measured frontal plane knee joint variability to determine the effect of QF on knee joint stability. Knee joint variability was calculated as standard deviation of movement of the lateral femoral epicondyle marker in the frontal plane. They reported no significant difference in the knee joint variability among any of their QF conditions. Knee joint variability was the only reported kinematic variable, and as such comparisons between their study and ours are difficult.

Our final hypothesis stating that peak knee extension moment will not change significantly with increased QF was supported by our data. Peak knee extension moment

was not significantly influenced by widened QFs. Similarly, peak vertical PRFs were not affected by increased QFs. Given the length of the lower extremity segments, the relatively small increase in mediolateral PRF (5.1 N, 8.3 N, and 9.8 N at each workload respectively, (Table 2) may not have been large enough to change the resultant PRFs. These results suggest that the overall knee joint loading is not changed with manipulation of inter-pedal distance. This may, in conjunction with the lack of effect of Q-Factor on RPE, comfort, or knee pain (Table 1), provide some benefits to knee OA and other related patients. One such benefit is that changing QF may prove to be a safe and effective tool in rehabilitation protocols and exercises, as QF can be manipulated without fear of increasing overall knee joint loading, perceived cycling intensity, or discomfort, while modulating frontal plane loading in safe manners of targeted patients.

One limitation of this study is that due to the construction of the instrumented force pedals, we were constrained in the mechanism to increase Q-Factor. In gait modification literature, step-width is often measured as a percent increase of leg length (Bennett et al., 2017a; Bennett et al., 2017b; Paquette et al., 2015; Paquette et al., 2014b; Yocum et al., 2018). Disley and Li (Disley and Li, 2014a, b) used a 'floating pedal' that permitted the rider's foot to move freely about the mediolateral axis of a lengthened pedal spindle. Given the location of the instrumented force sensors within the pedal body, we were only able to increase the QF with spacers at the crank arm/pedal insertion which constrained the QF to increases of 42 mm (Figure 2). Although Q150 and Q192 were similar in absolute width to the preferred and wide step-widths reported previously, the ability to determine custom QF from some anthropometric measurement may be

necessary to provide more tailored control to knee joint loading in rehabilitation programs.

5. Conclusion

The findings of this study indicate that as the QF of a stationary cycle is increased, peak KAbM will increase as well, suggesting increased medial compartment loading of the knee. Increasing the QF did not change the knee extension moment or sagittal plane loading patterns of the knee. Identifying appropriate QFs for different patients can be beneficial for exercise prescription in modulating frontal plane loading patterns during OA management and rehabilitation. Future studies should examine the effects of increased QF on obese individuals as well as OA and total knee arthroplasty patients.

LIST OF REFERENCES

Ainsworth, B.E., Haskell, W.L., Herrmann, S.D., Meckes, N., Bassett, D.R., Jr., Tudor-Locke, C., Greer, J.L., Vezina, J., Whitt-Glover, M.C., Leon, A.S., 2011. 2011 Compendium of Physical Activities: a second update of codes and MET values. Medicine and science in sports and exercise 43, 1575-1581.

Álvarez, G., Vinyolas, J., 1996. A new bicycle pedal design for on-road measurements of cycling forces. Journal of applied biomechanics 12, 130-142.

American College of Sports Medicine, 1995. Physical Activity Readiness Questionnaire. PAR-Q. ACSM's Guidelines for exercise testing and prescription. Philadelphia. EEUU: Williams & Wilkins, 14-15.

Andriacchi, T.P., Koo, S., Scanlan, S.F., 2009. Gait mechanics influence healthy cartilage morphology and osteoarthritis of the knee. The Journal of Bone and Joint Surgery. American volume. 91, 95.

Asplund, C., St Pierre, P., 2004. Knee pain and bicycling: fitting concepts for clinicians. The Physician and sportsmedicine 32, 23-30.

Asplund, C., Webb, C., Barkdull, T., 2005. Neck and back pain in bicycling. Current sports medicine reports 4, 271-274.

Bailey, M.P., Maillardet, F.J., Messenger, N., 2003. Kinematics of cycling in relation to anterior knee pain and patellar tendinitis. Journal of sports sciences 21, 649-657.

Baker, K.R., Xu, L., Zhang, Y., Nevitt, M., Niu, J., Aliabadi, P., Yu, W., Felson, D., 2004. Quadriceps weakness and its relationship to tibiofemoral and patellofemoral knee osteoarthritis in Chinese: the Beijing osteoarthritis study. Arthritis and rheumatism 50, 1815-1821.

Beekley, M.D., Brechue, W.F., Dehoyos, D.V., Garzarella, L., Werber-Zion, G., Pollock*, M.L., 2004. Cross-validation of the YMCA submaximal cycle ergometer test to predict VO2max. Research quarterly for exercise and sport 75, 337-342.

Bennet, H.J., 2016. Static Frontal Plane Tibiofemoral Alignments and Their Effects on Knee Biomechanics During Level Walking and Stair Ascent Tasks. . TRACE: Tennesse Research and Creative Exchange.

Bennett, H.J., Shen, G., Cates, H.E., Zhang, S., 2017a. Effects of toe-in and toe-in with wider step width on level walking knee biomechanics in varus, valgus, and neutral knee alignments. The Knee 24, 1326-1334.

Bennett, H.J., Zhang, S., Shen, G., Weinhandl, J.T., Paquette, M.R., Reinbolt, J., Coe, D.P., 2017b. Effects of toe-in and wider step width in stair ascent with different knee alignments. Medicine & Science in Sports & Exercise 49, 563-572.

Bini, R.R., Diefenthaeler, F., 2010. Kinetics and kinematics analysis of incremental cycling to exhaustion. Sports biomechanics 9, 223-235.

Bini, R.R., Rossato, M., Diefenthaeler, F., Carpes, F.P., 2010. Pedaling cadence effects on joint mechanical work during cycling. Isokinetics and Exercise Science 18, 7-13.

Bini, R.R.H., P.A.; Croft, J.L., 2011. Effects of bicycle saddle height on knee injury and performance. Sports Med 41, 463-476.

Bini, R.R.T., A.C.; Mota, C.B., 2010. Effects of saddle height pedaling cadence and workload on joint kinetics
Journal of Sports Rehab 19, 301-314.

BMI, O.C., 1998. Clinical guidelines on the identification, evaluation, and treatment of overweight and obesity in adults. NOE Initiative.

Borg, G., 1998. Borg's perceived exertion and pain scales. Human kinetics.

Boutcher, S.H., 2010. High-intensity intermittent exercise and fat loss. Journal of obesity 2011.

Broker, J.P., 2003. Cycling Biomechanics: Road and Mountain, High-tech cycling 2nd ed. Human Kinetics, pp. 119-146.

Broker, J.P., Gregor, R.J., 1990. A dual piezoelectric element force pedal for kinetic analysis of cycling. International Journal of Sport Biomechanics 6, 394-403.

Burke, E., 1986. Science of cycling. Human Kinetics Publishers.

Burke, E., Pruitt, A., 2003. Body Positioning For Cycling, High-tech cycling 2nd ed. Human Kinetics, pp. 69-92.

Burke, E.R., 1994. Proper fit of the bicycle. Clinics in sports medicine 13, 1-14.

D'Lima, D.D., Steklov, N., Patil, S., Colwell, C.W., Jr., 2008. The Mark Coventry Award: in vivo knee forces during recreation and exercise after knee arthroplasty. Clin Orthop Relat Res 466, 2605-2611.

Dawson, J., Linsell, L., Zondervan, K., Rose, P., Randall, T., Carr, A., Fitzpatrick, R., 2004. Epidemiology of hip and knee pain and its impact on overall health status in older adults. Rheumatology 43, 497-504.

de Vey Mestdagh, K., 1998. Personal perspective: in search of an optimum cycling posture. Applied ergonomics 29, 325-334.

Dempster, W.T., Gabel, W.C., Felts, W.J., 1959. The anthropometry of the manual work space for the seated subject. American journal of physical anthropology 17, 289-317.

Disley, B.X., Li, F.X., 2014a. The effect of Q factor on gross mechanical efficiency and muscular activation in cycling. Scand J Med Sci Sports 24, 117-121.

Disley, B.X., Li, F.X., 2014b. Metabolic and kinematic effects of self-selected Q Factor during bike fit. Research in sports medicine (Print) 22, 12-22.

Donelan, J.M., Kram, R., 2001. Mechanical and metabolic determinants of the preferred step width in human walking. Proceedings of the Royal Society of London B: Biological Sciences 268, 1985-1992.

Edeline, O., Polin, D., Tourny-Chollet, C., Weber, J., 2004. Effect of workload on bilateral pedaling kinematics in non-trained cyclists. Journal of Human Movement Studies 46, 493-517.

Ercison, M.O., Nisell, R., Nemeth, G., 1988. Joint Motions of the Lower Limb during Ergometer Cycling. The Journal of orthopaedic and sports physical therapy 9, 273-278.

Ericson, M., 1986. On the biomechanics of cycling. A study of joint and muscle load during exercise on the bicycle ergometer. Scandinavian journal of rehabilitation medicine. Supplement 16, 1-43.

Ericson, M., Nisell, R., Ekholm, J., 1984. Varus and valgus loads on the knee joint during ergometer cycling. Scand J Sports Sci 6, 39-45.

Ericson, M.O., 1988. Mechanical muscular power output and work during ergometer cycling at different work loads and speeds. European journal of applied physiology and occupational physiology 57, 382-387.

Ericson, M.O., Bratt, A., Nisell, R., Nemeth, G., Ekholm, J., 1986. Load moments about the hip and knee joints during ergometer cycling. Scandinavian journal of rehabilitation medicine 18, 165-172.

Ericson, M.O., Nisell, R., 1986. Tibiofemoral joint forces during ergometer cycling. The American journal of sports medicine 14, 285-290.

Ericson, M.O., Nisell, R., 1987. Patellofemoral joint forces during ergometric cycling. Phys Ther 67, 1365-1369.

Fang, Y., Fitzhugh, E.C., Crouter, S.E., Gardner, J.K., Zhang, S., 2016. Effects of Workloads and Cadences on Frontal Plane Knee Biomechanics in Cycling. Medicine and science in sports and exercise 48, 260-266.

Felson, D.T., Anderson, J.J., Naimark, A., Walker, A.M., Meenan, R.F., 1988. Obesity and knee osteoarthritis. The Framingham Study. Annals of internal medicine 109, 18-24.

Felson, D.T., Couropmitree, N.N., Chaisson, C.E., Hannan, M.T., Zhang, Y., McAlindon, T.E., LaValley, M., Levy, D., Myers, R.H., 1998. Evidence for a Mendelian gene in a segregation analysis of generalized radiographic osteoarthritis: the Framingham Study. Arthritis and rheumatism 41, 1064-1071.

Felson, D.T., Lawrence, R.C., Dieppe, P.A., Hirsch, R., Helmick, C.G., Jordan, J.M., Kington, R.S., Lane, N.E., Nevitt, M.C., Zhang, Y., Sowers, M., McAlindon, T., Spector, T.D., Poole, A.R., Yanovski, S.Z., Ateshian, G., Sharma, L., Buckwalter, J.A., Brandt, K.D., Fries, J.F., 2000. Osteoarthritis: new insights. Part 1: the disease and its risk factors. Annals of internal medicine 133, 635-646.

Flegal, K.M., Kruszon-Moran, D., Carroll, M.D., Fryar, C.D., Ogden, C.L., 2016. Trends in obesity among adults in the United States, 2005 to 2014. Jama 315, 2284-2291.

Focht, B.C., Rejeski, W.J., Ambrosius, W.T., Katula, J.A., Messier, S.P., 2005. Exercise, self-efficacy, and mobility performance in overweight and obese older adults with knee osteoarthritis. Arthritis and rheumatism 53, 659-665.

Fregly, B.J., Reinbolt, J.A., Chmielewski, T.L., 2008. Evaluation of a patient-specific cost function to predict the influence of foot path on the knee adduction torque during gait. Computer methods in biomechanics and biomedical engineering 11, 63-71.

Garber, C.E., Blissmer, B., Deschenes, M.R., Franklin, B.A., Lamonte, M.J., Lee, I.M., Nieman, D.C., Swain, D.P., 2011. American College of Sports Medicine position stand. Quantity and quality of exercise for developing and maintaining cardiorespiratory, musculoskeletal, and neuromotor fitness in apparently healthy adults: guidance for prescribing exercise. Medicine and science in sports and exercise 43, 1334-1359.

Gardner, J.K., 2013. Effects of lateral shoe wedges and toe-in foot progression angles on the biomechanics of knee osteoarthritis during stationary cycling. The University of Tennessee, Trace: Tennessee Research and Creative Exchange.

Gardner, J.K., Klipple, G., Stewart, C., Asif, I., Zhang, S., 2016. Acute effects of lateral shoe wedges on joint biomechanics of patients with medial compartment knee osteoarthritis during stationary cycling. Journal of Biomechanics 49, 2817-2823.

Gardner, J.K., Zhang, S., Liu, H., Klipple, G., Stewart, C., Milner, C.E., Asif, I.M., 2015. Effects of toe-in angles on knee biomechanics in cycling of patients with medial knee osteoarthritis. Clinical Biomechanics 30, 276-282.

Glass, S., Dwyer, G.B., Medicine, A.C.o.S., 2007. ACSM'S metabolic calculations handbook. Lippincott Williams & Wilkins.

Gregersen, C.S., Hull, M.L., 2003a. Non-driving intersegmental knee moments in cycling computed using a model that includes three-dimensional kinematics of the shank/foot and the effect of simplifying assumptions. J Biomech 36, 803-813.

Gregersen, C.S., Hull, M.L., 2003b. Non-driving intersegmental knee moments in cycling computed using a model that includes three-dimensional kinematics of the shank/foot and the effect of simplifying assumptions. Journal of biomechanics 36, 803-813.

Gregor, R.J., Cavanagh, P.R., LaFortune, M., 1985. Knee flexor moments during propulsion in cycling--a creative solution to Lombard's Paradox. J Biomech 18, 307-316.

Guo, M., Axe, M.J., Manal, K., 2007. The influence of foot progression angle on the knee adduction moment during walking and stair climbing in pain free individuals with knee osteoarthritis. Gait & posture 26, 436-441.

Hamley, E.y., Thomas, V., 1967. Physiological and postural factors in the calibration of the bicycle ergometer. The Journal of physiology 191, 55P-56P.

Hanavan Jr, E.P., 1964. A mathematical model of the human body. AIR FORCE AEROSPACE MEDICAL RESEARCH LAB WRIGHT-PATTERSON AFB OH.

Helbostad, J.L., Moe-Nilssen, R., 2003. The effect of gait speed on lateral balance control during walking in healthy elderly. Gait & posture 18, 27-36.

Hollman, J.H., Youdas, J.W., Lanzino, D.J., 2011. Gender differences in dual task gait performance in older adults. American journal of men's health 5, 11-17.

Holmes, J., Pruitt, A., Whalen, N., 1994. Lower extremity overuse in bicycling. Clinics in sports medicine 13, 187-205.

Johnston, T.E., 2007. Biomechanical considerations for cycling interventions in rehabilitation. Phys Ther 87, 1243-1252.

Kutzner, I., Heinlein, B., Graichen, F., Rohlmann, A., Halder, A.M., Beier, A., Bergmann, G., 2012. Loading of the knee joint during ergometer cycling: telemetric in vivo data. journal of orthopaedic & sports physical therapy 42, 1032-1038.

Lacasse, Y., Wong, E., Guyatt, G.H., King, D., Cook, D.J., Goldstein, R.S., 1996. Meta-analysis of respiratory rehabilitation in chronic obstructive pulmonary disease. The Lancet 348, 1115-1119.

Lawrence, R.C., Felson, D.T., Helmick, C.G., Arnold, L.M., Choi, H., Deyo, R.A., Gabriel, S., Hirsch, R., Hochberg, M.C., Hunder, G.G., Jordan, J.M., Katz, J.N., Kremers, H.M., Wolfe, F., 2008. Estimates of the prevalence of arthritis and other rheumatic conditions in the United States. Part II. Arthritis and rheumatism 58, 26-35.

Liebs, T.R., Herzberg, W., Rüther, W., Haasters, J., Russlies, M., Hassenpflug, J., 2010. Ergometer cycling after hip or knee replacement surgery: a randomized controlled trial. JBJS 92, 814-822.

Lohmander, L.S., Ostenberg, A., Englund, M., Roos, H., 2004. High prevalence of knee osteoarthritis, pain, and functional limitations in female soccer players twelve years after anterior cruciate ligament injury. Arthritis and rheumatism 50, 3145-3152.

Mangione, K.K., McCully, K., Gloviak, A., Lefebvre, I., Hofmann, M., Craik, R., 1999. The effects of high-intensity and low-intensity cycle ergometry in older adults with knee osteoarthritis. The journals of gerontology. Series A, Biological sciences and medical sciences 54, M184-190.

Martin, J., Spirduso, W., 2001. Determinants of maximal cycling power: crank length, pedaling rate and pedal speed. European journal of applied physiology 84, 413-418.

Messier, S.P., Gutekunst, D.J., Davis, C., DeVita, P., 2005. Weight loss reduces knee-joint loads in overweight and obese older adults with knee osteoarthritis. Arthritis and rheumatism 52, 2026-2032.

Messier, S.P., Loeser, R.F., Miller, G.D., Morgan, T.M., Rejeski, W.J., Sevick, M.A., Ettinger, W.H., Jr., Pahor, M., Williamson, J.D., 2004. Exercise and dietary weight loss in overweight and obese older adults with knee osteoarthritis: the Arthritis, Diet, and Activity Promotion Trial. Arthritis and rheumatism 50, 1501-1510.

Mornieux, G., Guenette, J.A., Sheel, A.W., Sanderson, D.J., 2007. Influence of cadence, power output and hypoxia on the joint moment distribution during cycling. European journal of applied physiology 102, 11-18.

Mündermann, A., Dyrby, C.O., Andriacchi, T.P., 2005. Secondary gait changes in patients with medial compartment knee osteoarthritis: increased load at the ankle, knee, and hip during walking. Arthritis & Rheumatology 52, 2835-2844.

Neptune, R., Hull, M., 1998. Evaluation of performance criteria for simulation of submaximal steady-state cycling using a forward dynamic model. Transaction-American Society of Mechanical Engineers Journal of Biomechanical Engineering 120, 334-341.

Nisell, R., OLSEN, H., NÈMETH, G., 1986. Biomechanical analysis of the tibiofemoral joint in extension of the knee. Acte Orthop Scand 57, 41-46.

Nordeen-Snyder, K.S., 1976. The effect of bicycle seat height variation upon oxygen consumption and lower limb kinematics. Medicine and Science in Sports 9, 113-117.

Ogden, C.L., Carroll, M.D., Lawman, H.G., Fryar, C.D., Kruszon-Moran, D., Kit, B.K., Flegal, K.M., 2016. Trends in Obesity Prevalence Among Children and Adolescents in the United States, 1988-1994 Through 2013-2014. Jama 315, 2292-2299.

Paquette, M.R., Klipple, G., Zhang, S., 2015. Greater Step Widths Reduce Internal Knee Abduction Moments in Medial Compartment Knee Osteoarthritis Patients During Stair Ascent. Journal of applied biomechanics 31, 229-236.

Paquette, M.R., Zhang, S., Milner, C.E., Fairbrother, J.T., Reinbolt, J.A., 2014a. Effects of increased step width on frontal plane knee biomechanics in healthy older adults during stair descent. The Knee 21, 821-826.

Paquette, M.R., Zhang, S., Milner, C.E., Fairbrother, J.T., Reinbolt, J.A., 2014b. Effects of increased step width on frontal plane knee biomechanics in healthy older adults during stair descent. The Knee 21, 821-826.

Pendleton, A., Arden, N., Dougados, M., Doherty, M., Bannwarth, B., Bijlsma, J.W., Cluzeau, F., Cooper, C., Dieppe, P.A., Gunther, K.P., Hauselmann, H.J., Herrero-Beaumont, G., Kaklamanis, P.M., Leeb, B., Lequesne, M., Lohmander, S., Mazieres, B., Mola, E.M., Pavelka, K., Serni, U., Swoboda, B., Verbruggen, A.A., Weseloh, G., Zimmermann-Gorska, I., 2000. EULAR recommendations for the management of knee osteoarthritis: report of a task force of the Standing Committee for International Clinical Studies Including Therapeutic Trials (ESCISIT). Annals of the rheumatic diseases 59, 936-944.

Peveler, W.W., 2008. Effects of saddle height on economy in cycling. The Journal of Strength & Conditioning Research 22, 1355-1359.

Poole, D.C., Ward, S.A., Whipp, B.J., 1990. The effects of training on the metabolic and respiratory profile of high-intensity cycle ergometer exercise. European journal of applied physiology and occupational physiology 59, 421-429.

Price, D., Donne, B., 1997. Effect of variation in seat tube angle at different seat heights on submaximal cycling performance in man. Journal of sports sciences 15, 395-402.

Reiser, R., 2001. Biomechanics of recumbent cycling: Instrumentation, experimentation, and modeling.

Rheumatology, A.C.o., 2000. Recommendations for the medical management of osteoarthritis of the hip and knee: 2000 update. American College of Rheumatology Subcommittee on Osteoarthritis Guidelines. Arthritis and rheumatism 43, 1905-1915.

Rowe, T., Hull, M., Wang, E., 1998. A pedal dynamometer for off-road bicycling. TRANSACTIONS-AMERICAN SOCIETY OF MECHANICAL ENGINEERS JOURNAL OF BIOMECHANICAL ENGINEERING 120, 160-164.

Ruby, P., Hull, M.L., Hawkins, D., 1992. Three-dimensional knee joint loading during seated cycling. J Biomech 25, 41-53.

Schipplein, O.D., Andriacchi, T.P., 1991. Interaction between active and passive knee stabilizers during level walking. Journal of orthopaedic research : official publication of the Orthopaedic Research Society 9, 113-119.

Sharma, L., Hurwitz, D.E., Thonar, E.J., Sum, J.A., Lenz, M.E., Dunlop, D.D., Schnitzer, T.J., Kirwan-Mellis, G., Andriacchi, T.P., 1998. Knee adduction moment, serum hyaluronan level, and disease severity in medial tibiofemoral osteoarthritis. Arthritis and rheumatism 41, 1233-1240.

Sharp, A., 1896. Bicycles & tricycles: an elementary treatise on their design and construction, with examples and tables. Longmans, Green.

Shen, G., Zhang, S., Bennett, H.J., Martin, J.C., Crouter, S.E., Fitzhugh, E.C., 2018. Effects of Knee Alignments and Toe Clip on Frontal Plane Knee Biomechanics in Cycling. Journal of sports science & medicine 17, 312.

Silberman, M.R., Webner, D., Collina, S., Shiple, B.J., 2005. Road bicycle fit. Clinical Journal of Sport Medicine 15, 271-276.

Skender, M.L., Goodrick, G.K., Del Junco, D.J., Reeves, R.S., Darnell, L., GOTTO, A.M., Foreyt, J.P., 1996. Comparison of 2-year weight loss trends in behavioral treatments of obesity: diet, exercise, and combination interventions. Journal of the American Dietetic Association 96, 342-346.

Slemenda, C., Brandt, K.D., Heilman, D.K., Mazzuca, S., Braunstein, E.M., Katz, B.P., Wolinsky, F.D., 1997. Quadriceps weakness and osteoarthritis of the knee. Annals of internal medicine 127, 97-104.

Slemenda, C., Heilman, D.K., Brandt, K.D., Katz, B.P., Mazzuca, S.A., Braunstein, E.M., Byrd, D., 1998. Reduced quadriceps strength relative to body weight: a risk factor for knee osteoarthritis in women? Arthritis and rheumatism 41, 1951-1959.

Tamborindeguy, A.C., Bini, R.R., 2011. Does saddle height affect patellofemoral and tibiofemoral forces during bicycling for rehabilitation? Journal of bodywork and movement therapies 15, 186-191.

Thomas, R.H., Resnick, D., Alazraki, N.P., Daniel, D., Greenfield, R., 1975. Compartmental evaluation of osteoarthritis of the knee: a comparative study of available diagnostic modalities. Radiology 116, 585-594.

Thompson, P.D., Arena, R., Riebe, D., Pescatello, L.S., 2013. ACSM's new preparticipation health screening recommendations from ACSM's guidelines for exercise testing and prescription. Current sports medicine reports 12, 215-217.

Too, D., Landwer, G.E., 2000. The effect of pedal crank arm length on joint angle and power production in upright cycle ergometry. Journal of sports sciences 18, 153-161.

Umberger, B., Scheuchenzuber, H., Manos, T., 1998. Differences in power output during cycling at different seat tube angles. Journal of Human Movement Studies 35, 21-36.

Umberger, B.R., Martin, P.E., 2001. Testing the planar assumption during ergometer cycling. Journal of Applied Biomechanics 17, 55-62.

Wert, D.M., Brach, J., Perera, S., VanSwearingen, J.M., 2010. Gait biomechanics, spatial and temporal characteristics, and the energy cost of walking in older adults with impaired mobility. Physical therapy 90, 977-985.

WHO, 2016. Obesity and Overweight

Wozniak Timmer, C.A., 1991. Cycling biomechanics: a literature review. Journal of Orthopaedic & Sports Physical Therapy 14, 106-113.

Yocum, D., Weinhandl, J., Faribrother, J., Zhang, S., 2018. Effects of Wide Step Width on Knee Biomechanics in Stair Ascent in Obese Participants. . Journal of Biomechanics.

Zhang, W., Moskowitz, R.W., Nuki, G., Abramson, S., Altman, R.D., Arden, N., Bierma-Zeinstra, S., Brandt, K.D., Croft, P., Doherty, M., Dougados, M., Hochberg, M., Hunter, D.J., Kwoh, K., Lohmander, L.S., Tugwell, P., 2008. OARSI recommendations for the management of hip and knee osteoarthritis, Part II: OARSI evidence-based, expert consensus guidelines. Osteoarthritis and cartilage 16, 137-162.

Zhao, D., Banks, S.A., Mitchell, K.H., D'Lima, D.D., Colwell, C.W., Jr., Fregly, B.J., 2007. Correlation between the knee adduction torque and medial contact force for a variety of gait patterns. Journal of orthopaedic research : official publication of the Orthopaedic Research Society 25, 789-797.

APPENDICES

Appendix A: Individual Subject Characteristics

Table 4: Individual Subject Characteristics.

Subject	Gender	Age (years)	Height (m)	Weight (kg)	BMI (kg/m^2)
1	M	21	1.89	85.90	24.05
2	M	22	1.91	77.07	21.13
3	M	24	1.84	76.98	22.74
4	M	22	1.89	89.11	24.95
5	F	22	1.61	59.75	23.05
6	F	23	1.61	62.71	24.19
7	F	22	1.62	60.72	23.14
8	F	20	1.66	65.67	23.83
9	F	21	1.69	61.58	21.56
10	F	21	1.67	65.73	23.57
11	F	21	1.72	61.66	20.84
12	M	20	1.82	66.11	19.96
13	F	24	1.63	59.64	22.45
14	M	23	1.69	61.09	21.39
15	M	21	1.76	74.76	24.13
16	M	31	1.83	78.64	23.48
Mean ± STD		22.38±2.60	1.74±0.11	69.20±9.75	22.78±1.43

Table 5: Group Mean RPE, comfort, and pain scores.

Variables	Workload (W)	Q150	Q192	Q234	Q276	Workrate	Q-Factor	Int
RPE	80	7.44±1.03	7.88±1.54	8.13±1.93	8.31±1.70	**p < 0.001**	0.101	0.110
	120[a]	9.38±1.71	10.06±1.84	9.63±2.13	9.56±2.10			
	160[a,b]	11.31±2.33	11.63±2.22	12.25±2.38	12.88±2.94			
	Q-Factor Test							
Comfort	80	0.80±0.63	1.10±1.20	1.50±1.18	2.40±1.84	0.061	0.179	0.881
	120	1.00±0.82	1.40±1.17	1.90±0.99	2.80±1.87			
	160	1.50±1.08	1.70±1.42	2.40±1.26	3.50±1.72			
	Q-Factor Test							
Pain	80	0.00±0.00	0.00±0.00	0.00±0.00	0.00±0.00	0.251	0.447	0.447
	120	0.00±0.00	0.10±0.3	0.00±0.00	0.00±0.00			
	160	0.10±0.30	0.10±0.30	0.10±0.30	0.20±0.40			
	Q-Factor Test							

Note:
[a]: significantly different from 80W, [b]: significantly different from 120W
[α]: significantly different from Q150, β: significantly different from Q192, γ: significantly different from Q234
[1]: significantly different from Q150 at same work load, [2]: significantly different from Q192 at same work load, [3]: significantly different from Q234 at same work load
Q-Factor Test: post hoc comparisons for Q-factor main effect.

Appendix B: Informed Consent Form

INFORMED CONSENT FORM

Effects of Increased Q-Factor on Knee Biomechanics during Stationary Cycling

Principal Investigator: Tanner Thorsen, B.S.
Address: 136 HPER
1914 Andy Holt Avenue
Knoxville, TN 37996
Phone: (865) 974-2091

Faculty Advisor: Songning Zhang, PhD
Address: 340 HPER
1914 Andy Holt Avenue
Knoxville, TN 37996
Phone: (865) 974-2091

Introduction

You are invited to participate in this research study because you are an adult between 18 and 35 years old. This research investigates the differences in knee joint function in both obese and normal weight people in response to increased Q-Factors of the bicycle. The Q-Factor of a bicycle refers to the inter-pedal width, or, in other words, how far apart the bicycle pedals are spaced. The Q-Factor of a bicycle may have an impact on knee joint function during cycling. Please ask the study staff to explain any words or information that you do not clearly understand. Before agreeing to participate in this study, it is important that you read and understand the following explanation of the procedures, risks, and benefits.

Testing Protocol

If you agree to participate, you will attend one study visit at the Biomechanics/Sports Medicine Lab on the UT campus. Your information from the demographic questionnaire and Physical Activity Readiness Questionnaire (PAR-Q), will be used for this study. The study visit will take approximately 1-1½ hours. You will need to wear clothing appropriate for exercise which includes spandex short and t-shirt. If you do not have spandex type of clothing, a spandex short or laboratory paper short will be provided**.**

We will measure your weight and height. We will place reflective markers on your feet, ankles, legs, knees, thighs, pelvis and trunk. This will allow motion cameras to capture your movements when performing the exercises. The cameras will not record images of you. If you have any questions, interests, or concerns about any equipment to be used in this test, please feel free to ask the investigator or other research personnel.

You will perform stationary cycling of the following conditions for 2 minutes each, at 80 revolutions per minute (rpm):

- Cycle at a Q-Factor of 150 mm.
- Cycle at a Q-Factor of 192 mm.
- Cycle at a Q-Factor of 234 mm.
- Cycle at a Q-Factor of 276 mm.

Trials need to be completed at 80 rpm. During testing trials, you will be asked to pedal within 5% of the established 80 rpm. If you are not within 5%, you will be asked to repeat the trial. It is anticipated that you will not be required to perform more than two minutes at each condition.

A break will be provided in between each testing condition, and you will be asked to remain seated on the cycle ergometer during these breaks. You can end any exercise early and do not have to complete the study visit.

Potential Risks

Risks associated with this study are minimal. There is a small risk of injury but it is no greater than the risk you experience similar recreational activities. You can practice the exercises before the testing and take breaks as needed. If you are injured the study visit, we will provide

standard first aid. In the unlikely event you are injured during the study, the University of Tennessee does not automatically provide reimbursement for medical care or other compensation and you will be responsible for any medical expenses. If you are injured, please notify Tanner Thorsen or his advisor, Dr. Songning Zhang (974-2091).

Every research study involves some risk to your confidentiality. It is possible that other people could find out you are in the study or see your study information. But we will do our best to keep your information confidential to minimize this risk.

Benefits of Participation

You may not benefit from participation in this study directly. However, you may learn about abnormalities that might be corrected with cycling movement modifications. You can receive an individual report of your study results to share with your personal physician. Results from the proposed study may help society better understand the role of obesity and cycling movement modifications such as increased Q-Factor on knee joint loading and function during stationary cycling.

Confidentiality

Your information will be kept confidential. Your research data and records will be stored securely and will be made available only to researchers who work on this study. The motion cameras will not record images of you. Your name will not be in any research data. Instead, a code number will replace your name on your data. Your name will not appear with the study results that will be presented at conferences and published in journals. Your data will be stored using password protected hard drives. Your research information may be used for future research studies [and/or other purposes (education, etc.), if applicable] or shared with other researchers for

use in future research studies without obtaining additional informed consent from you. If this happens, all of your identifiable information will be removed before any future use or distribution to other researchers. If you decide to withdraw from the study, data collected up to that point may be used for research purposes, unless you request that it be destroyed.

Contact Information

If you have any questions about the study at any time or if you experience any problems as a result of participating in this study you can contact Tanner Thorsen or Dr. Songning Zhang at 1914 Andy Holt Ave. 136 HPER Bldg., The University of Tennessee and/or (865) 974-2091. Questions about your rights as a participant can be addressed to Compliance Officer in the Office of Research at the University of Tennessee at (865) 974-7697.

Voluntary Participation and Withdrawal

Your participation is entirely voluntary and your refusal to participate will involve no penalty or loss of benefits to which you are otherwise entitled. You may withdraw from the study at any time without penalty or loss of benefits to which you are otherwise entitled. Your participation in this study may be stopped by if you fail to follow the study procedures or if the principal investigator believes it is in your best interest to stop participation.

Consent Statement

I have read the above information. I agree to participate in this study. I have received a copy of this form.

Subject's Name: _____

Subject's Signature: _____ Date: _____

Investigator's Signature: _____

Appendix C: Flyer

RESEARCH VOLUNTEERS NEEDED



THE UNIVERSITY OF TENNESSEE KNOXVILLE

BIOMECHANICS

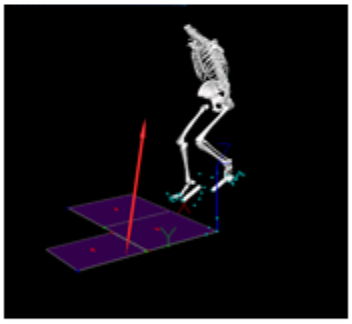
If you are:

- between the ages of 18 and 35
- free from lower extremity injury
- free from lower extremity surgery
- recreationally active
- available for **90 minutes**

UTK Biomechanics

Cycling Research

THE EFFECTS OF INCREASED **Q-FACTOR** ON KNEE JOINT BIOMECHANICS DURING CYCLING



Volunteer, and:

- support student research
- learn how to properly fit your bike
- get a report about your own cycling mechanics

To participate, or more information:

Please email **Tanner Thorsen** at the UT Biomechanics / Sports Medicine Lab:

Email: tthorsen@vols.utk.edu

Tanner Thorsen tthorsen@vols.utk.edu 865-974-2091

Appendix D: Physical Activity Readiness Questionnaire (PAR-Q)

PHYSICAL ACTIVITY READINESS QUESTIONNAIRE (PAR-Q)

Regular physical activity is fun and healthy, and increasingly more people are starting to become more active every day. Being more active is very safe for most people. However, some people should check with their doctor before they start becoming much more physically active.

If you are planning to become much more physically active than you are now, start by answering the seven questions in the box below. If you are between the ages of 15 and 69, the PAR-Q will tell you if you should check with your doctor before you start. If you are over 69 years of age and you are not used to being very active, check with your doctor.

No	Yes	
☐	☐	1. Has your doctor ever said that you have a heart condition <u>and</u> that you should only do physical activity recommended by a doctor?
☐	☐	2. Do you feel pain in your chest when you do physical activity?
☐	☐	3. In the past month, have you had chest pain when you were not doing physical activity?
☐	☐	4. Do you lose your balance because of dizziness or do you ever lose consciousness?
☐	☐	5. Do you have a bone or joint problem that could be made worse by a change in your physical activity?
☐	☐	6. Is your doctor currently prescribing drugs (for example water pills) for your blood pressure of heart condition?
☐	☐	7. Do you know of <u>any other reason</u> why you should not do physical activity?

Please note: If your health changes so that you then answer YES to any of these questions, tell your fitness or health professional. Ask whether you should change your physical activity plan.

If you answered YES to one or more questions

Talk to your doctor by phone or in person BEFORE you start becoming much more physically active of BEFORE you have a fitness appraisal. Tell your doctor about the PAR-Q and which questions you answered YES.

- You may be able to do any activity you want as long as you start slowly and build up gradually. Or you may need to restrict your activities to those which are safe for you. Talk to your doctor about the kinds of activities you wish to participate in and follow his/her advice.
- Find out which community programs are safe and helpful for you.

If you answered NO to all questions

Delay becoming much more active if:

If you have answered NO honestly to all PAR-Q questions, you can be reasonably sure that you can:

- Start becoming much more physical active – begin slowly and build up gradually. This is the safest and easiest way to go.
- Take part if a fitness appraisal – this is an excellent way to determine your basic fitness so that you can plan the best way for you to live actively.

- You are not feeling well because of a temporary illness such as a cold or a fever – wait until you feel better, or
  If you are or may be pregnant – talk to your doctor before you start becoming more active.

I understand that my signature signifies that I have read and understand all the information on the questionnaire, that I have truthfully answered all the questions, and that any question/concerns I may have had have been addressed to my complete satisfaction.

_____

Name (please print)

_____ _____

Signature Date

Appendix E: Borg's 6-20 scale, Comfort, Pain Numeric Visual Analog scale

Condition:_____

How would you rate your ***physical exertion*** during this bout of cycling (RPE)?

6 7 8 9 10 11 12 13 14 15 16 17 18 19 20

How comfortable were you during this bout of cycling? (0 = most comfortable, 10 = most ***un***comfortable)

0 1 2 3 4 5 6 7 8 9 10

How much knee pain did you experience during this bout of cycling? (0 = no pain, 10 = very painful)

0 1 2 3 4 5 6 7 8 9 10

Appendix F: Individual Results for Selected Variables

Table 6: Individual mean peak vertical PRF (N).

Subject	Q150			Q192			Q234			Q276		
	80 W	120 W	160 W	80 W	120 W	160 W	80 W	120 W	160 W	80 W	120 W	160 W
1	273.863	310.156	362.367	251.701	292.456	384.133	222.638	300.498	385.286	241.867	285.482	330.115
2	240.918	271.332	325.130	213.029	239.936	291.101	231.439	311.683	331.251	260.075	290.378	333.743
3	241.527	252.000	322.687	245.011	261.855	331.510	215.236	280.429	297.562	236.749	298.400	324.474
4	256.453	285.746	312.478	214.493	273.894	332.854	258.480	282.148	266.536	229.567	294.457	334.504
5	206.701	256.944	254.699	177.280	251.613	264.939	178.471	208.412	297.200	205.524	246.918	249.145
6	239.122	262.616	287.054	207.435	228.502	262.472	180.742	234.078	258.086	180.856	247.514	301.947
7	185.476	221.513	247.273	198.293	211.863	272.436	192.908	210.333	237.184	176.665	230.741	242.635
8	193.470	252.617	305.636	164.460	211.141	265.074	190.030	208.517	240.399	212.277	227.059	289.555
9	191.682	233.038	257.406	198.201	212.666	272.952	166.807	183.644	248.103	177.432	204.229	269.249
10	215.832	279.483	316.601	187.286	276.881	273.693	239.505	274.251	312.690	194.000	235.646	270.102
11	193.899	208.906	254.728	181.573	241.385	260.052	178.345	230.528	235.351	176.700	227.231	217.320
12	200.951	224.913	297.691	194.758	206.054	279.826	216.502	244.187	279.945	201.034	270.173	300.308
13	211.662	294.267	286.750	172.291	220.137	290.021	198.872	269.470	307.251	213.700	274.548	315.864
14	177.192	214.624	247.662	173.563	247.691	272.483	185.749	243.976	257.962	164.636	230.133	279.170
15	215.902	273.971	286.358	186.681	278.419	293.530	228.055	310.042	332.612	204.426	279.131	282.083
16	192.818	254.749	298.385	191.344	233.264	305.357	206.475	224.666	287.928	215.037	245.415	283.353
Mean	214.842	256.055	291.431	197.337	242.985	290.777	205.641	251.054	285.959	205.659	255.466	288.973
STD	27.886	29.527	32.962	24.568	27.524	33.506	25.903	39.699	41.593	27.006	29.139	34.485

Table 7: Individual mean peak mediolateral PRF (N).

Subject	Q150			Q192			Q234			Q276		
	80 W	120 W	160 W	80 W	120 W	160 W	80 W	120 W	160 W	80 W	120 W	160 W
1	-46.187	-47.795	-71.034	-37.014	-67.940	-96.522	-46.114	-76.222	-112.166	-65.713	-86.121	-101.706
2	-37.336	-42.083	-54.251	-47.272	-52.274	-76.315	-49.420	-83.232	-85.268	-54.266	-58.872	-65.228
3	-28.602	-31.921	-45.859	-47.409	-56.860	-74.305	-41.769	-62.238	-70.512	-55.077	-79.200	-84.062
4	-46.723	-51.135	-51.738	-56.864	-63.702	-81.517	-48.639	-60.857	-55.130	-53.875	-88.504	-96.569
5	-35.008	-42.785	-39.116	-35.172	-44.026	-58.682	-38.142	-44.849	-69.715	-57.997	-56.580	-65.570
6	-48.804	-58.472	-66.760	-47.473	-54.173	-72.125	-47.017	-60.562	-73.096	-55.238	-81.530	-107.710
7	-33.491	-38.889	-42.343	-34.889	-43.267	-59.626	-38.254	-51.456	-58.917	-42.936	-62.492	-72.271
8	-7.764	-11.571	-28.112	-19.120	-26.968	-38.136	-21.987	-39.623	-41.632	-23.623	-38.394	-53.628
9	-34.899	-43.557	-50.336	-43.879	-48.324	-62.855	-39.307	-43.560	-66.903	-43.923	-55.873	-78.371
10	-37.100	-57.674	-73.240	-44.189	-78.909	-81.755	-62.831	-83.905	-98.443	-59.883	-77.206	-98.136
11	-22.833	-28.368	-38.646	-29.241	-38.720	-46.430	-34.352	-52.730	-55.655	-34.674	-57.841	-48.598
12	-17.209	-37.67	-39.764	-28.574	-44.736	-47.880	-31.965	-43.264	-55.398	-23.310	-49.122	-57.408
13	-37.053	-55.833	-52.467	-33.893	-46.186	-66.144	-46.977	-70.165	-81.347	-57.745	-82.055	-101.051
14	-25.872	-38.67	-41.972	-37.457	-60.991	-60.141	-44.694	-68.289	-83.937	-45.898	-70.028	-90.724
15	-38.296	-49.914	-54.482	-35.358	-63.158	-61.091	-48.285	-76.094	-77.287	-56.573	-77.471	-83.326
16	-33.659	-47.975	-58.666	-41.564	-53.923	-73.165	-45.844	-46.413	-73.946	-44.836	-60.489	-74.086
Mean	-33.177	-42.77	-50.549	-38.711	-52.760	-66.043	-42.850	-60.216	-72.460	-48.473	-67.611	-79.903
STD	10.831	12.028	12.523	9.174	12.613	14.911	9.114	14.869	17.705	12.474	14.639	18.518

Table 8: Individual mean power phase COP (cm).

Subject	Q150			Q192			Q234			Q276		
	80 W	120 W	160 W	80 W	120 W	160 W	80 W	120 W	160 W	80 W	120 W	160 W
1	0.016±0.014	0.010±0.010	0.010±0.004	0.015±0.013	0.009±0.008	0.010±0.007	0.024±0.014	0.022±0.004	0.020±0.003	0.021±0.005	0.030±0.004	0.022±0.005
2	0.009±0.008	0.010±0.007	0.010±0.005	0.019±0.005	0.015±0.001	0.027±0.006	0.026±0.005	0.024±0.009	0.030±0.008	0.032±0.006	0.016±0.007	0.021±0.035
3	0.007±0.004	0.001±0.008	0.003±0.004	0.013±0.005	0.020±0.011	0.009±0.018	0.011±0.021	0.001±0.006	0.016±0.025	0.016±0.005	0.015±0.006	0.015±0.006
4	0.010±0.021	0.003±0.008	0.004±0.003	0.011±0.015	0.002±0.002	0.006±0.005	-0.003±0.014	0.011±0.008	-0.003±0.008	-0.001±0.003	0.012±0.013	0.004±0.004
5	0.015±0.009	0.007±0.013	-0.997±1.021	.±.	-0.163±0.000	.±.	0.017±0.009	0.004±0.039	-0.076±0.145	0.026±0.008	0.029±0.040	0.305±0.489
6	0.010±0.005	0.009±0.005	0.006±0.003	0.014±0.006	0.008±0.008	0.017±0.009	0.013±0.003	0.017±0.010	0.016±0.015	0.020±0.005	0.013±0.003	0.031±0.007
7	0.004±0.009	-0.025±0.034	-0.219±0.384	0.007±0.003	0.019±0.019	0.021±0.010	0.044±0.004	0.025±0.093	-2.636±6.173	0.058±0.056	0.052±0.041	0.025±0.091
8	0.030±0.003	0.011±0.007	-0.002±0.011	0.031±0.017	0.033±0.019	0.015±0.007	0.022±0.007	0.050±0.026	0.042±0.015	0.027±0.003	0.025±0.017	0.027±0.014
9	0.019±0.006	0.006±0.006	0.013±0.007	0.013±0.009	0.003±0.024	0.007±0.009	0.029±0.012	-0.024±0.056	2.048±0.000	0.014±0.006	0.034±0.024	-0.067±0.146
10	0.010±0.005	0.012±0.006	0.006±0.004	0.025±0.008	0.009±0.008	0.010±0.010	0.023±0.009	0.014±0.007	0.012±0.006	0.038±0.018	0.021±0.008	0.019±0.007
11	0.024±0.003	0.025±0.003	0.020±0.012	0.024±0.005	0.015±0.012	0.013±0.012	0.030±0.003	0.034±0.008	0.030±0.018	0.029±0.011	0.029±0.006	0.035±0.005
12	0.012±0.002	0.015±0.002	0.010±0.005	0.015±0.009	0.021±0.015	0.006±0.005	0.009±0.006	0.008±0.011	0.008±0.006	0.010±0.006	0.014±0.001	0.014±0.004
13	0.024±0.009	0.013±0.009	0.009±0.020	0.017±0.017	0.017±0.004	0.014±0.006	0.014±0.006	0.031±0.006	0.014±0.025	0.024±0.005	0.019±0.005	0.029±0.033
14	0.006±0.008	-0.011±0.039	-0.067±0.052	-0.024±0.031	-0.103±0.077	-0.168±0.152	0.007±0.020	-0.097±0.189	0.024±0.033	0.001±0.008	-0.031±0.000	-0.019±0.000
15	0.014±0.007	0.012±0.006	0.004±0.006	0.016±0.016	0.021±0.012	0.010±0.013	0.016±0.003	0.019±0.010	0.032±0.011	0.016±0.006	0.020±0.003	0.023±0.009
16	0.010±0.007	0.010±0.009	0.009±0.002	0.012±0.013	0.014±0.013	0.008±0.016	0.006±0.007	0.015±0.009	0.001±0.003	0.007±0.004	0.009±0.004	0.015±0.006
Mean±STD	0.014±0.007	0.007±0.011	-0.074±0.253	0.014±0.012	-0.004±0.052	0.003±0.047	0.018±0.011	0.010±0.033	-0.026±0.862	0.021±0.015	0.019±0.017	0.031±0.077

Table 9: Individual mean knee extension ROM (°).

Subject	Q150			Q192			Q234			Q276		
	80 W	120 W	160 W	80 W	120 W	160 W	80 W	120 W	160 W	80 W	120 W	160 W
1	62.337±1.157	63.379±1.378	63.389±1.307	60.990±1.145	62.410±1.662	64.890±1.195	60.603±1.565	64.616±1.057	64.004±1.086	64.259±1.189	64.873±2.219	64.916±0.833
2	59.880±1.167	61.105±0.722	59.790±0.797	61.066±0.415	64.390±1.571	62.581±0.806	64.061±1.004	62.615±1.059	64.205±1.684	63.260±1.572	63.094±0.494	62.443±1.474
3	71.277±0.566	72.328±0.507	73.444±2.476	73.818±1.784	73.439±1.367	72.539±0.464	72.793±1.176	76.002±1.798	75.793±2.034	74.273±0.802	74.905±1.996	75.647±1.348
4	68.419±0.987	68.527±0.931	67.504±0.467	70.165±0.807	70.296±1.607	68.622±0.584	69.908±0.912	68.511±0.930	68.444±1.075	70.705±1.164	71.366±0.804	68.778±0.653
5	80.125±0.780	77.652±1.874	77.823±2.390	78.412±0.916	79.093±1.984	79.091±1.679	78.605±0.949	78.993±0.798	79.994±0.921	80.684±1.181	82.031±0.693	81.217±1.268
6	68.030±0.938	66.162±0.771	68.912±0.537	70.756±1.294	71.003±0.982	68.415±0.548	69.665±1.164	70.744±1.410	70.529±1.912	70.890±2.234	72.233±0.736	76.492±0.426
7	71.479±0.336	72.217±0.776	69.709±0.625	72.777±0.441	71.262±1.302	71.290±0.791	74.558±0.703	74.600±0.786	72.612±0.411	73.419±0.867	75.671±1.896	74.450±1.522
8	71.540±0.707	66.141±1.374	64.354±0.819	70.456±1.734	68.315±0.857	68.740±1.208	69.323±0.923	69.216±2.107	71.309±0.693	68.271±0.700	69.811±2.303	69.825±1.408
9	67.917±0.975	67.125±0.614	65.208±0.952	69.625±1.205	66.592±0.791	66.616±1.397	68.940±1.215	67.175±1.019	67.312±1.578	68.888±1.047	68.274±1.093	69.490±1.870
10	69.394±0.581	70.479±0.911	68.064±0.944	70.184±0.747	71.656±0.458	70.563±0.969	73.655±0.504	73.015±1.258	71.353±0.727	74.218±1.052	72.162±0.882	71.400±0.561
11	76.517±0.704	77.371±1.068	79.335±0.872	79.320±0.601	79.305±0.613	79.550±0.983	77.054±0.729	79.073±0.786	78.300±1.302	78.169±0.806	79.453±2.049	77.503±0.630
12	75.493±0.479	71.106±0.873	75.304±0.530	74.264±1.156	76.441±0.882	75.147±0.939	78.467±1.439	77.406±2.201	79.604±1.506	76.642±1.793	76.862±1.033	79.210±1.129
13	82.924±1.539	88.812±3.880	87.743±2.558	82.687±1.304	88.422±1.328	89.901±3.161	83.322±1.562	85.441±1.574	92.503±2.931	84.417±1.586	86.237±1.581	91.025±0.733
14	70.609±1.086	68.617±1.086	71.616±1.298	68.930±0.935	69.356±1.928	70.818±0.755	69.276±1.841	71.142±1.819	70.770±2.547	77.522±1.489	72.078±1.749	72.423±2.804
15	72.537±1.070	72.121±0.226	71.942±0.365	70.339±1.146	72.633±1.888	70.989±2.022	72.150±0.961	73.597±0.950	73.578±1.552	71.883±0.448	71.993±1.025	72.542±0.848
16	70.431±1.023	71.654±0.190	72.294±0.830	71.761±0.188	72.039±1.010	72.718±0.479	71.682±0.429	71.345±0.691	71.573±0.723	71.984±0.238	73.103±0.625	75.155±0.508
Mean±STD	71.182±5.804	70.925±6.517	71.027±6.890	71.597±5.684	72.291±6.316	72.029±6.565	72.129±5.631	72.718±5.862	73.243±7.016	73.093±5.630	73.384±5.912	73.907±6.754

Table 10: Individual mean peak frontal plane knee angle (°).

Subject	Q150			Q192			Q234			Q276		
	80 W	120 W	160 W	80 W	120 W	160 W	80 W	120 W	160 W	80 W	120 W	160 W
1	1.104±0.681	0.756±0.484	-0.406±0.445	1.259±0.423	-0.827±0.642	-1.765±0.510	-0.537±0.727	-1.111±0.228	-4.373±2.070	-2.266±0.882	-1.845±0.633	-4.509±0.986
2	6.663±0.798	6.470±1.002	5.808±0.378	5.283±0.650	5.600±0.674	4.633±0.540	8.575±0.525	7.502±0.597	5.930±0.170	7.759±0.443	7.892±0.657	6.114±0.591
3	-1.546±1.222	-0.966±0.647	-0.521±0.799	-2.470±0.487	-2.298±1.394	-1.162±0.408	-3.133±0.940	-2.776±0.946	-1.836±0.547	-3.170±0.865	-3.116±0.873	-1.906±1.023
4	-0.599±0.280	0.310±0.555	-1.520±0.465	-2.369±0.868	-2.231±0.186	-2.268±0.366	-2.516±0.832	-1.481±0.519	-1.543±0.333	-3.745±0.371	-3.670±0.966	-4.023±0.783
5	11.474±0.979	10.239±1.501	10.181±1.267	9.064±0.825	8.440±1.519	8.226±1.341	3.651±1.625	6.344±1.352	7.442±1.515	5.169±1.494	6.456±0.939	5.959±1.708
6	1.528±0.682	1.584±0.303	0.676±0.490	-3.504±0.489	-1.526±1.155	-1.859±0.466	-2.650±0.651	-1.815±0.526	-1.385±0.424	-4.786±1.328	-2.546±1.242	-3.487±0.171
7	-3.894±0.464	-4.835±0.754	-3.906±1.216	-4.896±1.076	-6.161±0.722	-6.261±0.647	-7.829±1.444	-7.132±2.321	-8.217±0.641	-9.700±0.826	-7.545±1.977	-8.269±1.928
8	8.128±0.471	6.385±0.549	4.249±1.383	4.503±0.624	4.933±0.783	5.222±1.118	4.269±0.477	4.023±0.837	1.967±0.571	4.103±0.436	3.747±0.987	2.565±0.817
9	9.770±0.522	8.437±0.548	7.639±1.111	8.897±1.062	8.549±0.918	7.489±0.560	5.873±0.693	6.098±0.804	5.633±0.289	6.169±0.773	6.075±0.424	5.582±1.189
10	-2.024±0.767	-1.552±0.801	-2.621±0.375	-0.813±0.820	-1.118±1.692	-1.111±0.392	0.392±1.268	-0.906±0.775	-1.622±0.515	-2.411±1.184	-0.790±0.743	0.925±6.292
11	3.864±0.760	4.808±0.722	4.262±0.398	5.123±0.658	5.276±0.863	4.650±0.248	2.970±1.665	3.458±0.913	2.577±0.557	3.274±0.853	2.944±0.779	1.949±0.508
12	8.862±0.657	6.972±0.492	7.815±1.165	3.461±0.485	3.610±0.525	5.728±0.709	8.847±1.066	5.182±1.057	6.731±0.134	5.490±0.947	6.272±0.440	7.095±0.277
13	-2.141±0.779	-2.402±0.374	-2.161±0.418	-2.719±0.345	-2.295±0.800	-1.439±0.668	-3.770±0.807	-2.800±0.512	-3.772±0.705	-4.437±1.002	-3.343±0.828	-3.758±0.756
14	4.455±1.207	5.178±0.464	6.314±1.115	7.334±1.887	8.664±1.223	7.447±0.970	5.332±0.461	4.816±2.493	6.725±1.658	6.200±0.902	7.029±0.814	4.905±1.511
15	2.514±0.800	1.428±0.146	1.067±0.390	0.470±0.844	0.594±1.026	-0.524±0.572	-0.219±0.980	-1.107±1.399	-1.837±1.156	-0.146±1.418	-0.656±1.157	-2.771±0.709
16	-6.647±0.274	-5.595±0.612	-6.102±0.369	-5.951±0.703	-5.872±0.422	-7.051±0.777	-5.251±0.000	-5.275±0.256	.±.	-3.633±0.499	-3.981±0.612	-7.028±0.405
Mean±STD	2.594±5.315	2.326±4.758	1.923±4.776	1.417±4.917	1.459±4.997	1.247±4.920	0.875±4.964	0.814±4.504	-0.828±4.837	0.242±5.197	0.808±4.899	-0.041±5.043

Table 11: Individual mean knee abduction ROM (°).

Subject	Q150			Q192			Q234			Q276		
	80 W	120 W	160 W	80 W	120 W	160 W	80 W	120 W	160 W	80 W	120 W	160 W
1	-4.658±1.197	-5.065±0.389	-5.084±0.218	-3.270±0.631	-4.468±0.593	-5.457±0.605	-2.965±0.717	-2.996±0.302	-6.625±2.343	-3.903±1.210	-3.133±0.741	-5.024±0.883
2	-0.942±0.722	-0.589±0.800	-2.178±0.484	0.388±0.790	-0.760±0.604	-1.842±0.242	0.149±0.402	-0.450±0.479	-1.162±0.493	-0.118±0.676	-0.829±0.905	-2.860±0.947
3	-12.560±1.054	-11.922±0.687	-11.692±0.510	-12.696±1.139	-13.019±1.360	-12.659±1.483	-14.482±0.935	-13.698±1.030	-11.231±0.523	-11.292±1.490	-10.184±0.768	-8.842±1.480
4	-2.237±0.755	-0.289±0.699	-2.997±0.502	-0.119±1.066	-1.368±0.576	-0.466±0.632	-2.562±1.167	-1.648±0.689	-1.308±0.755	-1.412±0.240	-0.415±0.844	-0.967±1.239
5	-7.465±1.063	-8.306±1.655	-9.328±1.435	-6.216±1.614	-7.262±2.007	-8.973±2.366	-9.267±1.701	-8.684±1.728	-9.031±1.742	-6.815±2.148	-7.669±1.254	-8.410±2.735
6	-4.735±1.142	-6.019±0.552	-7.015±0.412	-7.667±0.750	-6.724±0.388	-7.347±1.045	-5.316±0.670	-5.835±0.561	-4.451±1.291	-5.647±1.641	-4.392±1.741	-6.412±0.425
7	-7.967±1.143	-9.324±1.243	-9.756±0.736	-7.483±1.190	-9.031±1.301	-7.411±1.328	-6.414±1.343	-7.140±2.392	-8.765±0.980	-7.582±1.403	-6.478±3.010	-8.069±1.453
8	-15.636±0.688	-18.771±0.983	-23.148±1.113	-14.056±1.158	-16.619±0.520	-16.568±1.376	-13.283±0.446	-12.867±2.032	-15.687±1.151	-14.390±1.257	-14.522±0.918	-15.839±0.992
9	-5.959±0.645	-5.688±1.161	-7.981±1.026	-6.109±1.583	-7.464±1.112	-7.538±1.406	-5.005±0.852	-6.598±1.452	-7.791±1.723	-4.983±1.099	-6.015±1.322	-6.543±0.627
10	-16.957±0.971	-16.491±1.700	-17.299±0.995	-15.991±0.981	-15.183±1.693	-15.949±0.449	-13.617±1.674	-14.674±0.925	-16.077±0.645	-10.880±0.536	-13.124±0.584	-11.815±6.481
11	-13.890±1.005	-14.416±0.728	-13.500±1.179	-12.661±0.620	-10.865±1.384	-11.585±0.585	-12.984±2.475	-10.848±1.216	-12.234±0.311	-10.469±1.231	-10.637±0.776	-11.176±1.018
12	-8.233±1.071	-8.134±0.477	-7.955±0.656	-11.385±0.686	-10.946±0.997	-8.815±0.833	-8.718±1.079	-9.351±1.145	-9.252±0.343	-9.432±0.675	-7.921±0.390	-6.664±0.376
13	-8.264±0.679	-10.496±3.491	-8.854±0.948	-6.234±0.818	-8.873±1.578	-7.095±0.831	-4.974±1.165	-3.965±0.519	-7.964±0.847	-2.771±1.109	-3.736±1.326	-3.111±0.904
14	-8.643±1.891	-5.220±0.418	-6.626±0.854	-6.756±3.568	-7.145±1.421	-6.373±2.308	-7.467±0.298	-7.045±2.506	-8.764±2.223	-5.923±0.894	-6.678±0.748	-7.375±2.136
15	-6.019±0.893	-6.937±0.440	-7.664±0.209	-5.594±0.507	-5.884±0.924	-6.707±0.487	-5.797±0.996	-6.092±1.599	-6.905±0.799	-4.417±1.550	-6.727±1.327	-4.895±0.852
16	-0.147±0.352	-0.285±0.398	0.517±0.421	0.285±0.437	0.696±0.150	0.571±0.435	1.152±0.000	0.751±0.340	.±.	0.805±0.723	1.421±0.244	0.999±0.223
Mean±STD	-7.769±4.957	-7.997±5.498	-8.785±5.765	-7.223±5.081	-7.807±4.908	-7.763±4.849	-6.972±4.828	-6.946±4.623	-8.483±4.312	-6.202±4.297	-6.315±4.453	-6.688±4.207

Table 12: Individual mean knee external rotation ROM (°).

Subject	Q150			Q192			Q234			Q276		
	80 W	120 W	160 W	80 W	120 W	160 W	80 W	120 W	160 W	80 W	120 W	160 W
1	-4.50±1.96	-1.43±1.48	-1.36±3.45	-1.44±4.41	-1.16±1.67	-0.72±1.08	-0.50±1.64	0.50±0.32	8.16±44.88	-0.15±1.26	0.15±0.20	0.85±0.73
2	.±.	-0.77±3.39	0.89±0.82	-1.87±4.88	-0.70±0.04	0.32±0.18	-0.60±0.99	0.60±0.40	1.23±0.90	1.37±0.04	2.53±0.00	0.89±0.00
3	-12.10±2.37	-7.85±1.42	-8.14±0.33	-10.83±2.42	-3.31±3.60	-5.40±2.36	-10.45±5.42	-9.94±1.02	-2.81±4.06	-6.58±2.84	-4.22±2.27	-6.10±3.40
4	-0.65±2.87	-0.92±1.69	-1.85±2.89	-0.83±2.49	-1.13±1.41	-1.44±0.99	0.44±1.95	-0.24±1.42	-2.43±0.63	-1.24±2.06	0.61±0.93	-0.40±0.98
5	-4.28±15.45	-1.08±0.00	-6.57±7.48	2.11±1.94	0.37±0.00	0.42±3.92	-8.01±6.60	-2.92±7.02	-2.35±5.31	-7.82±7.73	-6.36±6.27	-3.75±7.09
6	0.26±0.00	-1.74±4.24	-2.83±3.78	0.54±0.38	-3.15±3.43	-4.27±2.66	-1.58±3.41	-2.59±2.53	-0.24±2.03	-0.55±2.57	0.41±0.36	-5.16±1.11
7	1.19±0.29	1.08±0.78	3.75±1.56	2.72±0.94	2.16±1.04	4.56±1.33	3.80±1.45	3.50±2.12	5.61±1.65	3.95±0.89	4.70±2.34	4.45±1.71
8	0.90±0.91	1.67±0.87	.±.	-0.57±1.73	-0.29±0.18	-17.78±1.36	0.57±1.54	-11.00±0.00	-16.65±0.49	-5.89±7.00	-13.25±0.31	-14.49±1.55
9	1.21±1.03	1.80±0.28	0.22±1.61	0.06±1.40	-2.74±9.66	-5.90±8.75	-6.60±8.25	-9.33±9.38	-6.63±8.54	-0.33±0.81	-4.45±6.65	-8.00±5.75
10	-5.59±1.06	-4.88±0.34	-2.73±0.99	-8.36±0.64	-5.93±2.11	-4.81±1.36	-7.58±0.52	-4.05±1.55	-1.45±0.93	-2.56±2.06	-3.51±1.92	-2.88±2.03
11	0.69±0.17	0.68±0.26	0.63±0.37	.±.	0.37±0.21	0.59±0.39	1.31±0.46	-0.02±2.03	0.95±0.23	0.34±0.12	0.82±0.19	0.51±0.12
12	.±.	-3.15±7.36	0.39±0.00	.±.	.±.	1.07±0.05	1.59±0.00	-0.46±0.16	0.46±0.74	.±.	0.84±0.48	0.41±1.19
13	-3.58±2.26	-5.59±3.06	-0.13±0.33	-4.97±3.07	-4.52±1.85	-1.41±0.45	-1.99±1.00	-0.73±1.27	-4.44±3.64	-0.09±0.57	-1.17±1.41	-0.35±0.97
14	-11.02±7.73	-14.09±0.56	-16.05±0.55	-13.47±7.87	-17.57±0.94	-0.62±0.00	-12.59±1.66	0.26±0.00	-12.03±8.64	.±.	-7.75±11.30	-17.30±0.00
15	0.18±1.00	.±.	.±.	-3.60±2.73	-3.83±4.56	-0.57±0.82	-3.57±4.89	-1.91±1.78	-3.26±2.88	.±.	-10.23±0.00	-3.88±0.39
16	.±.	.±.	.±.	.±.	.±.	.±.	.±.	.±.	.±.	.±.	.±.	.±.
Mean±STD	-3.12±4.37	-2.59±4.20	-2.59±4.92	-3.0±4.796	-2.89±4.57	-2.52±4.92	-3.01±4.71	-2.60±4.14	-2.33±5.96	-1.63±3.33	-2.19±4.84	-3.66±5.73

Table 13: Individual mean peak ankle eversion angle (°).

Subject	Q150			Q192			Q234			Q276		
	80 W	120 W	160 W	80 W	120 W	160 W	80 W	120 W	160 W	80 W	120 W	160 W
1	-4.055±0.68	-3.979±0.87	-3.814±1.14	-4.968±0.78	-2.102±0.44	-2.135±0.62	-2.765±0.60	-2.657±0.41	-0.054±1.48	-2.481±1.04	-2.762±0.61	-1.478±0.78
2	4.374±0.90	2.327±1.63	3.071±0.19	5.228±0.65	1.079±0.42	0.991±0.78	-0.507±0.89	1.685±0.96	2.762±1.63	-0.254±0.57	-0.954±1.16	0.875±1.58
3	-1.531±0.77	-0.865±1.69	-1.799±0.82	0.666±1.16	0.058±0.82	1.974±1.69	-1.572±1.10	-0.722±1.10	0.578±1.04	-0.445±1.12	0.040±0.67	0.851±0.86
4	-2.882±0.54	-5.237±0.76	-3.930±0.35	-3.178±0.66	-2.636±1.34	-3.095±0.97	-3.931±0.66	-4.784±0.86	-3.170±0.65	-2.389±0.68	-0.787±1.78	-2.116±0.85
5	-0.402±0.30	1.019±1.76	-1.764±1.59	0.491±2.3	2.607±1.82	1.895±1.22	2.607±3.28	2.387±0.79	2.302±1.86	2.618±2.24	3.554±1.07	2.495±0.71
6	-5.772±0.50	-3.381±1.09	-7.499±0.71	-8.132±0.769	-6.616±1.11	-5.438±0.66	-5.377±0.55	-7.571±0.89	-7.272±0.38	-3.668±1.43	-5.466±0.82	-2.482±0.40
7	-7.006±0.36	-5.027±1.39	-6.467±1.49	-3.787±1.70	-2.441±1.44	-3.440±0.45	-0.887±1.17	-1.212±0.84	1.076±1.08	7.979±1.90	6.565±0.94	9.068±2.29
8	-4.737±0.41	-2.482±1.12	-1.358±0.94	-1.779±0.43	-2.226±0.72	-2.314±0.85	1.303±0.54	2.181±1.21	4.794±1.05	0.086±0.94	1.560±0.35	0.681±1.44
9	-1.145±1.21	0.320±0.51	-0.388±0.67	0.220±1.74	0.420±1.05	0.699±1.12	-1.135±0.64	-0.369±1.15	-1.919±1.30	0.005±1.02	-0.422±0.53	0.904±1.11
10	-0.933±0.42	-0.496±0.96	1.334±0.68	-1.734±0.88	-2.525±0.97	-0.671±0.09	-1.495±0.64	-2.160±1.29	-0.531±0.94	4.198±2.57	-3.189±0.72	-0.701±0.56
11	8.416±0.49	6.665±1.08	6.713±0.41	6.364±0.48	5.452±0.88	6.890±0.27	7.034±1.15	8.092±0.33	7.935±0.95	7.631±0.97	8.713±0.68	8.263±0.57
12	-1.932±0.55	4.181±0.57	1.302±1.00	6.606±1.03	5.173±5.45	2.079±1.12	-1.282±1.57	4.619±1.35	0.636±0.55	0.856±1.08	2.258±1.03	-2.696±0.35
13	-1.794±0.62	-2.189±1.08	-2.749±1.34	-0.452±1.01	-1.568±1.70	-2.863±1.28	-1.171±0.98	-2.712±1.04	-0.081±1.25	0.181±1.65	-0.265±0.36	-0.376±0.78
14	-1.754±1.53	-3.583±0.63	-4.818±1.36	-5.292±2.27	-4.930±1.06	-6.280±2.32	-1.743±2.37	-3.684±2.48	-1.182±2.01	-1.015±0.46	-0.522±1.06	-0.379±1.35
15	-3.682±0.79	-4.407±1.65	-1.080±0.58	-4.965±0.82	-1.214±2.46	-5.619±1.75	-1.579±1.17	0.929±2.60	-0.446±1.95	0.353±2.11	0.488±2.00	1.698±1.37
16	0.347±0.45	0.389±0.54	2.112±0.27	-9.415±0.34	-9.314±0.63	-7.651±0.37	-10.947±0.63	-11.229±0.43	-10.313±0.54	-11.904±0.60	-11.113±0.55	-9.603±0.35
Mean±STD	-1.531±3.74	-1.047±3.41	-1.321±3.67	-1.508±4.75	-1.299±3.87	-1.561±3.83	-1.466±3.75	-1.076±4.64	-0.305±4.27	0.109±4.585	-0.144±4.563	0.313±4.27

Table 14: Individual mean hip abduction ROM (°).

Subject	Q150			Q192			Q234			Q276		
	80 W	120 W	160 W	80 W	120 W	160 W	80 W	120 W	160 W	80 W	120 W	160 W
1	5.007±2.044	5.764±0.897	2.979±0.475	3.160±1.271	1.774±0.774	2.639±1.419	1.457±1.266	2.351±0.792	2.476±1.949	3.251±1.806	1.328±0.278	0.864±0.705
2	1.427±0.903	0.905±0.759	0.827±0.321	0.989±0.426	1.454±0.465	0.176±0.516	0.800±0.841	0.320±0.280	0.672±0.397	0.818±0.700	0.106±0.665	0.163±0.402
3	-0.574±1.862	0.115±0.313	0.153±0.372	0.150±0.204	0.422±0.477	0.652±1.044	0.716±0.804	0.075±0.101	0.059±0.081	0.537±0.295	-4.024±5.749	0.149±0.156
4	6.343±1.778	6.059±0.642	3.321±0.688	3.808±2.354	4.910±2.742	2.781±1.361	8.520±0.594	5.883±1.292	4.803±1.346	8.338±0.646	4.923±0.461	4.405±1.596
5	7.469±2.980	0.783±0.637	0.834±0.394	0.573±0.466	0.779±1.332	3.905±3.343	0.035±0.232	-0.045±0.270	0.359±0.452	-0.204±1.320	0.211±0.264	-0.005±0.095
6	1.398±0.638	2.072±0.496	1.852±0.428	1.033±0.672	1.483±0.792	0.841±0.606	1.567±0.199	1.190±0.570	0.916±1.009	0.635±0.501	1.195±0.508	1.524±0.873
7	5.821±1.110	4.388±1.017	3.711±1.240	6.338±0.701	3.768±2.262	1.795±1.255	3.775±0.753	2.707±1.005	2.130±1.475	3.443±0.894	3.457±1.617	3.026±1.357
8	1.895±0.410	2.157±0.435	1.946±0.717	2.070±1.424	2.239±0.622	2.094±0.887	3.110±1.293	1.693±0.766	1.323±0.757	1.720±0.341	2.452±0.959	2.433±0.552
9	1.012±0.643	2.015±0.377	1.337±0.337	1.579±0.805	1.614±0.406	1.551±0.526	0.756±0.737	0.973±0.217	1.500±0.733	1.124±0.538	1.640±0.682	1.216±0.782
10	1.212±0.488	2.498±0.913	1.457±1.163	0.922±0.417	1.163±0.793	1.919±0.466	1.206±0.763	1.518±0.440	2.466±0.942	0.334±0.141	0.858±0.471	0.919±0.628
11	-0.779±0.649	-1.205±1.051	-0.368±0.738	-3.297±3.028	-0.050±0.185	-0.471±1.010	-0.326±0.342	0.004±0.120	-0.345±0.551	0.010±0.018	-0.031±0.034	-0.065±0.186
12	0.753±1.749	0.429±0.292	0.418±0.322	2.624±1.329	4.077±1.074	1.048±0.820	0.902±0.676	1.513±1.264	1.203±0.454	1.671±1.028	0.879±0.201	1.170±0.442
13	1.331±0.602	2.831±1.553	1.182±1.057	5.145±1.435	1.514±0.530	0.752±1.134	1.844±1.047	0.070±0.168	1.999±1.870	0.978±0.791	0.279±0.394	0.916±0.938
14	6.763±2.693	2.089±0.947	6.174±2.088	5.827±3.853	2.676±0.827	4.597±2.392	1.565±2.214	4.398±2.636	2.608±0.882	6.466±1.298	3.474±1.682	2.392±1.978
15	10.431±0.852	8.247±0.403	8.360±1.412	5.243±2.160	6.785±2.669	4.757±2.454	8.786±1.703	7.501±1.243	5.679±0.956	8.453±2.249	8.221±1.092	3.684±2.064
16	0.079±0.055	0.387±0.177	0.495±0.411	0.277±0.171	0.226±0.121	0.312±0.277	0.150±0.116	0.267±0.134	0.380±0.468	0.268±0.087	0.099±0.139	0.174±0.201
Mean±STD	3.099±3.359	2.471±2.508	2.167±2.324	2.278±2.549	2.177±1.859	1.834±1.564	2.179±2.736	1.901±2.240	1.764±1.637	2.365±2.890	1.567±2.662	1.435±1.378

Table 15: Individual mean peak knee extension moment (Nm).

Subject	Q150			Q192			Q234			Q276		
	80 W	120 W	160 W	80 W	120 W	160 W	80 W	120 W	160 W	80 W	120 W	160 W
1	33.177±1.89	43.175±9.33	60.714±6.42	33.619±5.67	44.907±11.03	55.556±3.72	25.412±4.69	43.479±9.20	59.686±8.34	33.27±8.00	48.23±12.42	47.565±8.713
2	38.571±6.84	38.176±10.13	45.670±8.52	34.109±6.25	36.177±18.94	52.797±7.38	41.687±12.85	58.050±10.20	54.916±4.45	49.73±5.60	48.80±8.87	55.962±12.67
3	26.241±6.90	40.547±3.67	38.071±8.02	29.584±10.91	31.247±4.93	41.681±5.79	24.455±8.51	43.654±7.39	39.749±8.80	32.69±11.73	40.67±13.53	42.459±15.70
4	18.276±3.48	33.195±7.90	27.023±6.29	32.428±5.76	37.345±6.42	45.172±13.31	27.951±7.61	36.009±4.67	32.427±10.02	19.88±3.59	50.70±7.21	54.656±4.15
5	18.837±10.30	24.964±7.62	23.011±11.27	18.531±3.74	23.767±6.82	22.982±4.94	5.809±2.83	20.594±5.20	22.373±6.19	18.48±6.29	22.90±3.41	22.481±8.60
6	23.516±3.58	23.629±6.72	26.102±3.94	22.386±3.24	23.603±6.60	26.731±4.15	17.521±3.58	24.891±4.40	31.599±6.08	16.95±6.97	28.068±1.12	28.558±4.13
7	28.182±6.17	35.815±7.99	30.282±4.20	26.477±3.79	32.027±3.45	37.734±4.54	31.040±6.88	31.547±9.42	35.873±1.61	30.56±4.91	39.269±2.86	36.792±1.50
8	20.839±5.41	23.166±3.84	25.353±1.74	21.010±6.06	25.296±2.93	28.718±2.71	23.324±2.80	26.199±4.39	31.702±3.99	16.12±1.74	27.504±6.05	30.239±4.39
9	20.835±4.26	26.420±6.01	26.569±3.48	17.285±3.23	21.318±9.35	29.634±6.13	20.187±6.16	24.308±8.41	33.321±6.58	20.22±3.84	25.167±8.07	36.997±5.72
10	-2.328±2.57	5.659±2.83	1.864±1.60	2.012±1.86	5.755±2.09	8.049±1.61	3.020±1.63	2.091±3.15	0.682±1.40	6.31±2.40	1.421±0.50	5.389±1.40
11	16.872±4.52	21.518±4.14	36.895±5.41	16.280±1.99	24.529±6.02	24.749±5.58	15.238±5.67	25.819±3.02	26.911±3.40	14.54±1.72	26.427±3.10	20.785±3.91
12	15.383±2.01	14.825±6.07	36.483±7.08	17.949±4.23	27.961±5.95	41.152±8.82	23.238±1.84	29.404±6.65	30.927±5.46	13.96±4.56	28.736±4.38	34.664±3.32
13	23.155±6.23	36.630±7.08	35.048±2.73	18.377±1.78	25.423±6.52	37.767±9.19	24.144±3.11	37.295±3.61	40.292±3.44	27.74±6.38	37.751±3.30	42.663±9.93
14	16.398±12.53	34.324±7.49	36.717±15.69	22.426±5.40	34.443±3.14	38.574±7.25	16.721±5.56	29.498±4.47	34.271±4.95	29.20±6.71	39.176±8.19	43.052±6.79
15	27.047±6.01	35.621±2.90	34.954±3.29	19.372±5.09	40.102±14.22	31.924±6.45	30.768±4.30	42.152±13.43	48.001±9.24	27.56±7.63	35.028±8.94	36.366±4.31
16	15.172±1.82	30.021±2.37	34.591±4.29	23.799±2.11	30.663±3.25	47.081±0.92	18.175±2.56	16.809±3.38	40.341±6.62	25.01±3.98	29.388±2.32	35.182±1.34
Mean±STD	21.261±9.10	29.230±10.00	32.459±12.27	22.228±8.06	29.035±9.11	35.644±12.15	21.793±9.45	30.738±12.95	35.192±13.43	23.89±10.32	33.078±12.24	35.863±12.80

Table 16: Individual mean peak knee abduction moment (Nm).

Subject	Q150			Q192			Q234			Q276		
	80 W	120 W	160 W	80 W	120 W	160 W	80 W	120 W	160 W	80 W	120 W	160 W
1	-14.647±0.84	-17.917±2.35	-20.659±1.51	-15.414±0.92	-20.765±1.74	-28.818±3.41	-15.451±2.76	-23.608±4.10	-30.412±2.68	-19.460±2.06	-26.059±5.43	-28.485±5.58
2	-8.917±1.61	-11.024±2.45	-12.512±2.81	-12.988±2.41	-15.131±6.50	-21.128±2.63	-15.545±5.82	-21.946±5.04	-22.283±3.24	-16.236±2.10	-17.811±2.24	-16.681±4.37
3	-6.190±1.39	-6.475±0.65	-10.570±2.09	-9.043±1.26	-12.526±1.80	-15.184±2.47	-9.844±1.45	-15.732±2.04	-18.074±2.57	-13.435±3.62	-18.916±6.83	-20.573±5.61
4	-15.220±1.40	-19.601±1.94	-17.543±1.19	-21.245±1.44	-21.084±3.06	-25.852±5.29	-17.696±3.00	-18.600±2.21	-16.726±1.34	-21.054±1.63	-24.837±3.04	-25.311±2.26
5	-10.768±6.08	-11.210±1.33	-10.691±5.80	-9.042±1.73	-11.709±5.15	-16.939±5.24	-9.800±2.77	-11.484±3.13	-18.967±5.03	-15.965±5.35	-16.644±1.47	-19.486±3.59
6	-10.928±2.49	-12.775±1.44	-15.426±0.86	-9.239±2.02	-11.379±0.82	-14.076±2.48	-9.589±1.34	-13.434±2.52	-18.379±3.94	-10.019±2.67	-17.675±1.85	-25.168±2.43
7	-7.782±0.92	-7.749±1.81	-11.299±1.85	-8.957±0.83	-8.394±0.57	-13.236±2.16	-8.715±1.85	-11.217±1.47	-12.301±1.17	-10.102±1.63	-11.429±1.47	-17.066±2.40
8	-5.418±1.53	-6.414±1.31	-10.029±1.14	-5.986±1.45	-8.927±1.61	-11.844±2.22	-7.148±0.70	-10.568±2.19	-10.830±0.61	-6.169±0.74	-9.094±2.13	-11.834±1.92
9	-10.188±1.81	-13.237±1.82	-15.051±0.89	-12.399±3.22	-13.352±3.17	-18.964±2.22	-11.507±2.66	-12.828±3.61	-19.457±1.84	-12.909±1.27	-17.647±4.09	-22.902±3.76
10	-10.349±0.99	-17.899±1.83	-22.521±2.12	-14.197±3.58	-27.294±1.51	-26.777±1.15	-21.721±2.92	-30.272±3.41	-34.447±1.62	-19.588±4.15	-27.252±3.16	-35.415±1.10
11	-4.215±0.58	-6.794±1.05	-9.702±1.99	-6.682±0.98	-8.198±1.82	-9.394±1.26	-9.039±2.10	-12.826±1.46	-13.069±2.36	-8.430±1.12	-14.945±2.13	-9.907±1.40
12	-6.406±0.63	-6.813±2.44	-10.601±2.10	-5.186±1.54	-9.998±2.37	-12.517±3.68	-10.902±1.46	-11.483±2.54	-14.410±3.31	-4.658±1.10	-11.726±1.99	-17.394±1.61
13	-9.379±3.36	-13.641±3.31	-10.949±0.21	-9.188±0.64	-10.687±1.18	-18.558±4.46	-12.430±1.35	-17.160±1.80	-19.409±1.53	-14.229±2.47	-18.770±2.05	-23.357±3.97
14	-7.593±3.55	-12.972±4.25	-17.037±8.29	-12.094±2.52	-21.527±2.00	-19.699±3.53	-15.073±4.45	-21.123±3.43	-24.735±3.76	-16.388±3.45	-23.721±4.36	-28.985±5.62
15	-9.857±1.50	-13.849±1.03	-14.663±3.52	-11.073±1.30	-17.771±5.17	-17.938±4.02	-12.138±1.05	-18.003±6.05	-19.018±3.40	-14.838±3.37	-22.545±4.84	-21.445±2.81
16	-10.975±0.94	-13.420±0.94	-12.898±0.43	-12.971±1.50	-14.505±1.51	-18.776±2.54	-16.472±1.02	-16.162±1.20	-23.817±1.88	-15.766±1.18	-19.663±1.37	-22.871±1.11
Mean±STD	-9.302±3.03	-11.987±4.27	-13.884±3.92	-10.981±4.01	-14.578±5.61	-18.106±5.53	-12.692±3.94	-16.653±5.46	-19.771±6.32	-13.703±4.76	-18.671±5.29	-21.680±6.45

Table 17: Individual mean peak knee external rotation moment (Nm).

Subject	Q150			Q192			Q234			Q276		
	80 W	120 W	160 W	80 W	120 W	160 W	80 W	120 W	160 W	80 W	120 W	160 W
1	12.781±0.580	14.823±1.451	18.977±1.491	12.983±1.445	19.520±1.700	25.148±1.755	13.401±2.513	20.324±1.207	30.520±2.545	17.82±2.15	23.043±3.033	26.422±4.802
2	9.329±1.198	11.519±3.140	14.625±3.318	10.640±2.138	15.723±8.421	21.399±3.232	14.661±5.365	23.615±6.228	24.805±3.154	15.35±1.30	17.559±3.022	19.877±2.888
3	6.783±1.779	7.379±1.047	9.997±1.110	10.689±2.788	14.752±3.541	19.676±2.782	10.630±4.714	17.259±2.493	17.733±2.724	14.33±5.91	19.912±6.244	22.597±5.869
4	17.348±2.330	17.658±1.567	17.946±1.691	15.785±1.908	18.398±3.861	24.210±6.163	14.940±1.979	19.265±3.509	17.923±1.943	16.73±0.80	22.209±3.351	27.730±1.347
5	7.927±0.761	9.331±1.881	6.250±2.412	6.541±1.612	8.132±1.771	11.087±2.524	9.508±1.749	7.808±1.107	13.715±2.345	11.79±1.80	9.235±1.352	11.363±2.344
6	12.398±0.925	14.110±2.259	14.868±0.983	13.957±1.161	14.798±3.592	19.695±2.199	12.461±1.828	16.174±1.454	18.217±4.035	13.80±2.69	19.548±1.372	21.981±1.392
7	9.263±2.018	9.946±1.711	11.951±1.920	8.741±2.100	10.900±1.064	16.177±3.020	8.937±1.756	12.917±3.030	14.711±0.754	9.96±1.77	15.138±1.613	17.816±1.622
8	-1.562±0.610	.±.	-3.119±0.286	-0.610±0.632	1.484±0.839	3.146±1.918	0.287±0.664	2.794±1.883	2.309±0.847	-0.04±0.60	1.740±1.715	2.082±1.442
9	6.833±0.409	9.056±1.389	11.151±0.993	9.324±1.521	10.902±2.285	14.656±1.418	9.045±1.573	9.399±2.829	16.513±1.637	9.325±1.15	13.602±2.008	16.919±2.650
10	9.471±1.058	16.106±1.639	19.646±1.224	12.120±2.316	22.360±1.603	23.030±0.758	16.524±0.929	23.144±2.300	28.039±1.275	13.81±2.67	22.493±2.370	29.483±1.899
11	2.758±0.210	3.782±0.561	3.843±0.964	3.998±0.661	4.015±1.118	6.093±1.022	6.095±0.821	8.601±0.575	9.915±2.554	5.71±0.78	9.572±1.363	7.151±0.998
12	2.458±0.371	7.920±1.427	4.265±0.554	3.216±1.442	6.624±1.529	7.601±3.028	6.346±1.181	6.896±1.505	10.087±2.413	2.46±1.17	8.776±1.564	10.723±1.021
13	6.490±1.624	9.689±2.755	9.306±0.480	5.822±0.607	8.970±0.825	11.974±2.663	7.453±0.738	11.654±0.858	13.515±1.988	9.14±1.47	13.983±1.697	16.947±3.197
14	7.312±2.396	10.841±3.196	11.801±4.726	13.383±0.866	17.944±2.041	19.097±3.114	13.514±3.869	19.734±3.383	24.465±4.806	11.94±1.84	17.110±2.530	22.935±3.100
15	11.163±1.373	14.835±1.243	15.212±2.270	11.185±1.498	17.507±4.600	18.006±3.246	13.074±0.932	20.514±6.472	20.321±2.411	14.80±3.90	20.937±3.785	21.243±2.154
16	11.250±0.744	14.078±0.781	16.253±2.044	14.183±2.096	18.404±1.171	20.988±2.844	16.333±0.841	17.276±0.824	25.376±1.610	14.53±1.11	19.539±1.591	21.113±1.444
Mean±STD	8.250±4.545	11.405±3.787	11.436±6.223	9.497±4.588	13.152±6.051	16.374±6.679	10.826±4.393	14.836±6.353	18.010±7.444	11.35±5.04	15.900±6.065	18.524±7.521

Table 18: Individual mean peak ankle eversion moment (Nm).

Subject	Q150			Q192			Q234			Q276		
	80 W	120 W	160 W	80 W	120 W	160 W	80 W	120 W	160 W	80 W	120 W	160 W
1	-1.446±0.70	-1.874±0.36	-1.417±0.17	-2.319±1.54	-3.920±0.45	-4.063±2.33	-4.702±0.81	-6.805±0.83	-10.103±3.29	-7.644±1.28	-7.820±4.00	-10.009±1.01
2	-1.068±0.32	-1.359±0.38	-0.984±0.33	-6.979±0.85	-6.898±1.30	-8.635±0.78	-4.261±1.10	-6.015±1.61	-6.589±0.78	-3.350±0.68	-3.181±0.31	-2.793±0.36
3	0.732±0.67	0.875±0.15	0.541±0.62	-1.243±0.18	-1.578±0.82	-2.344±0.55	-2.522±0.62	-1.904±1.70	-4.560±0.52	-4.527±0.73	-5.452±0.78	-6.433±1.34
4	-5.497±1.24	-6.765±0.76	-7.417±0.34	-10.292±0.53	-10.532±1.03	-12.865±2.03	-8.219±1.38	-7.779±0.82	-7.354±0.22	-12.681±0.96	-14.030±0.81	-15.157±0.95
5	-2.398±0.92	-2.150±0.44	-1.885±0.35	-2.244±0.74	-2.997±0.85	-3.381±0.59	-4.590±0.94	-3.696±0.78	-5.487±1.16	-6.701±0.84	-7.186±0.98	-5.745±3.15
6	-0.408±0.24	-0.300±0.34	-0.202±0.03	-2.490±0.57	-1.657±0.39	-1.742±0.19	-3.338±0.65	-3.315±0.30	-3.612±0.97	-4.394±0.48	-5.074±0.23	-4.518±0.50
7	-3.527±0.28	-4.113±0.58	-4.304±0.65	-5.007±0.37	-4.713±0.61	-6.004±0.67	-6.027±0.56	-6.770±0.58	-7.616±0.62	-8.382±0.48	-8.987±0.63	-10.975±1.52
8	1.702±0.15	2.360±0.16	2.875±0.44	1.094±0.37	1.047±0.20	0.902±0.13	0.137±0.11	-0.432±0.51	-0.301±0.16	-0.515±0.08	-0.224±0.16	-0.232±0.35
9	-0.413±0.21	-0.233±0.09	-0.385±0.14	-2.108±0.42	-1.858±0.15	-2.552±0.28	-3.009±0.47	-3.137±0.66	-5.310±5.92	-4.652±0.34	-5.856±0.84	-6.550±0.44
10	-0.364±0.14	-1.333±0.32	-2.616±0.52	-2.801±0.74	-5.605±0.94	-5.779±0.89	-6.494±0.57	-8.729±0.85	-9.769±0.64	-8.052±1.21	-8.660±0.92	-12.830±0.57
11	1.518±0.16	1.621±0.12	0.977±0.06	0.919±0.42	1.360±0.39	0.672±0.10	-0.663±0.98	0.373±0.17	0.238±0.04	-0.743±0.25	-0.412±0.51	-0.414±0.18
12	0.792±0.18	0.596±0.22	0.745±0.18	0.535±0.22	-0.139±0.38	0.005±0.15	-1.625±0.39	-2.326±0.99	-2.119±0.85	-2.780±0.46	-3.661±0.33	-3.972±0.44
13	0.070±0.17	-0.291±0.18	0.103±0.37	-1.425±0.17	-1.115±0.31	-2.238±0.25	-1.544±0.28	-1.734±0.59	-1.092±0.55	-3.649±0.79	-3.165±0.35	-3.153±0.84
14	-1.063±0.41	-1.716±0.36	-0.679±0.18	-3.503±0.71	-3.741±0.20	-3.794±0.40	-4.617±0.29	-3.266±1.48	-6.391±0.49	-5.753±0.53	-8.486±1.14	-8.287±1.78
15	-1.473±0.25	-1.656±0.29	-2.150±0.92	-2.906±0.39	-4.198±0.95	-4.266±0.41	-4.208±0.56	-5.869±1.62	-5.292±0.34	-6.349±1.09	-9.871±2.32	-8.864±1.33
16	-4.912±0.14	-6.341±0.24	-7.248±0.35	-4.462±0.31	-5.293±0.24	-6.321±0.70	-6.412±0.31	-6.239±0.23	-9.538±0.87	-7.618±0.71	-9.173±0.39	-9.731±0.31
Mean±STD	-1.110±2.10	-1.417±2.55	-1.503±2.81	-2.827±2.91	-3.240±3.06	-3.900±3.54	-3.881±2.28	-4.228±2.70	-5.306±3.27	-5.487±3.09	-6.327±3.66	-6.854±4.29

Table 19: Individual mean peak ankle external rotation moment (Nm).

Subject	Q150			Q192			Q234			Q276		
	80 W	120 W	160 W	80 W	120 W	160 W	80 W	120 W	160 W	80 W	120 W	160 W
1	-4.525±0.44	-6.346±0.98	-7.621±0.54	-4.529±2.28	-7.277±0.88	-10.618±0.87	-5.374±0.92	-9.167±1.13	-12.650±0.87	-8.278±1.40	-11.487±2.11	-11.890±2.40
2	-3.128±0.41	-5.005±0.89	-4.946±2.26	-6.057±2.96	-8.315±3.46	-11.516±1.31	-7.141±2.14	-11.369±2.48	-11.059±1.39	-7.241±0.77	-9.568±1.50	-7.805±1.22
3	-2.844±0.48	-2.731±0.50	-4.777±1.02	-4.188±0.50	-5.675±1.24	-5.645±2.79	-5.056±1.01	-7.359±1.12	-8.562±1.16	-6.827±2.05	-9.684±3.34	-9.659±2.98
4	-6.789±0.98	-8.304±1.07	-7.654±0.92	-8.833±1.33	-9.169±1.73	-12.074±2.96	-7.196±1.59	-9.774±0.86	-7.477±1.13	-8.698±0.56	-13.665±1.59	-15.670±0.76
5	-3.657±1.44	-4.635±0.53	-4.407±1.83	-3.884±0.40	-4.667±1.58	-7.102±1.90	-4.755±0.50	-5.358±0.99	-8.202±1.31	-6.780±1.83	-7.443±0.52	-8.524±1.38
6	-4.789±0.78	-4.708±0.52	-5.872±0.42	-5.126±1.03	-5.493±0.20	-7.186±0.98	-5.394±0.74	-6.893±0.71	-8.908±1.55	-5.981±1.33	-8.657±0.94	-11.131±0.88
7	-3.686±0.88	-3.756±1.02	-3.839±1.03	-3.444±0.50	-3.944±0.76	-5.421±0.90	-4.293±0.54	-6.464±0.93	-6.267±1.03	-6.242±1.00	-9.133±1.04	-10.761±0.77
8	-0.001±0.33	-0.986±0.36	-2.719±0.24	-1.773±0.96	-2.056±0.77	-3.252±0.49	-2.827±0.31	-4.318±0.76	-4.527±0.65	-3.165±0.31	-3.444±0.74	-4.297±2.29
9	-3.823±0.77	-4.210±0.29	-4.794±0.23	-4.724±0.35	-4.382±0.47	-5.388±0.48	-4.007±0.78	-2.958±1.39	-8.588±7.02	-4.010±0.47	-4.684±2.44	-6.966±1.28
10	-4.975±0.37	-7.099±0.56	-8.519±0.42	-6.475±1.39	-11.243±0.60	-10.449±0.20	-9.215±0.98	-11.964±0.88	-12.522±0.46	-9.712±1.88	-10.940±0.87	-12.890±0.53
11	-1.458±0.27	-1.408±0.31	-2.199±0.38	-2.427±0.62	-2.413±0.32	-2.949±0.31	-3.157±0.58	-4.468±0.45	-4.851±0.92	-3.212±0.48	-5.650±0.90	-4.177±0.55
12	-1.769±0.25	-3.043±0.54	-2.965±0.78	-1.311±0.87	-3.832±1.15	-4.667±1.69	-3.272±0.76	-4.396±0.88	-5.798±1.25	-1.884±0.45	-4.843±0.84	-7.064±0.53
13	-3.485±0.79	-5.160±1.15	-4.304±0.42	-3.688±0.19	-4.415±0.59	-7.619±1.96	-5.518±0.72	-8.041±0.73	-8.378±0.95	-6.819±1.27	-9.466±0.95	-11.099±1.63
14	-2.181±0.85	-3.250±1.12	-4.459±2.01	-3.855±0.36	-5.920±0.69	-6.744±0.96	-5.584±1.77	-9.943±1.22	-8.953±1.99	-6.289±1.85	-7.862±1.22	-11.210±1.45
15	-3.315±0.35	-4.801±0.78	-4.433±0.93	-3.736±0.43	-6.495±1.87	-6.624±1.24	-4.826±0.37	-6.783±2.06	-6.818±1.14	-6.557±1.47	-9.316±1.86	-8.874±0.90
16	-3.802±0.32	-5.757±0.47	-6.218±0.85	-4.392±0.71	-5.900±0.40	-7.357±0.92	-5.931±0.37	-5.935±0.49	-9.968±0.91	-5.756±0.55	-7.807±0.63	-8.701±0.43
Mean±STD	-3.389±1.58	-4.450±1.93	-4.983±1.80	-4.278±1.82	-5.700±2.42	-7.163±2.76	-5.222±1.65	-7.199±2.66	-8.345±2.41	-6.091±2.11	-8.353±2.70	-9.420±3.02

Table 20: Individual mean peak hip abduction moment (Nm).

Subject	Q150			Q192			Q234			Q276		
	80 W	120 W	160 W	80 W	120 W	160 W	80 W	120 W	160 W	80 W	120 W	160 W
1	-25.121±2.26	-30.34±3.35	-34.720±3.68	-20.81±12.94	-39.137±3.03	-50.679±6.13	-26.50±4.37	-39.969±5.21	-58.328±6.85	-34.32±3.64	-44.085±6.18	-52.88±10.35
2	-13.332±3.25	-12.84±4.17	-14.775±3.78	-19.097±4.61	-24.347±9.55	-32.193±4.04	-23.64±7.18	-33.087±8.47	-36.491±4.64	-23.94±3.52	-23.638±1.87	-27.236±5.33
3	-10.017±1.88	-12.77±0.43	-17.770±2.58	-19.632±5.02	-23.632±3.94	-34.140±4.49	-20.61±5.17	-29.924±5.10	-31.093±4.26	-25.37±9.02	-35.48±13.90	-27.17±15.84
4	-20.905±3.34	-23.82±3.59	-21.692±2.11	-28.916±2.19	-30.344±4.96	-34.922±8.19	-28.24±4.05	-26.520±2.87	-22.310±3.89	-30.29±4.19	-39.602±4.93	-37.058±2.53
5	-11.125±3.67	-10.32±2.32	-10.471±6.40	-13.199±2.50	-13.787±4.74	-19.800±6.12	-15.45±2.66	-14.607±1.65	-20.389±6.14	-20.35±5.55	-18.509±3.87	-24.371±5.36
6	-12.034±1.58	-16.66±1.80	-18.389±1.63	-15.053±2.63	-17.571±3.82	-21.739±2.18	-14.41±1.96	-18.636±3.83	-21.483±4.24	-15.96±4.31	-25.770±3.43	-31.788±2.59
7	-16.426±2.98	-18.70±3.66	-22.116±2.27	-19.442±1.53	-19.407±2.35	-29.659±6.09	-19.25±2.77	-24.839±5.57	-29.904±1.12	-20.17±2.37	-27.800±1.66	-35.459±4.17
8	-4.184±0.86	1.15±1.23	0.313±1.33	-0.259±1.58	-1.968±1.51	-3.560±1.14	-1.46±0.98	-3.358±1.98	-4.914±0.60	-0.84±1.39	-2.522±2.24	-1.732±1.50
9	-12.797±3.17	-15.53±1.73	-15.157±2.00	-17.398±4.43	-17.435±3.90	-21.343±2.76	-17.26±2.70	-19.625±4.57	-25.736±3.91	-19.14±2.82	-22.985±5.44	-30.876±5.68
10	-9.158±1.21	-15.91±1.96	-19.704±3.48	-11.790±3.18	-20.822±2.25	-22.468±1.81	-14.40±1.86	-21.898±2.76	-24.911±2.72	-15.86±4.06	-20.674±3.31	-26.825±2.24
11	-4.171±0.52	-3.43±0.74	-5.042±1.34	-4.360±0.69	-4.002±1.33	-5.945±0.88	-6.72±1.60	-9.513±1.40	-8.288±1.84	-7.00±1.23	-9.398±1.63	-5.449±1.74
12	-5.341±0.71	-10.37±2.39	-10.380±2.05	-10.651±3.36	-16.225±3.23	-18.220±5.61	-14.72±2.14	-16.382±4.77	-20.924±4.41	-6.28±2.66	-17.854±3.54	-23.018±1.73
13	-19.628±6.41	-28.23±8.26	-26.239±1.45	-19.153±0.83	-22.480±1.06	-32.332±6.63	-24.96±2.71	-30.999±3.00	-39.014±4.88	-26.60±3.72	-34.230±3.22	-45.117±7.45
14	-12.996±3.08	-16.68±7.14	-19.619±7.49	-19.096±1.52	-28.327±2.61	-27.991±5.24	-17.26±3.19	-29.375±3.39	-27.689±4.59	-23.87±2.68	-28.075±4.05	-33.401±7.03
15	-16.524±2.85	-22.06±1.67	-24.546±4.95	-20.999±2.58	-34.059±9.39	-31.734±8.41	-23.15±3.64	-36.850±12.73	-38.382±6.44	-22.89±5.93	-35.778±11.51	-36.970±5.76
16	-18.544±2.10	-25.87±1.04	-26.781±1.98	-27.887±4.52	-32.521±2.49	-40.924±5.47	-28.77±2.09	-25.249±3.25	-39.436±4.31	-25.97±1.89	-32.188±2.23	-39.495±1.19
Mean±STD	-13.269±6.05	-16.40±8.53	-17.943±8.71	-16.734±7.49	-21.62±10.13	-26.72±11.98	-18.55±7.52	-23.802±9.86	-28.08±12.86	-19.92±9.00	-26.16±10.96	-29.92±12.89

Table 21: Individual RPE scores.

Subject	Q150			Q192			Q234			Q276		
	80 W	120 W	160 W	80 W	120 W	160 W	80 W	120 W	160 W	80 W	120 W	160 W
1	7	10	13	8	11	13	7	9	14	7	9	12
2	6	8	7	6	11	11	6	7	10	6	10	10
3	7	6	12	8	12	12	9	9	12	7	11	13
4	7	7	7	7	7	7	6	6	7	6	6	7
5	7	9	13	8	9	13	8	10	12	8	10	21
6	9	10	8	9	11	13	9	11	12	9	11	12
7	9	9	11	10	11	13	11	12	15	10	11	13
8	8	11	11	11	13	14	12	12	14	11	13	13
9	9	11	14	9	12	16	8	11	16	9	12	16
10	7	8	13	7	9	9	6	9	14	10	7	14
11	6	12	14	6	8	11	6	12	13	9	9	13
12	7	9	10	6	8	9	8	7	9	7	6	11
13	7	12	13	7	10	11	8	9	14	8	10	13
14	9	10	12	9	11	13	10	10	13	9	11	13
15	7	10	13	9	11	11	10	13	11	11	10	14
16	7	8	10	6	7	10	6	7	10	6	7	11
Mean±STD	7.44±1.0	9.38±1.7	11.31±2.3	7.88±1.5	10.06±1.8	11.63±2.2	8.13±1.9	9.63±2.1	12.25±2.3	8.31±1.7	9.56±2.1	12.88±2.9

Table 22: Individual comfort scores.

Subject	Q150			Q192			Q234			Q276		
	80 W	120 W	160 W	80 W	120 W	160 W	80 W	120 W	160 W	80 W	120 W	160 W
1												
2												
3												
4												
5												
6												
7	1	1	2	1	2	2	0	1	2	1	1	1
8	2	2	2	3	3	4	3	3	3	4	4	4
9	1	2	3	3	3	4	2	3	3	5	6	6
10	0	0	0	0	0	0	0	0	0	0	0	0
11	1	2	2	0	0	2	1	2	3	0	0	3
12	0	1	1	0	1	1	1	1	1	0	1	2
13	0	0	0	1	1	1	3	3	3	4	4	5
14	1	0	1	1	2	1	0	1	2	1	2	3
15	1	1	1	0	0	0	1	1	1	4	4	3
16	0	0	0	0	0	0	1	1	1	2	2	2
Mean±STD	0.80±0.63	1.00±0.82	1.50±1.08	1.10±1.20	1.40±1.17	1.70±1.42	1.50±1.18	1.90±0.99	2.40±1.26	2.40±1.84	2.80±1.87	3.50±1.72

Table 23: Individual pain scores.

Subject	Q150			Q192			Q234			Q276		
	80 W	120 W	160 W	80 W	120 W	160 W	80 W	120 W	160 W	80 W	120 W	160 W
1												
2												
3												
4												
5												
6												
7	0	0	1	0	0	1	0	0	0	0	0	1
8	0	0	0	0	0	0	0	0	0	0	0	0
9	0	0	0	0	0	0	0	0	0	0	0	0
10	0	0	0	0	0	0	0	0	0	0	0	0
11	0	0	0	0	0	0	0	0	0	0	0	0
12	0	0	0	0	1	0	0	0	0	0	0	0
13	0	0	0	0	0	0	0	0	0	0	0	0
14	0	0	0	0	0	0	0	0	1	0	0	1
15	0	0	0	0	0	0	0	0	0	0	0	0
16	0	0	0	0	0	0	0	0	0	0	0	0
Mean±STD	0.00±0.00	0.00±0.00	0.10±0.3	0.00±0.00	0.10±0.3	0.10±0.3	0.00±0.00	0.00±0.00	0.10±0.3	0.00±0.00	0.00±0.00	0.20±0.4

Table 24: Group mean peak pedal reaction force (PRF) and pedal center of pressure.

Variables	Workload (W)	Q150	Q192	Q234	Q276	Workload	Q-Factor	Int
Vertical PRF (N)	80	214.8±27.9	197.3±24.6	205.6±25.9	205.7±27.0	**p < 0.001**	0.183	0.339
	120[α]	256.1±29.5	243.0±27.5	251.1±39.7	255.5±29.1			
	160[α,β]	291.4±33.0	290.8±33.5	286.0±41.6	289.0±34.5			
	Q-Factor Test							
Mediolateral PRF (N)	80	-33.2±10.8	-38.7±9.2	-42.9±9.1[1]	-48.5±12.5[1,2]	**p < 0.001**	**p < 0.001**	**0.016**
	120[α]	-42.8±12.0	-52.8±12.6[1]	-60.2±14.9[1]	-67.6±14.6[1,2]			
	160[α,β]	-50.6±12.5	-66.0±14.9[1] α	-72.5±17.7[1] α,β	-79.9±18.5[1,2] α,β,γ			
	Q-Factor Test							
Power Phase COP (cm)	80	1.4±0.7	1.4±0.12.0	1.8±1.1	2.1±1.5	0.583	**0.014**	0.182
	120	0.7±0.1	-0.4±5.2	1.0±3.3	1.9±1.7			
	160	-7.4±25.3	0.0±4.7	-2.6±86.2	3.1±7.7			
	Q-Factor Test							

Note:
[a]: significantly different from 80W, [b]: significantly different from 120W
[α]: significantly different from Q150,
[1]: significantly different from Q150 at same work load, [2]: significantly different from Q192 at same work load, [3]: significantly different from Q234 at same work load
Q-Factor Test: post hoc comparisons for Q-factor main effect.

Table 25: Group mean peak lower extremity joint angles and power phase ROM.

Variables	Workload (W)	Q150	Q192	Q234	Q276	Workload	Q-Factor	Int
Knee Extension ROM	80	71.1±5.8	71.6±5.7	72.1±5.6	73.1±5.6	0.603	**p < 0.001**	0.663
	120	70.9±6.5	72.3±6.3	72.7±5.9	73.4±5.9			
	160	71.0±6.9	72.0±6.6	73.2±7.0	73.9±6.8			
	Q-Factor Test		α	α,β	α,β,γ			
Frontal Plane Knee Angle	80	2.6±5.3	1.4±4.9	0.9±4.9	0.2±5.2	0.770	**0.006**	0.155
	120	2.3±4.8	1.5±5.0	0.8±4.5	0.8±4.9			
	160	1.9±4.8	1.3±4.9	0.8±4.8	0.0±5.0			
	Q-Factor Test				α			
Knee Abduction ROM	80	-7.8±5.0	-7.2±5.1	-7.0±4.8	-6.2±4.3	0.083	**0.022**	0.562
	120	-8.0±5.5	-7.8±4.9	-7.0±4.6	-6.3±4.5			
	160	-8.8±5.8	-7.8±4.9	-8.5±4.3	-6.7±4.2			
	Q-Factor Test				α,β			
Knee External Rotation ROM (deg)	80	-2.9±4.6	-3.1±5.0	-3.1±4.9	-1.6±3.5	0.709	0.644	0.310
	120	-2.6±4.4	-3.0±4.8	-2.6±4.3	-2.7±5.0			
	160	-2.6±5.1	-2.4±5.1	-2.4±6.2	-3.7±6.0			
	Q-Factor Test							
Peak Ankle Eversion Angle (deg)	80	-1.5±3.8	-1.5±4.8	-1.5±3.8	0.1±4.6	0.268	0.385	0.268
	120	-1.1±3.4	-1.3±3.9	-1.1±4.6	-0.1±4.6			
	160	-1.3±3.7	-1.7±3.8	-0.3±4.3	0.3±4.3			
	Q-Factor Test							
Hip Abduction ROM (deg)	80	3.1±3.4	2.3±2.6	2.2±2.7	2.4±2.9	0.084	0.129	0.633
	120	2.4±2.5	2.2±1.9	1.9±2.2	1.6±2.7			
	160	2.2±2.3	1.8±1.6	1.8±1.6	1.4±1.4			
	Q-Factor Test							

Note:
[a]: significantly different from 80W, [b]: significantly different from 120W
[α]: significantly different from Q150, β: significantly different from Q192, γ: significantly different from Q234
[1]: significantly different from Q150 at same work load, [2]: significantly different from Q192 at same work load, [3]: significantly different from Q234 at same work load
Q-Factor Test: post hoc comparisons for Q-factor main effect.

Table 26: Group mean peak lower extremity power phase joint moments.

Variables	Workload (W)	Q150	Q192	Q234	Q276	Workload	Q-Factor	Int
Knee Extension Moment (Nm)	80	21.3±9.1	22.2±8.1	21.8±9.5	23.9±10.3			
	120[a]	29.2±10.0	29.0±9.1	30.7±13.0	33.1±12.2	**p < 0.001**	0.146	0.332
	160[a,b]	32.5±12.3	35.6±12.2	35.2±13.431	35.9±12.8			
	Q-Factor Test							
Knee Abduction Moment (Nm)	80	-9.3±3.0	-11.0±4.0	-12.7±3.9[1]	-13.7±4.8[1,2]			
	120[a]	-12.0±4.31	-14.6±5.6[1]	-16.7±5.5[1,2]	-18.7±5.3[1,2]	**p < 0.001**	**p < 0.001**	**0.020**
	160[a,b]	-13.9±3.9	-18.1±5.5[1]	-19.8±6.3[1]	-21.7±6.5[1,2]			
	Q-Factor Test		α	α,β	α,β,γ			
Knee External Rotation Moment (Nm)	80	8.3±4.6	9.5±4.6	10.8±4.4[1,2]	11.4±5.1[1,2]			
	120[a]	11.4±3.8	13.2±6.1[1]	14.8±6.4[1]	15.9±6.1[1,2]	**p < 0.001**	**p < 0.001**	**p < 0.001**
	160[a,b]	11.4±6.2	16.4±6.7[1]	18.0±7.4[1]	18.5±7.5[1,2]			
	Q-Factor Test		α	α,β	α,β,γ			
Ankle Eversion Moment (Nm)	80	-1.1±2.1	-2.8±2.9[1]	-3.9±2.3[1]	-5.5±3.1[1,2,3]			
	120[a]	-1.4±2.6	-3.2±3.1[1]	-4.2±2.7[1]	-6.3±3.7[1,2,3]	**0.005**	**p < 0.001**	**0.035**
	160[a,b]	-1.5±2.8	-3.9±3.5[1]	-5.3±3.3[1]	-6.9±4.3[1,2,3]			
	Q-Factor Test		α	α,β	α,β,γ			
Ankle External Rotation Moment (Nm)	80	-3.4±1.6	-4.3±1.8[1]	-5.2±1.7[1]	-6.1±2.1[1,2,3]			
	120[a]	-4.5±1.9	-5.7±2.4[1]	-7.2±2.7[1]	-8.4±2.7[1,2,3]	**p < 0.001**	**p < 0.001**	**0.021**
	160[a,b]	-5.0±1.8	-7.2±2.8[1]	-8.3±2.4[1]	-9.4±3.0[1,2]			
	Q-Factor Test		α	α,β	α,β,γ			
Hip Abduction Moment (Nm)	80	-13.3±6.1	-16.7±7.5[1]	-18.6±7.5[1,2]	-20.0±9.0[1,2]			
	120[a]	-16.4±8.5	-21.6±10.1[1]	-23.8±9.9[1]	-26.1±11.0[1,2]	**p < 0.001**	**p<0.001**	**0.001**
	160[a,b]	-17.9±8.7	-26.7±12.0[1]	-28.1±12.9[1]	-30.0±12.9[1]			
	Q-Factor Test		α	α,β	α,β			

Note:
[a]: significantly different from 80W, [b]: significantly different from 120W
[α]: significantly different from Q150, β: significantly different from Q192, γ: significantly different from Q234
[1]: significantly different from Q150 at same work load, [2]: significantly different from Q192 at same work load, [3]: significantly different from Q234 at same work load
Q-Factor Test: post hoc comparisons for Q-factor main effect.

VITA

Tanner Thorsen was born in Provo, Utah, to the parents of Byron and Sidney Thorsen. He attended elementary through high school in Arlington, TX. After his graduation from James W. Martin high school, he attended Brigham Young University and received his Bachelor of Science degree in Exercise Science. After his graduation, he was accepted by the University of Tennessee in to the Master of Science in the department of Kinesiology, Recreation, and Sport Science with an emphasis in biomechanics. He graduated with a Master of Science degree in 2018.